LARGE STRAIN SHEAR MODULUS OF SAND AS A FUNCTION OF CONFINEMENT AND RELATIVE DENSITY

by

Behzad Soltanbeigi

B.S., Civil Engineering, Islamic Azad University,Tabriz Branch, 2011

Submitted to the Institute for Graduate Studies in
Science and Engineering in partial fulfillment of
the requirements for the degree of
Master of Science

Graduate Program in Civil Engineering
Boğaziçi University

2013

`

LARGE STRAIN SHEAR MODULUS OF SAND AS A FUNCTION OF CONFINEMENT AND RELATIVE DENSITY

APPROVED BY:

AssociateProf. Özer ÇİNİCİOĞLU……..

(Thesis Supervisor)

Prof. Erol GÜLER……..

Assist. Prof.M. Kubilay KELEŞOĞLU……..

DATE OFAPPROVAL: 23.08.2013

ACKNOWLEDGEMENTS

My sincere thanks are due to Assoc. Prof. Özer ÇİNİCİOĞLU for his sparkling ideas, invaluable assistance, advice, and meticulous comments throughout writing my M.S. thesis. I believe that my advisor's wholehearted support established the main framework of this study.

I would like to make acknowledgment to the member of the thesis committee, Prof. Erol GÜLER and Assist. Prof. Kubilay KELEŞOĞLU for their efficient comments.

Finally, I would like to thank myparents for their life-long support and for my friends for their patience in laboratory, for which I will remain grateful forever.

ABSTRACT

LARGE STRAIN SHEAR MODULUS OF SAND AS A FUNCTION OF CONFINEMENT AND RELATIVE DENSITY

Shear modulus of soils (G) is dependent on so many factors, such as, plasticity, mineralogy of soil particles and particle shape, relative density, overburden pressure, shear strain magnitude, number of cycles and some more. Meanwhile, for clean sands two significant factors prevail upon the others; relative density and confining pressure. Investigation on stiffness of soils against induced loads has always been a crucial issue for geotechnical engineers. On the other hand, this critical property of soil can be surveyed through in-situ and laboratory tests, which are costly and a long time is needed to obtain precise results. Due to these problems, engineers often prefer to use simple and straightforward empirical approaches to calculate the value of magnitude of G. In this thesis, nearly 200 Direct Simple Shear tests were conducted on two types of sands to understand and quantify the influences of relative density (R_D) and vertical effective stress (σ_v') on shear modulus as a function of shear strain. Additionally, an equation was proposed to estimate G as a function of R_D,σ_v' and shear strain within the range of 0.1 to 10%. The outstanding advantage of proposed equation is that it uses directly measurable and calculable parameters (R_D and σ_v').

ÖZET

KUMLARDA BÜYÜK DEFORMASYON ŞARTLARINDA KAYMA MODÜLÜNÜN GERİLME VE SIKILIK İLE DEĞİŞİMİ

Zeminlerin kesme modülü birçok faktöre bağlıdır. Bu faktörlerden bazıları zemin plastisitesi, daneciklerin minerolojisi ve şekli, göreceli yoğunluk, ortamdaki basınç, kesme gerinimi ve yükleme tekrar sayısı olarak sıralanabilir. Bununla birlikte, temiz kum için zeminin görecrli yoğunluğu ve çevresel basınç diğer faktörlere göre daha baskın durumdadır. Etkin yüklere bağlı olarak zemin rijitliğinin değişimi hakkındaki araştırmalar, geoteknik mühendisliği için önemli bir konu olmuştur. Diğer bir yandan, toprağın bu kritik özelliği, maliyetli ve hassas sonuçlar alabilmek için uzun zaman gerektiren arazi ve labaratuvar deneylerinden faydalanılarak araştırılabilir. Bu problem sebebiyle, mühendisler G değerinin büyüklüğünü hesaplamak için genelde basit ve yaklaşık olan ampirik yaklaşımlar kullanırlar. Bu tezin hazırlanışı sırasında, toprağın görecrli yoğunluğu (R_D) ve düşey efektif gerilmesinin (σ_v') kesme modülü üzerindeki etkisini kesme geriniminin bir fonksiyonu gibi anlamak ve onu sayısallaştırmak amacıyla yaklaşık 200 tane basit kesme deneyi gerçekleştirilmiştir. Ayrıca toprağın göreceli yoğunluğunun (R_D), düşey efektif gerilmesinin (σ_v') ve %0.1 ve %10 aralığındaki bir kesme geriniminin bir fonksiyonu olarak düşünülen G'nin tahmin edilebilmesi için bir denklem geliştirilmiştir. Önerilenbu denklemin göze çarpan avantajı ise denklemin toprağın göreceli sıkılığı (R_D) ve düşey efektif gerilmesi(σ_v') gibi direkt olarak ölçülebilir ve hesaplanabilir parametrelerden oluşmasıdır.

TABLE OF CONTENTS

ACKNOWLEDGEMENTS iii

ABSTRACT iv

ÖZET v

LIST OF FIGURES viii

LIST OF TABLES xiii

LIST OF SYMBOLS xv

LIST OF ACRONYMS/ABBREVIATIONS xvii

1. INTRODUCTION 1
   1.1. Objective of Thesis 2
   1.2. Organization of Thesis 2
2. LITERATURE REVIEW 4
   2.1. Historical Background of DSS Test 4
   2.2. Summary of ASTM Testing Requirements 7
   2.3. Constant Volume / Constant Load Tests 9
   2.4. Wire-reinforced and Stacked Rings Membrane 10
      2.4.1. Comparison of Consolidation Data 11
      2.4.2. Comparison of Shear Data 12
   2.5. Typical Results Can be Obtained in DSS Test 13
      2.5.1. Correction Factors 15
      2.5.2. Specimen Size Effect 19
      2.5.3. Stress Rotation 20
      2.5.4. Shear Stiffness Determination 21
      2.5.5. Pore Pressure Determination 24
   2.6. Shear Modulus of the soil 25
      2.6.1. Low Amplitude Shear Modulus 27
      2.6.2. Strain Dependent Shear Modulus 35
3. DIRECT SIMPLE SHEAR TEST METHODOLOGY 36
   3.1. Testing Equipment 36

3.2. Testing Procedure……..……..... 37
3.2.1. Specimen Preparation and Setting up the Test Apparatus……..…….. 37
3.3. Properties of Soils Tested……..……..…… 41
3.3.1. Silivri Sand……..…….. 41
3.3.2. Standard Ottawa Graded Sand……..……..…….. 44
3.4. Geocomp DSS Software PID Settings…….…… 46
3.5. Consolidation Test……..…. 47
4. EVALUATION of DIRECT SIMPLE SHEAR TEST RESULTS…….…….. 49
4.1. Silivri Sand DSS Test Results…….……...…… 49
4.1.1. Effect of Relative Density on Shear Modulus of Silivri Sand..……51
4.1.2. Quantifying G as a function of σ_v', R_D and γ for Silivri Sand……..... 61
4.2. Standard Ottawa Graded Sand DSS Test Results…….…….... 73
4.2.1. Effect of Relative Density onShear Modulus of Standard Ottawa Graded Sand..……. 75
4.2.2. Quantifying Shear ModulusAs a Function of σ_v', R_D and γ for Standard Ottawa Graded Sand……... 87
5. DISCUSSION……..100
5.1. Comparison of Obtained Results for Silivri Sand with Proposed Equation… 100
5.2. Comparison of Obtained Results for Standard Ottawa Graded Sand with Proposed Equation……. 106
6. CONCLUSION……116
6.1. Recommendations for Future Work……..…… 117
REFERENCES…….. 118

LIST OF FIGURES

Figure 2.1. SGI Simple Shear Device. ..…….. 5

Figure 2.2. NGI Direct Simple Shear Device. ……... 5

Figure 2.3. NGI DSS Membrane stretcher (a) and NGI DSS Set-up (b). …… 6

Figure 2.4. GEOCOMP direct simple shear test device. …….. 7

Figure 2.5. Schematic Diagram of Essential Direct Simple Shear Components. ……. 8

Figure 2.6. Samples prepared for DSS testing using (a) Stacked rings and (b) Wire-reinforced. ……..… 10

Figure 2.7. Shear stress and excess pore pressure verses strain from DSS test.…… 12

Figure 2.8. Stress paths for a.) Gulf of Mexico Clay, and b.) Organic Silt. ……... 13

Figure 2.9. Shear Stress-Strain behavior of Silivri sand. …….. 14

Figure 2.10. Stress-strain relationship for samples of water. ……..…… 16

Figure 2.11. Calibration of membrane resistance. ……..……. 17

Figure 2.12. NGI's Wire Reinforced Membrane chart by membrane size. …...…….. 18

Figure 2.13. Stress rotation representation in DSS test. …… 21

Figure 2.14. Applied Stress during DSS Testing. ……..……... 22

Figure 2.15. Normalized undrained shear strength for TC, DSS and TE test results as a function of plasticity index. ..……..…….…….. 23

Figure 2.16. Comparison of Pore Pressure from Constant Volume and Undrained DSS test Results. ……..…….…….. 25

Figure 2.17. Variation in shear modulus with different shear strain levels. ……. 26

Figure 2.18. Back-bone curve. …….. 28

Figure 2.19. Typical modulus and height change with time for clay. ……... 32

Figure 2.20. Modulus increase ratio versus plasticity index. ……....… 33

Figure 2.21. Typical modulus change with time for sand. ……..……..…… 34

Figure 3.1. Simplified diagram of the DSS device. ……..…….. 38

Figure 3.2. Specimen preparation and setting up the DSS test.……..…….. 39

Figure 3.3. Air-pluviation set-up for sample preparation.…….……..40

Figure 3.4. Variation of the void ratio with raining height.…….…… 41

Figure 3.5. Gradation curve for well-graded Silivri sand. …….…… 42

Figure 3.6. Relative density test apparatus.…….…… 44

Figure 3.7. Gradation curve for standard Ottawa graded sand. …….……. 45

Figure 3.8. PID Input Manual Geocomp Software.…….. 46

Figure 3.9. Consolidation test result, interpretation of t100 parameter.…….…..48

Figure 4.1. Stress-strain curve of soil and G_{tan} determination.……..…. 52

Figure 4.2. Shear modulus variation with shear strain between 0.1 to 10 % for$\sigma'_v = 10\ Kpa$ (a) and (b). ……..……..…… 52

Figure 4.3. Shear modulus variation with shear strain between 0.1 to 10 % for $\sigma'_v = 20\ Kpa$ (a), (b), (c) and (d). ……..……...…….54

Figure 4.4. Shear modulus variation with shear strain between 0.1 to 10 % for$\sigma'_v = 30\ Kpa$ (a) and (b). ……..……... 55

Figure 4.5. Shear modulus variation with shear strain between 0.1 to 10 % for$\sigma'_v = 50\ Kpa$ (a) and (b). ……..……..57

Figure 4.6. Shear modulus variation with shear strain between 0.1 to 10 % for $\sigma'_v = 70\ Kpa$ (a) and (b). ……..……..……59

Figure 4.7. Variation of fitting parameters with R_D , for $\sigma'_v = 10\ Kpa$.……..…….64

Figure 4.8. Variation of fitting parameters with R_D , for $\sigma'_v = 20\ Kpa$.……..…… 65

Figure 4.9. Variation of fitting parameters with R_D , for $\sigma'_v = 30\ Kpa$.……..... 66

Figure 4.10. Variation of fitting parameters with R_D , for $\sigma'_v = 50\ Kpa$.…….. 67

Figure 4.11. Variation of fitting parameters with R_D , for $\sigma'_v = 70\ Kpa$.…….. 68

Figure 4.12. Fitting parameters variation with σ'_v/p_a (a). ……..…..……..... 69

Figure 4.13. Shear modulus variation with shear strain between 0.1 to 10 % for$\sigma'_v =$ 10 Kpa.……...……..... 75

Figure 4.14. Shear modulus variation with shear strain between 0.1 to 10 % for$\sigma'_v =$ 50 Kpa.……..…….... 76

Figure 4.15. Shear modulus variation with shear strain between 0.1 to 10 % for $\sigma'_v =$ 70 Kpa (a), (b), (c) and (d). ……..…….……. 77

Figure 4.16. Shear modulus variation with shear strain between 0.1 to 10 % for$\sigma'_v =$ 90 Kpa (a) and (b). ……..……..…..…… 78

Figure 4.17. Shear modulus variation with shear strain between 0.1 to 10 % for $\sigma'_v =$ 110 Kpa(a), (b), (c) and (d). ……..……..... 80

Figure 4.18. Shear modulus variation with shear strain between 0.1 to 10 % for$\sigma'_v =$ 130 Kpa (a), (b), (c) and (d).……..…….. 82

Figure 4.19. Shear modulus variation with shear strain between 0.1 to 10 % for$\sigma'_v =$ 160 Kpa(a) and (b). ……... 83

Figure 4.20. Shear modulus variation with shear strain between 0.1 to 10 % for$\sigma'_v =$ 200 Kpa(a) and (b). ……..…… 85

Figure 4.21. Variation of fitting parameters with R_D , for $\sigma'_v = 10\ Kpa$.…… 88

Figure 4.22. Variation of fitting parameters with R_D , for $\sigma'_v = 50\ Kpa$.…… 89

Figure 4.23. Variation of fitting parameters with R_D , for $\sigma'_v = 70\ Kpa$.…… 90

Figure 4.24. Variation of fitting parameters with R_D , for $\sigma'_v = 90\ Kpa$.…… 91

Figure 4.25. Variation of fitting parameters with R_D , for $\sigma'_v = 110\ Kpa$.……. 92

Figure 4.26. Variation of fitting parameters with R_D , for $\sigma'_v = 130\ Kpa$.…….. 93

Figure 4.27. Variation of fitting parameters with R_D , for $\sigma'_v = 160\ Kpa$.……. 94

Figure 4.28. Variation of fitting parameters with R_D , for $\sigma'_v = 200\ Kpa$……. 95

Figure 4.29. Fitting parameters variation with σ'_v/P_a(a). …..…….…… 96

Figure 5.1. Comparison of obtained data from DSS test for Silivri sand with proposed equation at σ'_v =10 Kpa.…….……....… 101

Figure 5.2. Comparison of obtained data from DSS test for Silivri sand with proposed equation at σ'_v =20 Kpa.……..…… 102

Figure 5.3. Comparison of obtained data from DSS test for Silivri sand with proposed equation at σ'_v =30 Kpa.…….……..… 103

Figure 5.4. Comparison of obtained data from DSS test for Silivri sand with proposed equation at σ'_v =50 Kpa.…….……....… 104

Figure 5.5. Comparison of obtained data from DSS test for Silivri sand with proposed equation at σ'_v =70 Kpa. …….……....… 105

Figure 5.6. Comparison of obtained data from DSS test for SOG sand with proposed equation at σ'_v =10 Kpa.…….. 107

Figure 5.7. Comparison of obtained data from DSS test for SOG sand with proposed equation at σ'_v =50 Kpa.…….. 108

Figure 5.8. Comparison of obtained data from DSS test for SOG sand with proposed equation at σ'_v =70 Kpa.…….. 109

Figure 5.9. Comparison of obtained data from DSS test for SOG sand with proposed equation at σ'_v =90 Kpa.…….. 110

Figure 5.10. Comparison of obtained data from DSS test for SOG sand with proposed equation at σ'_v =110 Kpa.…… 111

Figure 5.11. Comparison of obtained data from DSS test for SOG sand with proposed equation at σ'_v =130 Kpa.……. 112

Figure 5.12. Comparison of obtained data from DSS test for SOG sand with proposed equation at σ'_v =160 Kpa.……. 113

Figure 5.13 Comparison of obtained data from DSS test for SOG sand with proposed equation at σ'_v =200 Kpa..... 114

LIST OF TABLES

Table 2.1. Summary of maximum vertical strain during consolidation. …….. 12

Table 2.2. NGI's Wire Reinforced Membrane chart by membrane strength.…… 17

Table 2.3. Summary of steps for correction factor determination. …… 19

Table 2.4. Summary of shear strength results for different modes of loading. …… 24

Table 2.5. Values of k in the Factor,OCR^k…… 29

Table 2.6. Summarized formulas for void ratio functions and constants in proposed empiricalequations on Small Strains Modulus.……...……...30

Table 2.7. Effect of Environmental and Loading Conditions on Modulus Ratio. …. 35

Table 3.1. Engineering properties summary of Silivri Sand.……..47

Table 3.2. Engineering properties summary of Standard Ottawa graded Sand.….. 46

Table 4.1. Details of DSS test conducted on Silivri sand.……..50

Table 4.2. Summary of power functions of trend-lines and R^2 value.……62

Table 4.3. Summary of the equations corresponding to trend-lines for ζ and η parameters.……..69

Table 4.4. Fitting parameters variation with $\sigma'_{v.}$ …… 71

Table 4.5. Summary of $k_{1,\ldots,8}$ values of trend-lines for α_ζ , β_ζ , α_η and $\beta_\eta$parameters. ……72

Table 4.6. Summary of the equations corresponding and R^2 value of trend-lines for α_ζ ,β_ζ , α_η and β_η parameters. …… 72

Table 4.7. Details of DSS tests conducted on standard Ottawa graded sand.…..... 73

Table 4.8. Summary of the equations corresponding to trend-lines for ζ and η parameters. …….. 96

Table 4.9. Fitting parameters variation with σ'_v/P_a. ……..…...……98

Table 4.10. Summary of $k_{1,\ldots,8}$ values of trend-lines for α_ζ , β_ζ , α_η and β_η parameters. ……..… 99

Table 4.11. Summary of the equations corresponding and R^2 value of trend-lines for α_ζ ,β_ζ , α_η and β_η parameters. ….……..……...……...……... 99

LIST OF SYMBOLS

C Cohesion of the soil

C_c Coefficient of Curvature

C_u Coefficient of uniformity

e Void ratio

G Shear modulus

G_{max} Maximum shear modulus

G_{tan} Tangent shear modulus

OCR Over consolidated ratio

P_a Atmospheric pressure

PI Plasticity index

R_D Relative density

Su Undrained shear strength

t Time

U Percent of consolidation

α_ζ Slope of the line correlating ζ with σ'_v

α_η Slope of the line correlating η with σ'_v

β_ζ Zero intercept of line correlating ζ with σ'_v

β_η Zero intercept of line correlating η with σ'_v

γ Shear strain

γ_{et} Elastic threshold strain

γ_r Cyclic strain amplitude

ε_a Normal (axial) strain

ζ Unit-independent fitting parameter

η Unit-independent fitting parameter

σ_2 Intermediate principal stress

σ_0' Mean effective stress

σ_t Tangential stress

σ_v' Vertical effective stress

σ'_{vc} Vertical effective consolidation stress

τ_{max} Maximum Shear stress

$\emptyset$ Friction angle of the soil

LIST OF ACRONYMS/ABBREVIATIONS

ASTM American Society for Testing and Materials

DSS Direct Simple Shear

NGI NorwegianGeotechnical Institute

PIDProportional Integral-Derivative

RC Resonant Column

SGISwedish Geotechnical Institute

SOG Standard Ottawa Graded

TC Triaxial Compression

TE Triaxial Extension

WRM Wire Reinforced Membrane

1. INTRODUCTION

To construct safe and economic structures, it is crucial to investigate and quantify the engineering properties of the materials used and the behavior of the soil underneath. Both economy and safety should be satisfied in all engineering activities, so neither over nor under-estimations are desirable. Nonlinear behavior of soil presents a sort of uncertainty especially to conventional linear design of geo-structures. Furthermore, the need to build larger and heavier structures such as dams, bridges and skyscrapers and the accompanying scarcity of lands with stable and strong soils, impose an ever-increasing demand on engineers to understand and quantify soil behavior under different stresses and strains. A serious problem to tackle for geotechnical engineers is the prediction of soil respond to strong ground motions that are generally induced by earthquakes. Of all diverse soil types, cohesionless soils, in particular sands, present some of the most major challenges since they are routinely used as backfill materials. If engineers have the ability to quantify the degradation of a soil's stiffness as it endures shear strains, it would help to improve design techniques for structures and, moreover, consider an optimized factor of safety.

Because of the nonlinearity of the stress-strain behavior of soils, the shear modulus is always a function of strain amplitude, so, quantification of shear modulus becomes crucial when it comes to evaluation of strain level induced by both loading scheme and soil specifications. The amount of strain and its effect on soil shear modulus become increasingly of interest in the past decades, specifically in areas such as embankment design problems, marine structures subjected to the cyclic action of waves, ground response analysis,pavements under traffic loading conditions, and soil structure interaction under dynamic and static loads.

In situ tests such as cross-hole seismic testing or surface wave testingallows the estimationof G_{max}in practice. Three-dimensional models for soil elasticity are capable ofapproximatingvariation in G_{max} that happen with loading, which isconsequence of stresses and soil density changes. On the other hand, over the past years, many researchers

have widely investigated modulus reduction relationships for soils through laboratory experiments. Large-strain stiffness can be obtained in triaxial, simple shear and the resonant column apparatuses. This thesis used Direct Simple Shear test to investigate stress-strain behavior of the well-graded Silivri sand and also an standard Ottawa graded Kavakli sand. Shear modulus of the sands were computed from data obtained from Geocomp DSS test device data acquisition. A testing program was established to monitor the effect of both relative density and vertical stress on shear modulus of the prepared samples.

1.1.The Objectives of Thesis

The first objective of this thesis is to quantify the shear modulus of Silivri sand in large strains as a function of vertical effective stress and relative density. Moreover, the second objective is to evaluate proposed equation for another type of sand, a standard Ottawa graded sand.

These objectives will be fulfilled by conducting Direct Simple Shear test on sand specimens that are prepared in different relative densities and induced predetermined vertical effective stresses, as two variables, and undergo two phases of consolidation and shearing.

1.2.Organization of Thesis

Chapter 2 consists of a literature review, in which the theory behind the direct simple shear test, historical development of device, ASTM summary of testing requirements, interpretation of constant volume-load procedures used for the shear phase, types of membranes used in this test and their effect on both consolidation and shearing of the specimen, typical results that can be obtained in this test and also needed correction factors, the effect of specimen size on results gained, explanation of stress rotation takes place during shear phase, shear stiffness and pore pressure determination and eventually a brief description on shear modulus in its thresholds.

Chapter 3 includes testing equipment description, Consolidation phase summary, PID (Proportional Integral-Derivative) settings for Geocomp Shear Track II system, DSS testprocedure which consist of Specimen preparation and setting up the test apparatus, properties of the sands tested.

Chapter 4 comprises DSS test results obtained for both sands. Initially, relative density was chosen as a variable, and vertical stress kept as a constant. To observe the effect of changing in relative density, variation of normalized shear modulus vs. shear strain was plotted for every single family of data (also named as degradation curve). Therewith, a trend-line has drawn by Excel for each degradation curve so that a mathematical equation, as a power function, obtained. This led to generating an equation for estimation of shear modulus degradation in a boundary of 0.1 to 10 % of shear strain as a function of confinement and relative density.

Chapter 5 contains results from DSS test for both Silivri and Kavakli sands, and furthermore, the plots of proposed equations for each type of sand are available, which are computed in chapter 4 from data points. The obtained normalized shear modulus vs. shear strain plots, which are restricted to 0.1 to 10 % of shear strain, can be compared to the power function estimated values.

2. LITERATURE REVIEW

2.1.Historical Background of DSS Test

In 1936 the Swedish Geotechnical Institute (SGI) built the first direct simpleshear device that was able to uniformly deform a soil specimen in pure shear. This device confined specimens using a rubber membrane and aluminum rings. The ringswere packed tightly together and the sample was consolidated using lead weights. Apicture of a typical sample using this equipment can be seen in Figure 2.1(Kjellam, 1951).

Since SGI's device was built in 1936 there have been many additional DSS devices. In 1953 a device was designed at the university of Cambridge using a square box for sand specimens. A device using a square sample (dimensions 60x60x20 mm) was designed with straight lateral boundaries (Roscoe 1953) in order to improve on the previous devices. The lateral boundaries are frictionless whereas the top and bottom boundaries are rough. This experimental device is the first of a long series developed in Cambridge University and thoroughly studied in details by several researchers during the following decades. These devices could not perform truly undrained tests since no back pressure could be applied for full saturation. Later, Direct Simple Shear device testing samples enclosed in a pressurized cell were developed (Franke 1979, Dyvik 1987) with the objective to ensure a full saturation of the sample and provide accurate pore pressure measurements in the soil specimen.

In the 1960's the Norwegian Geotechnical institute (NGI) created a device that was able to strain in simple shear after vertical loading using a rubber membrane reinforced with a wound wire encased by the rubber (DeGroot *et al.*, 1992) as shown in Figure 2.2. NGI created the wire-reinforced membrane used in their DSS testing along with a special trimming apparatus allowing for minimal sample disturbance as shown in Figure 2.3. In the 1990's data acquisition and control systems became relatively inexpensive and several companies in the U.S. and the United Kingdom developed automated triaxial, direct simple shear, consolidation, and cyclic systems.These companies sell direct simple shear

equipment exclusively with stacked rings to avoid the high costs of wire reinforced membranes.

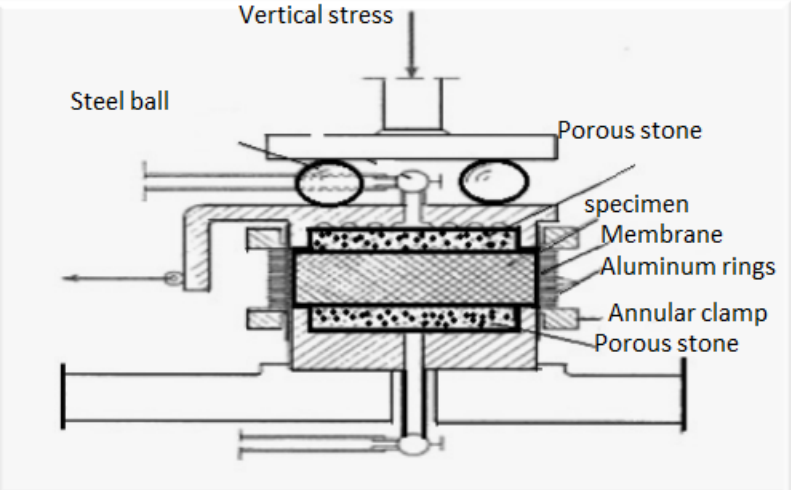
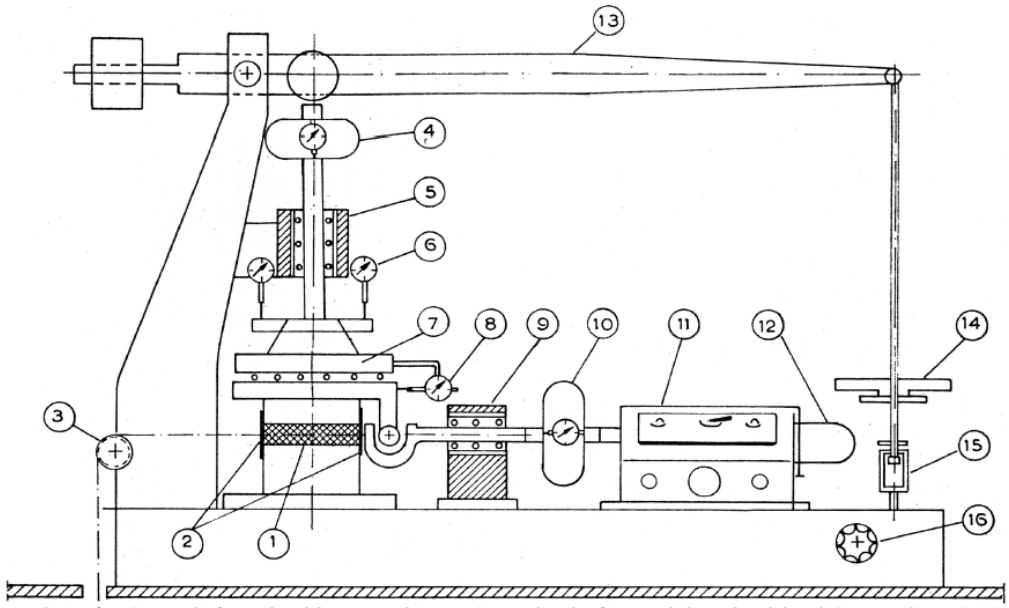
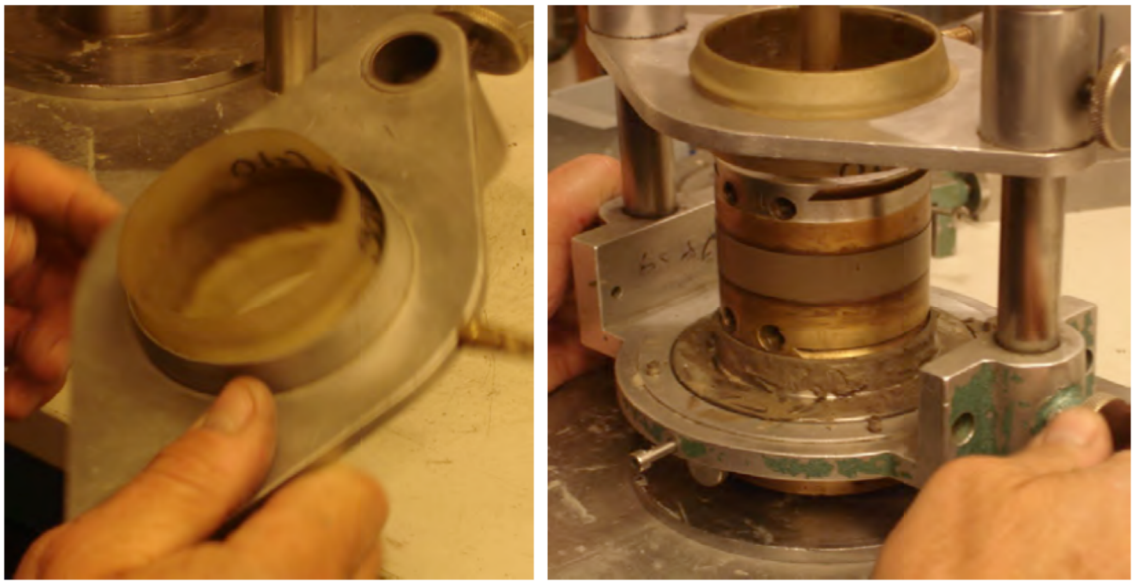


Figure 2.1.SGI Simple Shear Device 1936 (Kjellam, 1951).



1 - Sample, 2 - Reinforced rubber membrane, 3 - Wheels for applying dead load (contr. Stress), 4 - Load gauge for vertical load, 5 - Ball bushing, 6 - Dial gauges for measurement of vertical deformation, 7 - Sliding box, 8 - Dial gauge for measurement of horizontal deformation, 9 - Ball bushing, 10 - Load gauge for horizontal force, 11 - Gear box, 12 - Exchangeable servogear motor, 13 - Lever arm, 14 – Weights, 15/16 - Clamping and adjusting mechanism used for constant-volume tests

Figure 2.2. General principal of direct simple shear apparatus (NGI 1965).



(a) (b)

Figure 2.3.NGI DSS Membrane stretcher (a) and NGI DSS Set-up (b).

An example of one of these newer automated direct simple shear devices is a system created by the GEOCOMP Corporation called the 'Universal Shear Device', shown in Figure 2.4. This device is able to run monotonic and cyclic DSS tests under undrained conditions. The automated system dramatically reduces the labor involved in testing as the consolidation steps and shearing phases are pre-set before the test is started. The breakthrough of this device comes from using PID adaptive control technology to apply vertical and horizontal forces to the test specimen. The adoptive control permits rapid and precise control to produce the following operation :

- Application of constant vertical stress during consolidation;
- Maintenance of undrained conditions during shear by automatically adjustingthe vertical stress to maintain constant specimen height;
- Application of a constant horizontal displacement rate during shear;
- Automatic acquisition of load, displacement, and pore pressure data.

With this system the steps to measure shear stiffness for a stability analysis are reduced to :

- Prepare the sample to standard shape and size;
- Mount the soil sample into membrane (surrounded by stack rings);
- Define the vertical stress for consolidation and shearing rate for shearing phase;
- Run the test (after calibration the LVDT);

- Monitor progress of consolidation and shearing phases ;
- Dismount the sample and put it in oven-dry (to find moisture content);
- Prepare test report(Marr, 2003).

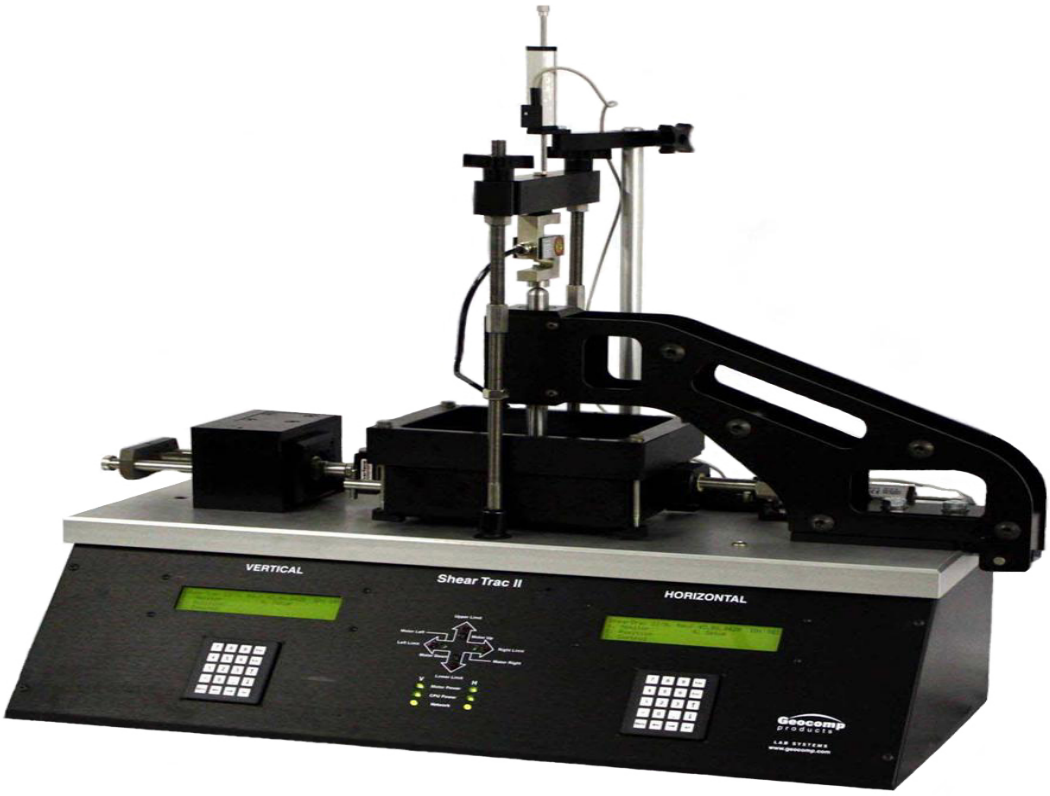


Figure 2.4.GEOCOMP direct simple shear test device.

2.2. Summary of ASTM Testing Requirements

According to ASTM D6528 the standard method for Consolidated Undrained Direct Simple Shear Testing of Cohesive Soils, Figure 2.5 provides a diagram outlining specimen set-up, involves the following:

- A specimen of cohesive soil is constrained axially between two parallel, rigid platens and laterally, such that the cross sectional area remains constant.
- The specimen is loaded axially and allowed to consolidate one dimensionally. Each normal load increment is maintained until excess pore water pressures are essentially dissipated as interpreted from interpretation of the axial displacement rate. The maximum normal load is maintained until completion of one cycle of

secondary compression or one day longer than the end of excess pore water pressure dissipation.

- The specimen is sheared by displacing one platen tangentially relative to the other at a constant rate of displacement and measuring the resulting shear force. The platens are constrained against rotation and axial movement throughout shear.
- The specimen volume is held constant during shear to simulate undrained conditions. Constant volume is achieved by changing the normal load applied to the specimen to maintain constant specimen height. Since the pore pressure is zero through shear, the change in normal stress is equal to the change in effective stress and assumed to be equal to the change in pore water pressure that would occur in a sealed specimen confined by a constant total stress.

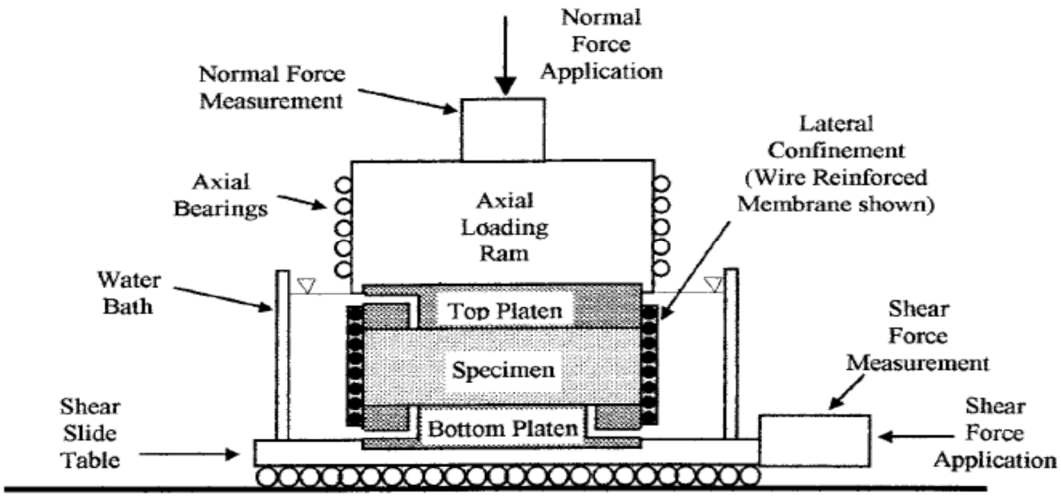


Figure 2.5.Schematic Diagram of Essential Direct Simple Shear Components(ASTM D6528).

2.3.Constant Volume / Constant Load Tests

Two main procedures are in use for the shear phase of direct simple shear tests: maintaining a constant vertical load during shearing or maintaining the volume of the soil specimen constant by keeping the height of the sample constant. The former is considered to yield drained shear stiffness parameters; the latter undrained shear stiffness parameters. For granular soils (sand), Direct Simple Shear tests are usually performed drained with a

constant load since the drained parameters are most likely to be investigated. For soft soils (clay, peat), the parameters of interest are more likely to be investigated in undrained conditions. In most of the simple shear apparatus, it is not possible to perform truly undrained tests since no back pressure can be applied with mean of cell pressure around the sample. So, the undrained simple shear response is normally investigated by performing drained tests at constant volume. Bjerrum and Landva (1966) proposed this equivalence between the two tests and furthermore, stated that the change in vertical stress observed in a constant volume test is similar to the change in pore pressure that would have occurred in a constant load undrained test.

Dyvik *et al*., (1987) performed tests to validate the ”constant volume” hypothesis. They designed a chamber for the NGI Direct Simple Shear device that provides the capability of performing truly undrained tests with pore pressure measurements inside the soil specimen. The authors compared truly undrained tests and constant volume drained test results on normally consolidated clay and obtained very similar results in both case. These conclusions only apply to normally consolidated saturated clay for shear strain lower than 10%. Unfortunately, it was not investigated for other materials. It needs not be correct for unsaturated soils. Budhu and Britto (1987) performed a finite element modelling of the evolution of pore pressure in the core of the NGI specimen. Using Speswhite Kaolin properties and the modified Cam Clay model, they obtained results in accordance with Bjerrum’s predictions for the same range of shear strain.

2.4.Wire-Reinforced and Stacked Rings Membrane

DSS testing in its current form is credited to Krey, Terzaghi, and Casagrande (Young & Townsend, 1981). The current method can be performed using circular or square sample and consists of a normal loading phase and a shear phase. The sample is confined on all sides, loaded with a normal force, and shearedwhile maintaining a constant sample volume. ASTM Standard D6528 − 07was published in 2000, allowing use of both stacked metal rings and the wire reinforced membrane as confinement methods. The two primary methods of circular confinement are:

- Metal rings stacked on top of each other along the entire specimen height(Figure 2.6a).
- A wire-reinforced rubber membrane constructed at the Norwegian Geotechnical Institute (NGI) (Figure 2.6b).

The Kjellman's apparatus has been improved then by Landva at the Norwegian Geotechnical Institute (NGI) (Bjerrum and Landva, 1966). The major new feature of this device was the use of a reinforced membrane to surround the sample laterally and to enforce constant area. The reinforcement consists of a spiral winding of wire having a diameter of 0.15mm and being wound at 25 turns per cm. This reinforced membrane is applied on the sample with vacuum and fit perfectly to the lateral boundaries. The reinforced membrane is supposed to be stiff enough to ensure one dimensional consolidation of the soil specimen and to have the capacity to conserve a constant volume during shearing. The NGI device accommodates samples of h=10mm and D=80mm.

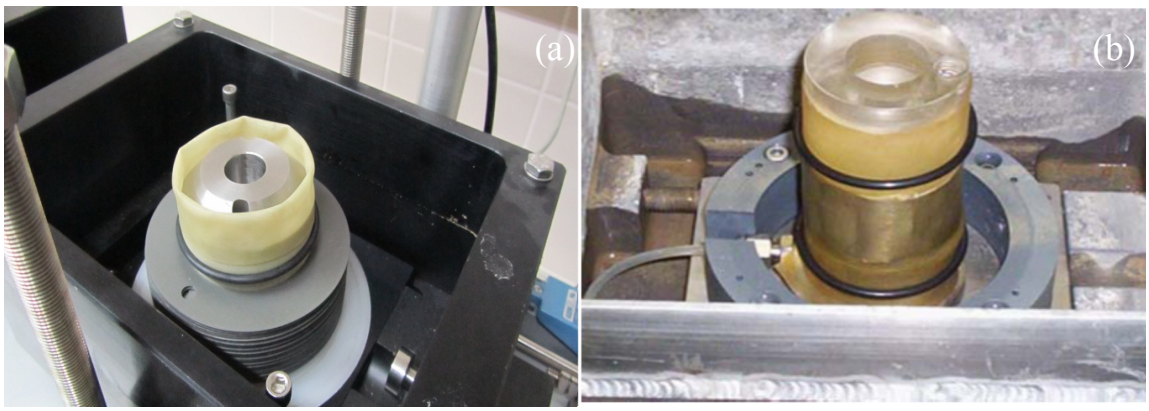


Figure 2.6. Samples prepared for DSS testing using (a) Stacked rings and (b) Wire-reinforced.

Although stacked rings were developed over 50 years ago, wire reinforced membranes have been used almost exclusively in practice. Over the past 10 years automated testing systems such as the Geocomp Sheartrac-II have become readily available in the United States. These systems are tailor-made for DSS testing. Most of the manufacturers of these systems sell stacked rings as DSS test confinement types. Gecomp, Corp., GeoTac, and GDS Instruments are examples of companies selling stacked rings with automated shear systems. This has caused a significant increase in the popularity of stacked rings in the US. They have become the dominant confiningsystem.

Use of the two confining systems may produce slightly different results in terms of measured stiffness, strength, and stress-strain behavior. This may be due to differing rigidity of the two systems, or some other mechanism (Baxter *et al.,* 2010). Below is a comparison the results of using stacked rings and wire reinforced membranes as a confining system for direct simple shear tests:

2.4.1. Comparison of Consolidation Data

The effects of the two confining methods on the vertical consolidation behavior were evaluated indirectly by comparing the vertical strains required to reach the final consolidation stress. A summary of the total vertical strains at the end of consolidation are summarized by soil type and confinement method in Table 2.1. For both soil types, the samples confined in the wire-reinforced membranes had higher strains during consolidation relative to the rings. This could be interpreted in one of two ways: a) the wide flanges of the rings may provide higher lateral stiffness, or b) the rings may be resisting the vertical load thereby reducing stresses in the soil (Baxter *et al.,* 2010).

Table 2.1. Summary of maximum vertical strain during consolidation (Baxter*et al.*, 2010).

Soil Type	Vertical Effective Stress (Kpa)	Vertical Strain to Consolidation Stress (%)	
		Ring	Wire
Gulf of Mexico Clay	50	7.3	8.9
	100	14.1	14.7
	200	18.2	24.0
Organic silt	50	16.4	17.7
	100	18.5	27.3

If the rings provide increased lateral stiffness, than the zero lateral strain assumption is even more valid. However, it is unclear if lateral stiffness is the true cause of the observed differences in vertical strains. Table 2.1 also indicates that the vertical strains were higher in the silt samples than in the clay samples. The higher strains are the result of preparing the silt from a slurry rather than the more consolidated nature of the intact clay specimens.

2.4.2. Comparison of Shear Data

The corrected stress-strain and excess pore pressure-strain relationships are shown for both soil types and confining methods in Figure 2.7. The stress paths for the same tests are also shown in Figure 2.8. As shown in these figures, there is good agreement in the shear stress and excess pore pressure behavior for both confinement methods.

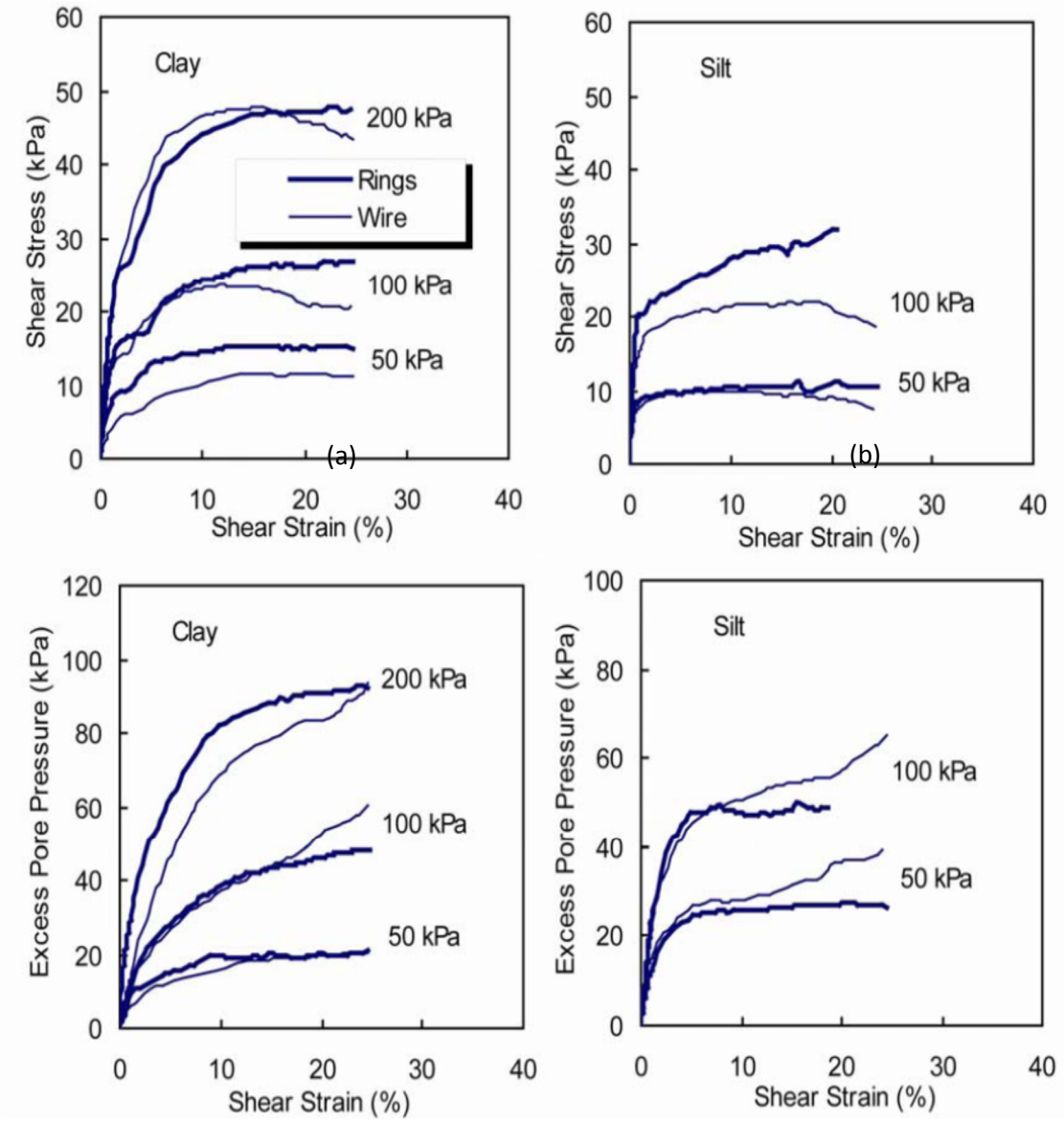


Figure 2.7. Shear stress and excess pore pressure verses strain from DSS test for a) Gulf of Mexico Clay, and b) Organic Silt (Baxter*et al.,* 2010).

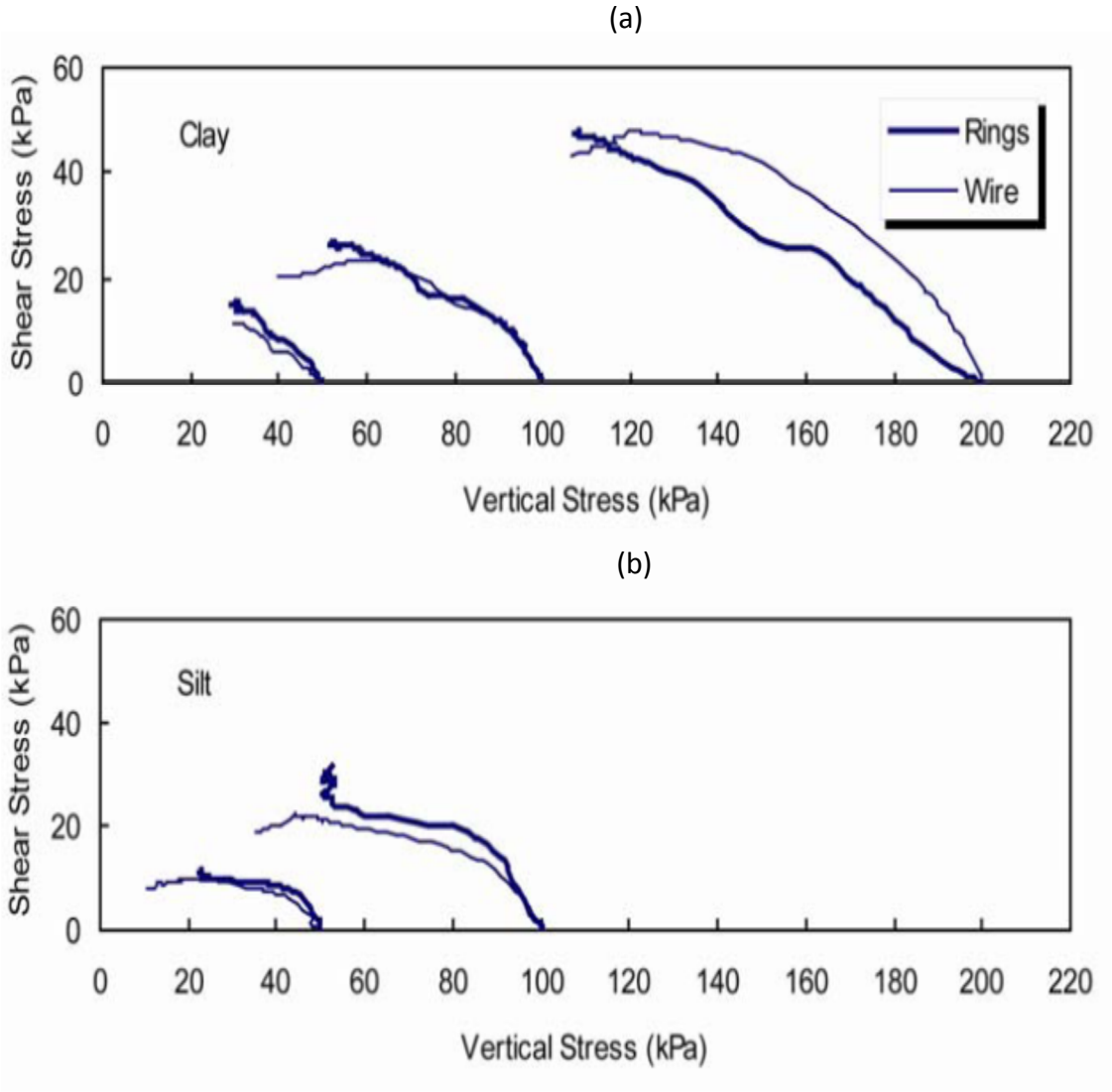


Figure 2.8.Stress paths for a) Gulf of Mexico Clay and b) Organic Silt.(Baxter*et al.,* 2010).

2.5.Typical Results can be Obtained in DSS Test

In a first phase, a normal force is applied at the top of the box and in a second phase, a shearing force is applied at the top (or bottom) of the split box, causing the soil to shear along the plane between the two parts of the box. The shear and vertical stresses are measured as functions of the horizontal displacement. A peak in the stress-strain curves is often observed, as shown by point (F), Figure 2.9. The evolution of the vertical displacement in function of the horizontal deformation provides information concerning the contractive or dilative behavior of the soil (Terzaghi, Peck and Mesri 1996).

The major advantages of this device are to impose a constant area of potential sliding (compared to the direct shear box) and also to obtain a better homogeneity of the stress distribution. In a comparable way to the direct shear box, the direction of the major principal stress σ_1 is verticalduring consolidation (the minor being horizontal) and then it rotates during shearing. The amplitude and direction of principal stresses remain difficult to trace during shearing in such a device.

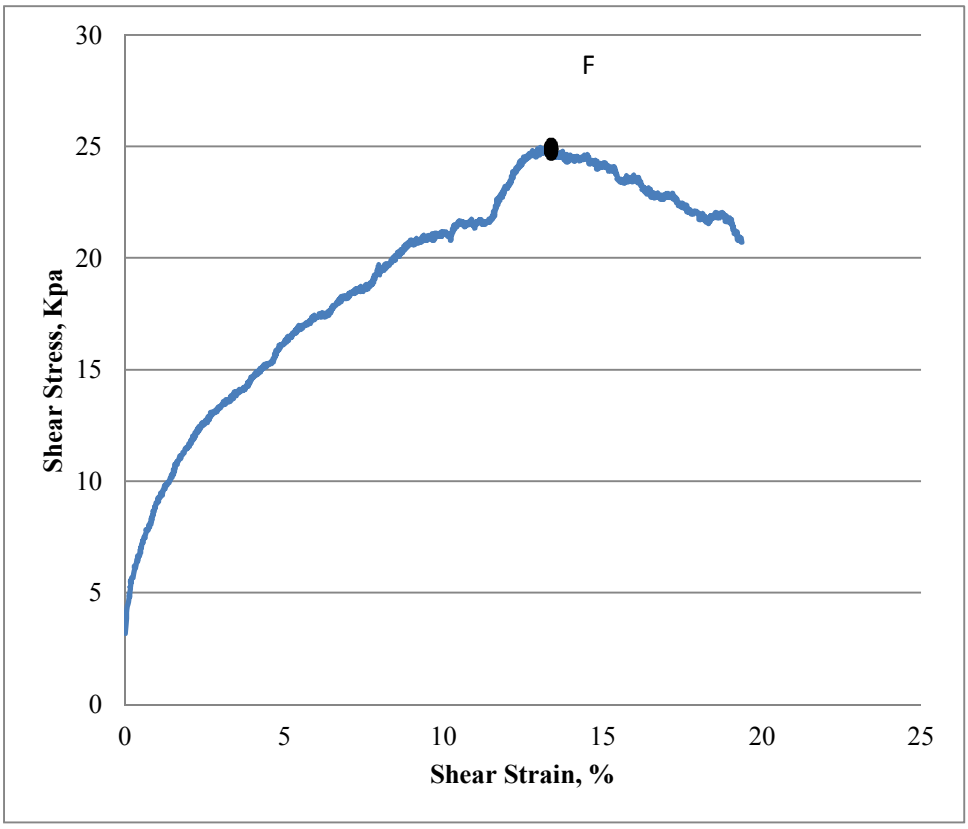


Figure 2.9. Shear Stress-Strain behavior of Silivri sand. Point (F) is shear stress peak.

The shear strain (γ) in simple shear is defined as the horizontal displacement divided by the height of the specimen. The typical results obtained from direct simple shear tests are the shear stress, the change in vertical stress (or the change in vertical displacement) as functions of the shear strain. The shear modulus can be deduced from the slope of the shear stress-shear strain curve.

The typical results mentioned above can be obtained from other shear devices but are not likely to provide similar results. (Saada *et al.,*1983) compared results from various shear tests such as triaxial or hollow cylinder. For both clay and sand, shear strength and shear modulus are among the lowest compared to the results from others apparatuses. Bjerrum and Landva (1966) also observed the same trend. It can be explained by the difference in the stress conditions in the simple shear and in other devices. For instance, in simple shear tests the intermediate principal stress (σ_2) is neither independent of nor it is equal to either the major or minor principal stress (contrary to triaxial test which impose σ_1 and $\sigma_2=\sigma_3$). Furthermore, the simple shear conditions allow the rotation of principal stresses during the test. In this way stress state of the sample during a DSS test is closer to the in situ conditions compared to the triaxial device which is only able to exchange major and minor principal stress.

2.5.1. Correction Factors

Baxter *et al*. (2010) evaluated running some tests with water instead of soil. This was done to calculate correction factors for both wire-reinforced membrane and Teflon rings confinement systems. The assumption made was that the water has no shear strength, therefore any measurable shear strength is caused by the confinement system and should be subtracted from the data collected when testing soil specimens.

The shear resistance attributed to each confinement system was investigated. This was done by performing tests on water instead of soil and directly measuring the shear stress resisted by the rings or wire reinforced membrane. For the ring tests, the water pressure was increased to evaluate a possible stress dependence on the shear resistance. The results of the water tests are shown in Figure 2.10 for both the rings and wire membrane. Below strains of about 15%, the resistance is similar and negligible in both methods, increasing monotonically up to about 1 Kpa. In the ring tests, the effect of increasing the internal pressure had no significant effect on the resistance and the trend of the data was repeatable.

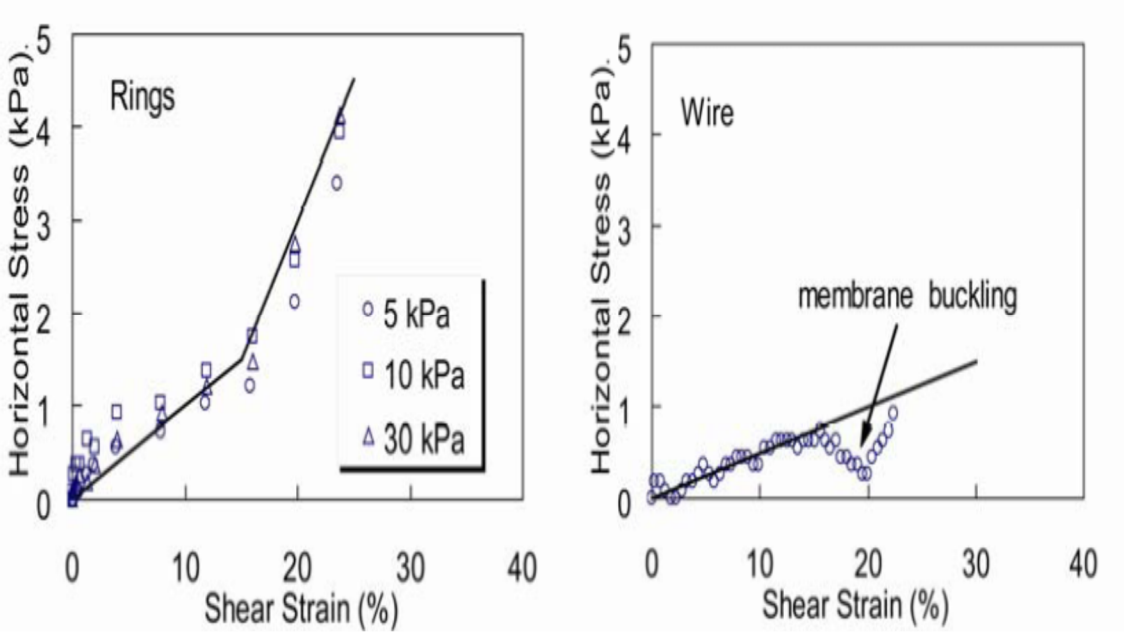


Figure 2.10.Stress-strain relationship for samples of water used to correct the DSS test result for the effect of the Teflon rings and the WRM (Baxter *et al.,* 2010).

Above about 15% strain, the resistance increases more dramatically in the rings but remains approximately linear. Therefore, a bi-linear function was used to represent the shear resistance of the rings up to 25% strain. Buckling of the wire-reinforced membrane (WRM) was observed at about 15% strain and thus the resistance was extrapolated up to 25% strain using the early portion of the curve. Using the linear resistance functions shown in Figure 2.11, all soil test data were corrected to remove the effects of the confining system as a function of shear strain.

Similarly to Baxter's correction factors, researchers at MIT performed testing on WRM's and calculated a correction factor that is shown in Figure 2.12. They also concluded the correction factors for the WRM's were nearly negligible, and stated the correction was ~1 kPa for the range of normal stresses they were interested in. At normal loads higher than 300 Kpa the O-rings experienced slipping, not allowing for good data (Ladd & Degroot, 2003).

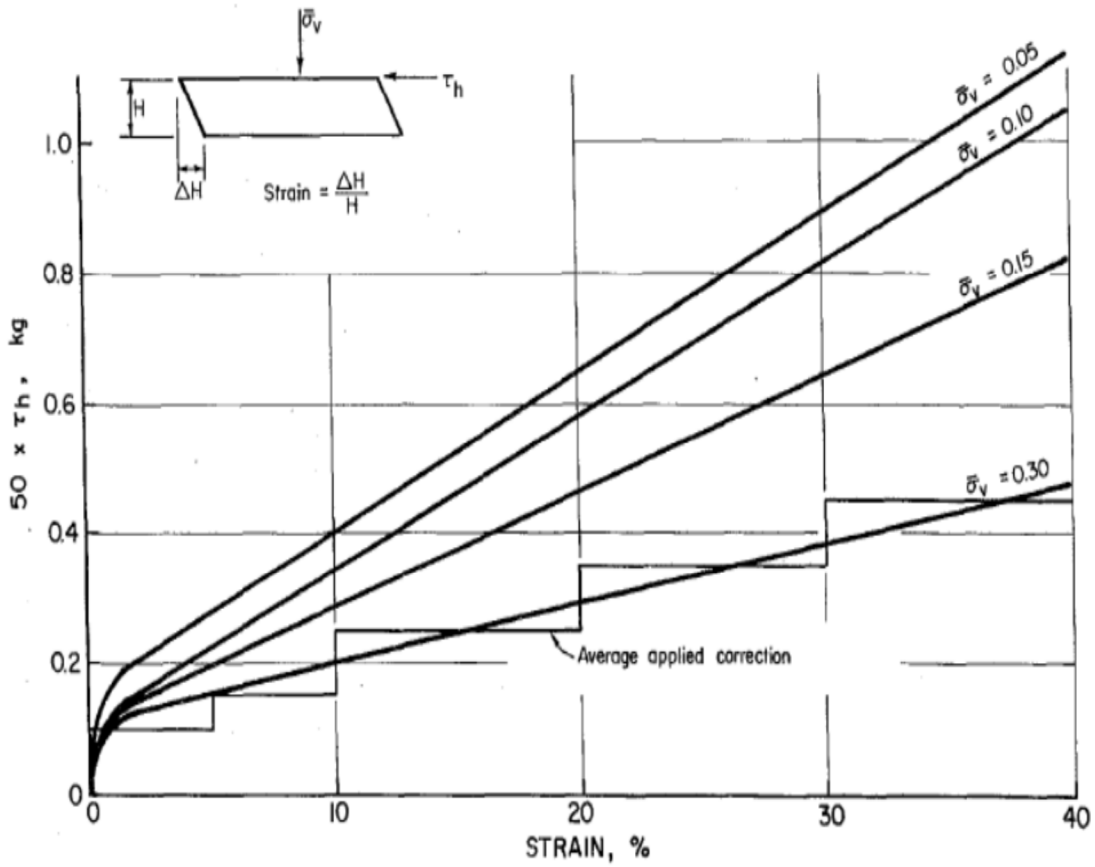


Figure 2.11.Calibration of membrane resistance (Ladd & Degroot, 2003).

The Norwegian Geotechnical Institute (NGI) performed a correction factor analysis on their WRM. Their calculation takes both membrane thickness and size in to account. This is shown in Table 2.2 and Figure 2.12.

Table 2.2.NGI's Wire Reinforced Membrane Correction Factor Table for Different Membrane thicknesses (Brylawski & Berre, 1992; rev 1997).

C (Membrane type)	F(Membrane correction revising factor), t (membrane thickness)
1	F=t/0.6
1.25	F=(t+0.0306)/0.6
1.5	F=(t+0.0696)/0.6

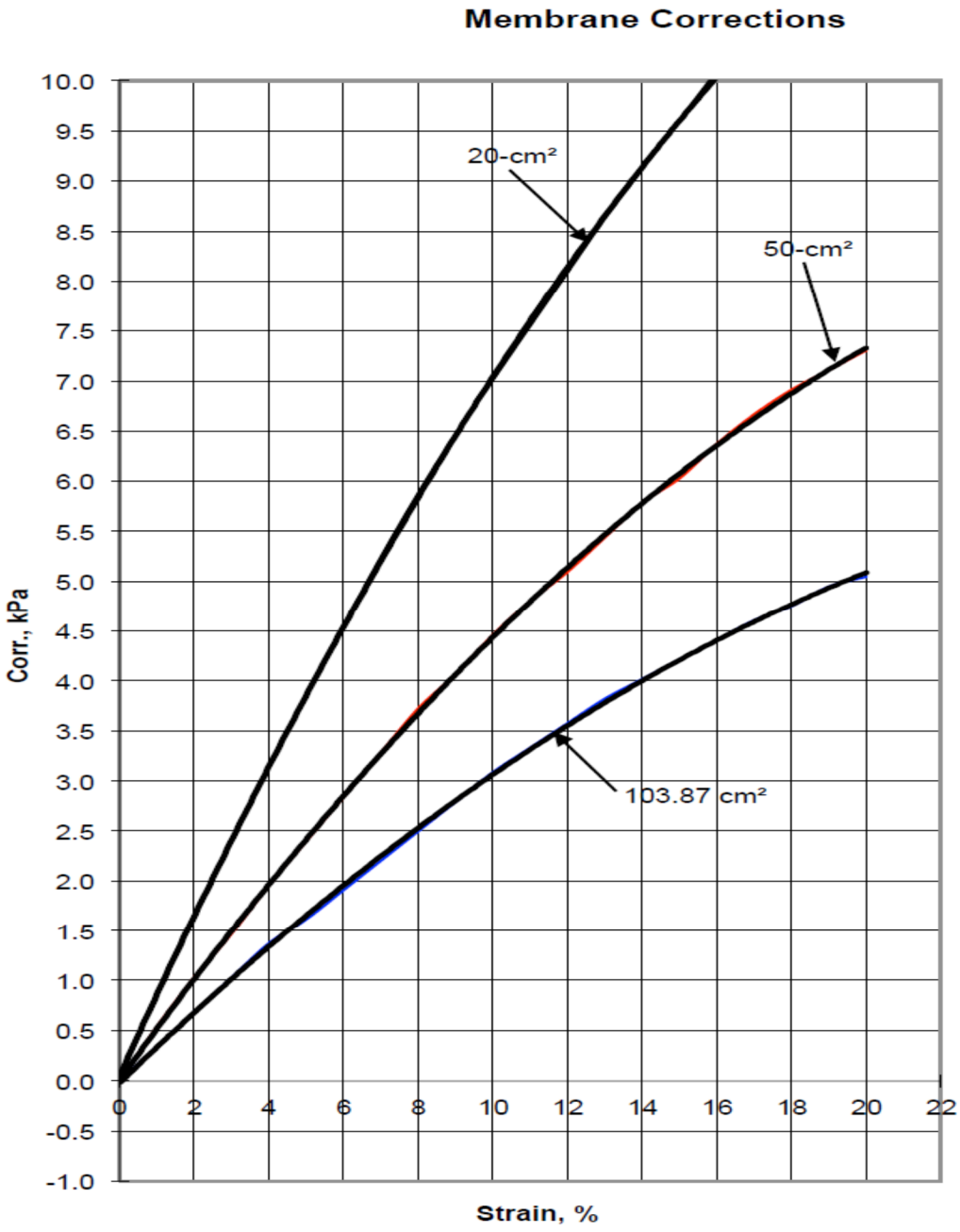


Figure 2.12.NGI's Wire Reinforced Membrane chart by membrane size (Brylawski, 1992).

Using Figure 2.12, Table 2.3, and the following calculations taken from Ed Brylawski's report (1997) NGI's Wire-Reinforced-Membrane correction factors can be determined (Brylawski & Berre, 1992; rev 1997).An example of correction factor calculation is on Table 2.3 (Seth McGuire, 2011):

Table 2.3. Summary of steps for correction factor determination(Seth McGuire, 2011).

Steps	Description	Quantity
1	Membrane type, Table 2.2	C=1
2	Amount of consolidation	$\varepsilon_v = 10\ \%$
3	Area of sample	A=50 cm^2
4	Membrane correction forA=50 cm^2, Figure 2.12	$mem_{corr} =$ 4.45 Kpa
5	Membrane thickness	t=0.65mm
6	Revising factor, Table 2.2	$f = \frac{0.65}{0.6} = 1.083$
7	Revised membrane correction	$mem^*_{corr} = 4.45 \times 1.083 = 4.82\ Kpa$
8	Actual measured vertical stress	$\sigma_{actual} = 50\ Kpa$
9	Vertical consolidation stress	$\sigma_v = \sigma_{actual} - mem^*_{corr} = 50 - 4.82 = 45.18\ Kpa$
10	Membrane Correction as a percentage of vertical stress	$\frac{mem^*_{corr}}{\sigma_{actual}} = \frac{4.82}{50} = 9.6\ \%$

It's clear there are non-uniformities in specimens when performing DSS tests using either Teflon rings or WRM. However, these non-uniformities are slight and do not affect the center of the specimen. Additionally, the DSS test provides a relatively average shear stiffness result when compared to other methods. From the limited comparisons of Teflon rings vs. WRM in the literature, it's apparent that they should produce similar results, with somewhat different strain softening paths and potential variability at higher strains. These variabilities may require the recalculation of correction.

2.5.2. Specimen Size Effect

Vucetic and Lacasse (1982) conducted tests on a medium stiff laminated clay with three different H/D ratio specimens (0.32; 0.20 and 0.14). The tests were carried out at two over-consolidation ratios. The results obtained, determined a very close results for the three different H/D ratios and the authors concluded that the H/D ratio has no significant influence on the strength and deformation characteristics of this soil. These results should be considered with caution regarding the specific laminated structure of the material tested.

2.5.3. Stress Rotation

A key feature of simple shear loading is that the principal stress directions are not fixed but rotate during shearing as depicted in Figure 2.13. According to Roscoe KH (1970), Simple shear devices, where the sample is constrained from deforming laterally, have only two degrees of freedom corresponding to the shear and vertical deformations. Thus, the principal stress rotation cannot be directly controlled and only limited rotation can be achieved.

Marte Gutierrez(2009), concluded thatexperimental determination of the degree of principal stress rotation requires measurement of the variation of the lateral confining stress during shearing. However, this measurement is difficult to perform and is not usually carried out in routine DSS tests.

Due to anisotropy, the response of sands during loading depends on the principal direction. Experimental data obtained by Arthur JRF (1980), shows that the shear strength and deformation of sands are dependent on the loading direction. Due to anisotropy, soils are expected to deform during principal stress rotation even when the shear stress level or the mobilized friction angle is kept constant.

Another important effect of principal stress rotation is the non-coincidence or non-coaxiality of the principal stress and principal plastic strain increment directions. Extensive experimental data from Hollow Cylindrical Testing have shown that the principal stress direction lags behind the principal plastic strain increment direction when the principal stresses are rotated, (Gutierrez M, 2000).

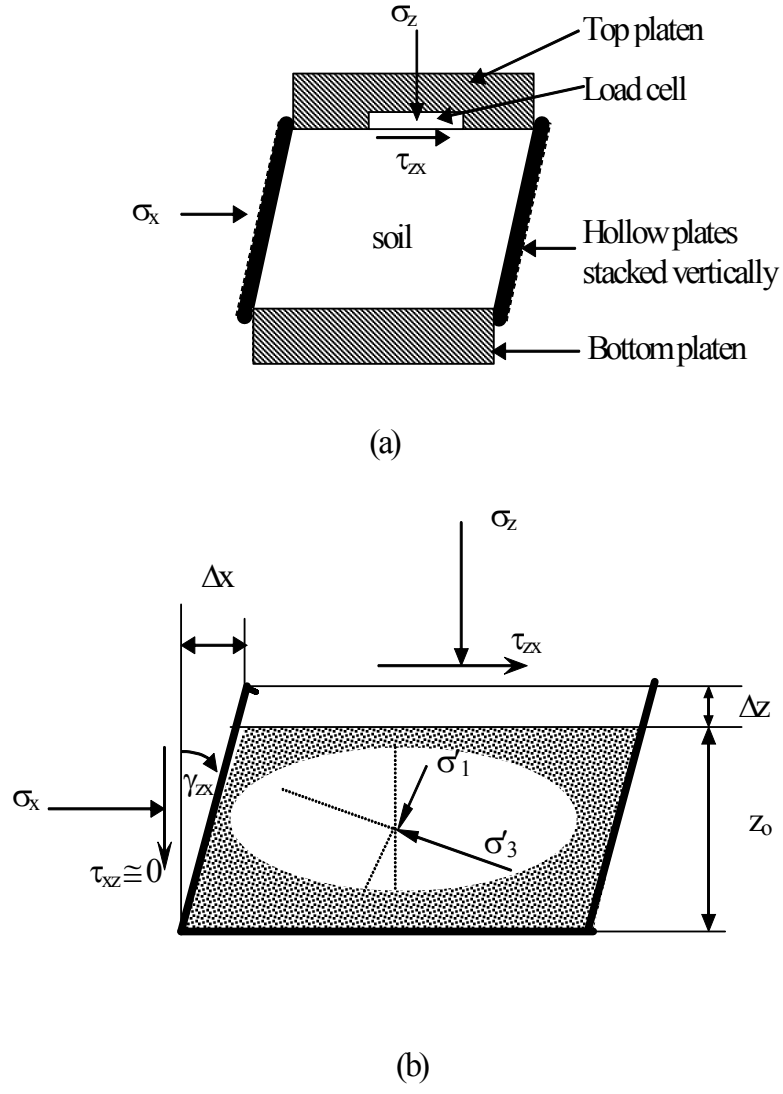


Figure 2.13 Stress rotation representation in DSS test, a) Test schematic view and b) Stress rotation interpretation (Roscoe KH 1970).

2.5.4. Shear Stiffness Determination

The term 'Simple Shear' is in reference to a state of strain. According to Degroot (1991) it is "a plane strain state where under constant volume condition an element

deforms only in one direction. Through deformation the height remains constant, requiring the sides to elongate." The term 'Pure Shear' is said to occur when an element is under two equal and opposite principle stresses (DeGroot *et al.,* 1991).

Figure 2.14 shows the normal and shear stresses acting on the vertical and horizontal planes during a direct simple shear test.

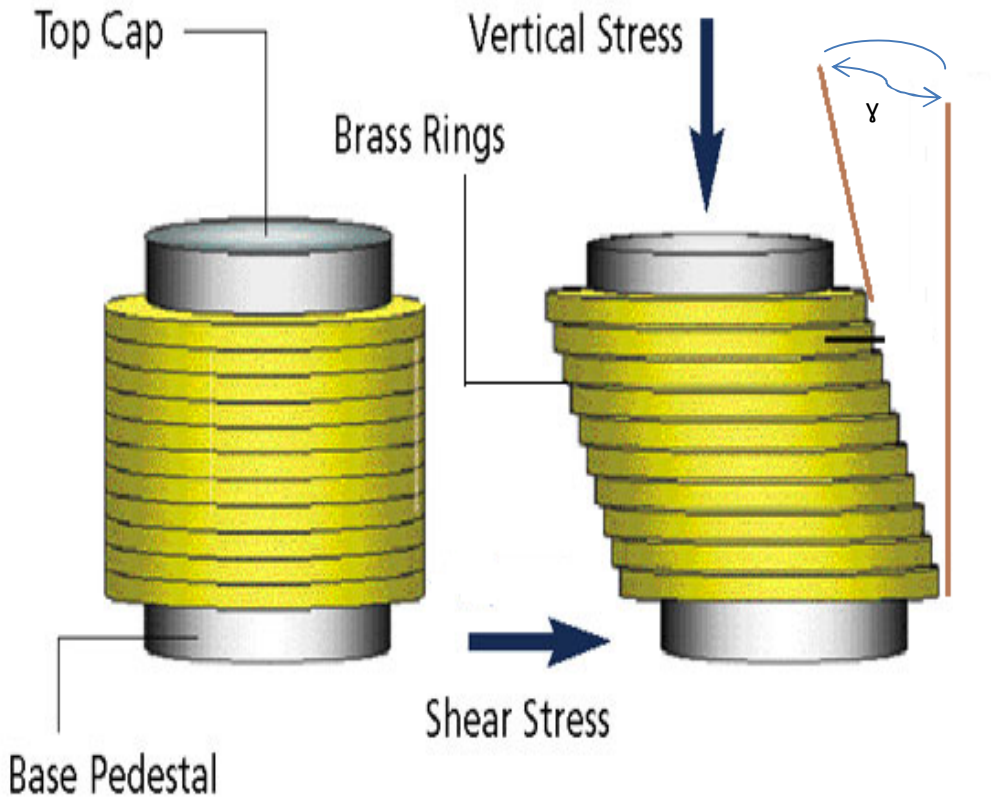


Figure 2.14.Applied Stress during DSS Testing (GEOCOMP DSS test manual 2012).

The DSS test has been found to be a good overall representation of shear strength along a roughly horizontal failure plane, which is applicable to many loading conditions in situ (e.g. slope stability, bearing capacity, etc.). In addition, values of undrained shear strength from DSS tests are between values measured using triaxial compression and extension tests (Ladd and Degroot, 2003), as shown in Figure 2.15.

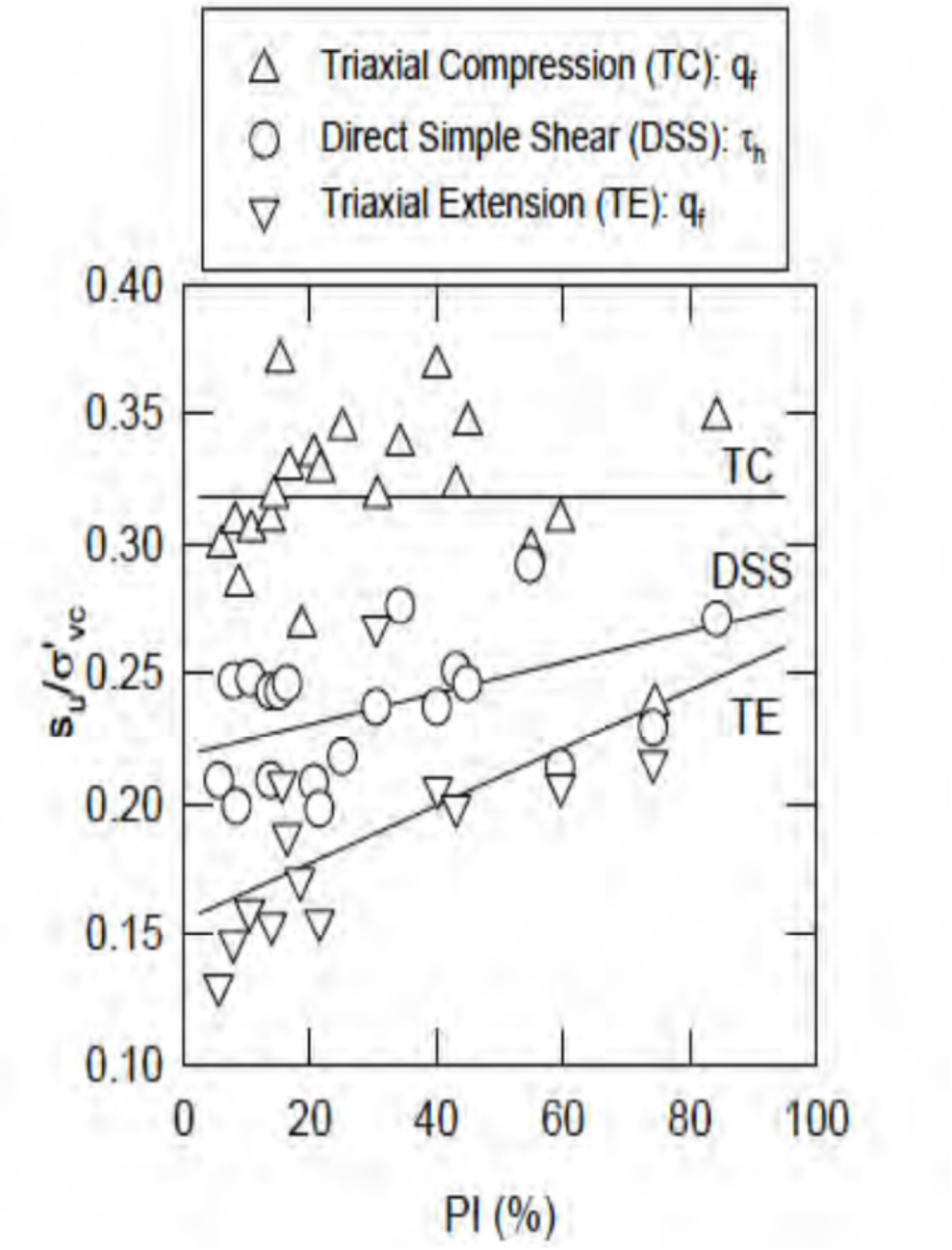


Figure 2.15.Normalized undrained shear strength for TC, DSS and TE test results as a function of plasticity index (Ladd and Degroot, 2003).

Table 2.4 (Marr, 2003) also shows values of undrained shear strength normalized by the vertical effective consolidation stress (S_u/σ'_{Vc}) for different modes of loading (compression, extension, simple shear). It reinforces the idea that DSS tests provides good average values of shear strength.

Table 2.4.Summary of shear strength results for different modes of loading (Marr, 2003).

Boston Blue Clay	
Stress Condition	**Value**
Triaxial compression	0.32
Triaxial extension	0.16
Direct simple shear	0.22
Average of compression and extension	0.24
Average of compression and extension and DSS	0.23

2.5.5. Pore Pressure Determination

The DSS test is in principle comparable to a consolidated undrained triaxial test, in that there is a consolidation stage (under 1-D conditions) followed by undrained shear through application of shear stress in the horizontal direction. However, DSS tests are not typically back pressure saturated and pore pressures are not measured.

Excess pore pressure during undrained shear is inferred from the change in total stress required to maintain constant volume (i.e. height) conditions. For example, if the total vertical stress decreases during shear to maintain constant volume, then that change in vertical stress is assumed to be equal to positive pore pressure development within the sample. This was determined to be true through testing by (Dyvik *et al*., 1988) on saturated cohesive soils. (Dyvik *et al.,*1988) ran consolidated undrained DSS tests and constant volume DSS tests. In the cases of the constant volume tests pore pressure assumed to be equal to the change in vertical applied load, whereas the undrained tests measured pore pressure with a pore pressure transducer. Whether the pore pressure was measured through the use of a pore pressure transducer or the change in vertical applied load the results were in close agreement as shown in Figure 2.16.

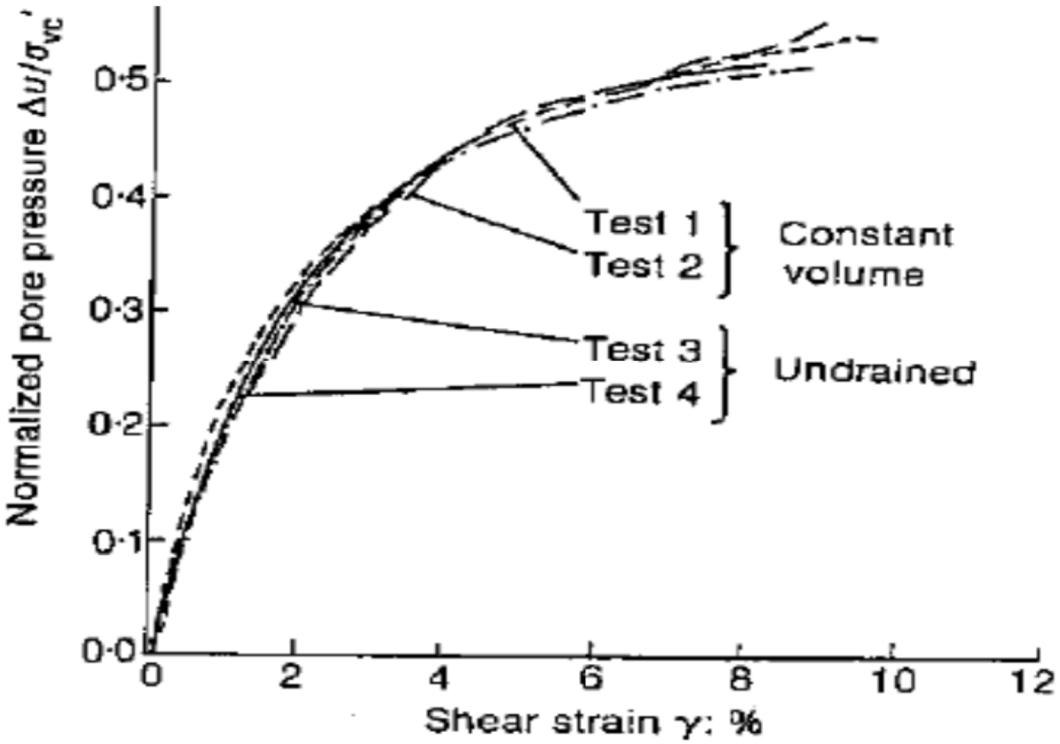


Figure 2.16. Comparison of pore pressure from constant volume and undrained DSS test results (Dyvik *et al*., 1988).

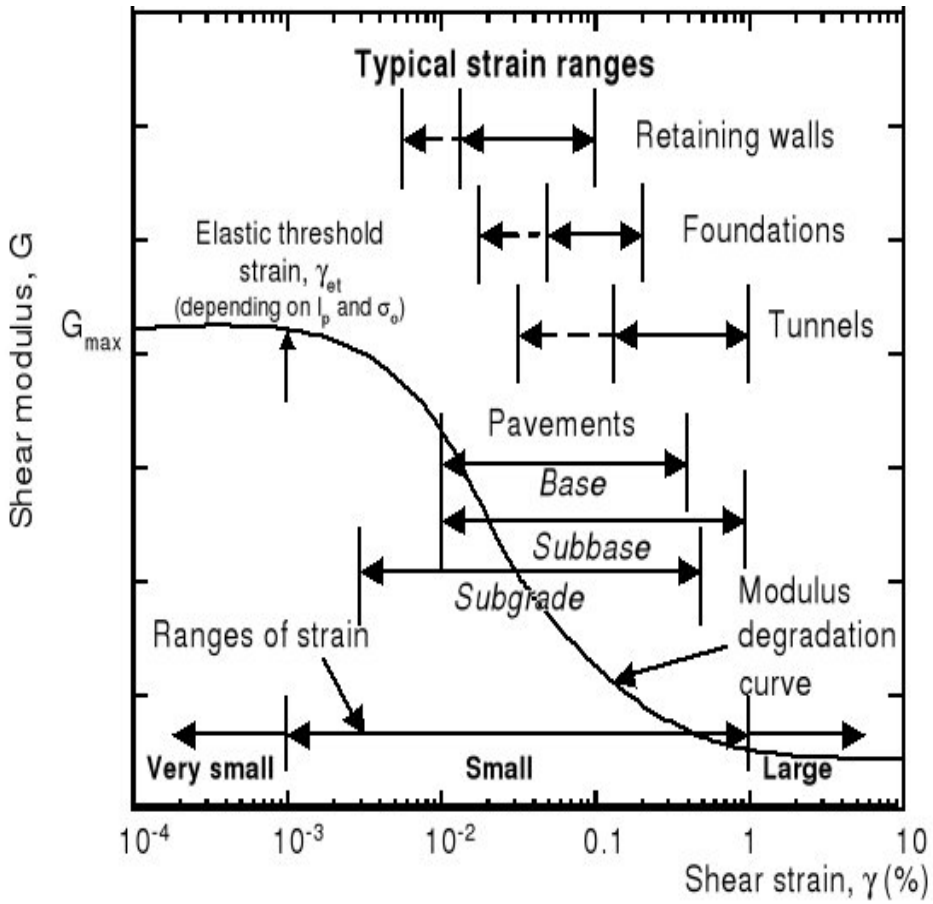
2.6. Shear Modulus of Soil

One of the important engineering properties of soils commonly used in design and analysisis the stiffness. Stiffness primarily describes the deformation characteristics of a soilthat is used to support engineering structures. Understanding the stiffness behavior of soil is therefore essential for improving design and analysis of structural behavior under various loading and environmental conditions.

Over the past 20 years,the importance of stiffness measurementsfrom small to large strains has gained major importance, in both static and dynamic analyses. The resonant column and torsional shear devices have been widely used for many years to study cyclic and dynamic properties of soils at strains ranging from 10^{-4} to 0.1% (Drnevich 1985, Saada 1988).

Based on the typical variation of shear modulus (G) with shear strain (ɣ) levels shown in Figure 2.17 (after Atkinson and Sallförs 1991, Mair 1993, Ishihara 1996,

Sawangsuriya *et al.,* 2005), three strain ranges are defined: (i) very small strain, (ii) small strain, and (iii) large strain.



Phenomena		Wave propagation, vibration	Crack, differential settlement	Slide, compaction, liquefaction
Soil behavior		Elastic	Elastic-plastic	Failure
Soil properties		Shear modulus, Poisson's ratio, damping		Angle of internal friction, cohesion
Effect of load repetition		←	→	
Effect of loading frequency		←	→	
In situ measure-ment	Seismic wave method	←		
	In situ vibration test		→	
	Repeated loading test		→	
Laboratory measure-ment	Wave propagation test	←		
	Resonant column test		→	
	Repeated loading test		→	

Figure 2.17. Variation in shear modulus with different shear strain levels for different geoengineering applications, in-situ tests, and laboratory tests (after Atkinson and Sallfors 1991, Mair 1993, Ishihara1996, Sawangsuriya *et al*., 2005).

2.6.1. Low Amplitude Shear Modulus

At small strains, which are typically below 10^{-5} % , the soil behaves linearly with its maximum shear modulus and deformational characteristics of soil are independent of strain amplitude, which is shown as elastic threshold strain (γ_{et}),. This modulus is called maximum shear modulus or low amplitude shear modulus, and denoted by G_{max}. This is a basic parameter in dynamic soil analyses.

The secant shear modulus, at low strain amplitudes, is high but it decreases as the strain amplitude increases with number of cycles. The locus of points corresponding to the tips of the hysteresis loops of various cyclic strain amplitude is called the "back-bone" curve as defined in Figure 2.18. Its slope at the origin corresponding to the cyclic strain amplitude γ_r is termed is maximum shear modulus, G_{max} , thus,

$$G_{max} = \frac{\tau_{max}}{\gamma_r} \qquad (2.1)$$

A number of laboratory studies have been made to establish empirical formulas to predict the low amplitude shear modulus from the void ratio, the effective stress, and other factors such as stress history, age and plasticity. Hardin and Black (1968) suggested the following expression for the small-strain shear modulus, Gmax:

$$G_{max} = \frac{1230 \times (2.97-e)^2 OCR^k}{1+e} (\sigma_0')^{0.5}, \qquad (2.2)$$

where,G_{max} is the small-strain shear modulus in Psi, e is thevoid ratio, OCR is over consolidation ratio, kis function of plasticity index, σ_0' is mean effective stress in Psi and the value of k varies between 0 and 0.5, depending on the plasticity index, PI. Therecommended values of k are given in Table 2.5.

Hardin and Black (1968) suggested a generalized equation to express the low amplitude shear modulus, G_{max}, for normally consolidated Kaolinite as:

$$G_{max} = A.F(e).(\sigma_0')^n, \qquad (2.3)$$

where, A is soil constant that accounts for stiffness, F(e) is a term that accounts for the change in void ratio, σ_0' is the mean effective stresses, and n is exponent for σ_0'. Several different void ratio functions F(e), have been proposed in Table 2.6.

Hardin (1978) modified Equation 2.4 normalizing it by atmospheric pressure (p_a)to make the expression independent of units:

$$G_{max} = A.F(e).P_a^{1-n}.(\sigma_0')^n \qquad (2.4)$$

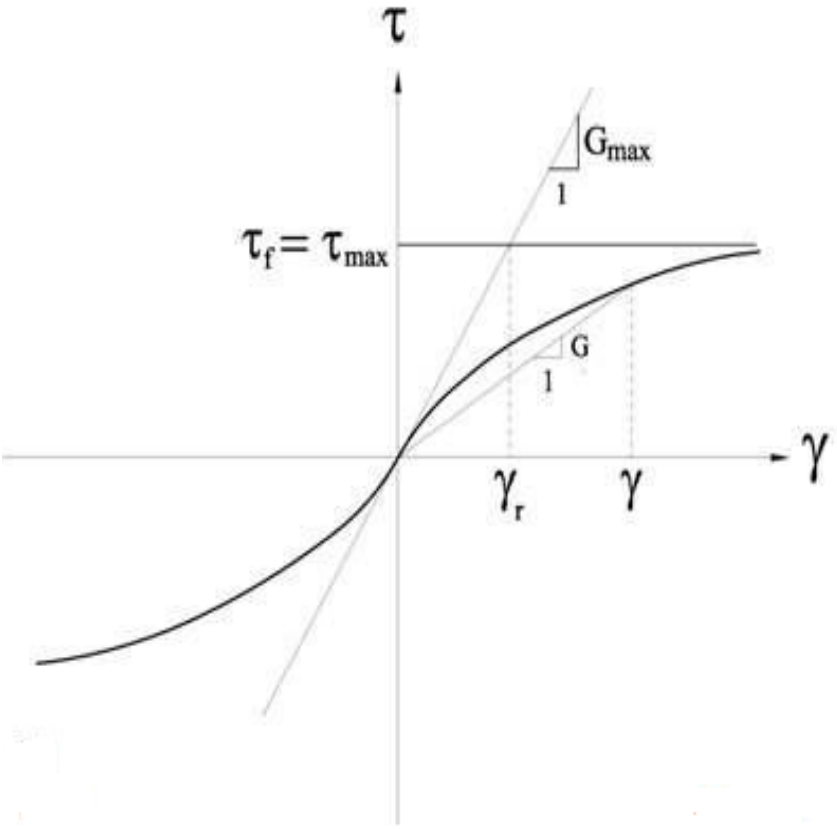


Figure 2.18. Back-bone curve.

Table 2.5.Values o f k in the Factor,OCR^k.

PI	k
0	0.00
20	0.18
40	0.30
60	0.41
80	0.48
≥ 100	0.50

It has been observed that the low-amplitude shear modulus increases with increasing mean effective stress (σ_0'). The effect of(σ_0') is expressed by $(\sigma_0')^n$ as an independent variable as shown in Equation 2.5. Hence the low amplitude shear modulus varies with (σ_0') to the power of n without including the effects of void ratio or aging effects. The plot of G_{max} vs (σ_0') is described by a line on a log-log scale. Yu and Richart (1984) considered stress condition in resonant column test and suggested using following Equation for (σ_0') using cylindrical coordinates:

$$\sigma_0' = \frac{\sigma_t + \sigma_v}{2}, \qquad (2.5)$$

where,$\sigma_t$is tangential stress, and$\sigma_v$is vertical stress.

The low amplitude shear modulus varies with time as well as with void ratio and with effective stress. The increase due to consolidation can be accounted for by thecorresponding decrease in void ratio. A secondary increase in G_{max} with time at aconstant effective stress is an aging effect resulting from strengthening of particlebonding not related to changes in void ratio (Ishihara 1996).

Typical changes in low amplitude shear modulus with time for clay are illustratedin Figure 2.19. The two distinct of modulus-time response are very evident in Figure 2.19a. First, during primary consolidation, values of the shear modulus increase rapidlyand begin to level off. Second, after primary consolidation, values of the modulusincrease linearly with the logarithm of time. Figure 2.19b presents the vertical height change of clay

specimen. Comparing the height change results with the modulus-timecurve, it is evident that the end of the initial phase in the modulus-time response coincided with the end of primary consolidation. The point of transition in the modulustimeresponse curve is defined as the end of primary consolidation (Anderson and Stokoe 1978). The rate of secondary increase in shear modulus or shear wave velocity is a function of logarithm of time and the magnitude of secondary increase was found to varywith soil type. Initially time effect were investigated on artificially prepared specimens of cohesive soils, but later a similar effect was found to exist in undisturbed samples ofcohesive soils and sands (Stokoe and Richart 1973).

Table 2.6.Summarized formulas for void ratio functions and constants in proposed empirical equationson Small Strains Modulus for both sand and clays(Kokusho, 1987).

	Researchers	A	F(e)	n	Soil type	Test type
Sand	Hardin-Richart (1963)	700	$(2.17-e)^2/(1+e)$	0.5	Round grained Ottawa sand	RC
		330	$(2.97-e)^2/(1+e)$	0.5	Angular grained crushed quartz	RC
	Shibata-Soelamo (1975)	4200	$0.67-(1/(1+e))$	0.5	Three kinds of clean sand	Ultra Pulse
	Iwasaki-Tatsuoka *et al.*, (1978)	900	$(2.17-e)^2/(1+e)$	0.4	Eleven kinds of clean sand	RC
	Kokusho (1980)	840	$(2.17-e)^2/(1+e)$	0.5	Toyoura sand	Cyclic Triaxial
	Yu-Richart (1984)	700	$(2.17-e)^2/(1+e)$	0.5	Three kinds of clean sand	RC
Clay	Hardin-Black (1968)	330	$(2.97-e)^2/(1+e)$	0.5	Kaolinite, etc	RC

Table 2.6.Summarized Formulas for Void Ratio Functions (Cont.).

	Marcuson-Wahls (1972)	450	$(2.97-e)^2/(1+e)$	0.5	Kaolinite, Ip = 35	RC
		45	$(4.4-e)^2/(1+e)$	0.5	Bentonite, Ip = 60	RC
	Zen-Umerhara (1978)	200-400	$(2.97-e)^2/(1+e)$	0.5	Remolded clay, I_P = 0 - 50	RC
	Kokusho-Yoshida *et al*., (1982)	14.1	$(7.32-e)^2/(1+e)$	0.6	Undisturbed clay, I_P = 40 — 85	Cyclic Triaxial

Afifi and Richart (1973) proposed the use of a coefficient to describe the long-term effect defined as:

$$I_G = \frac{\Delta G}{log_{10}(\frac{t_2}{t_1})}, \qquad (2.6)$$

where, t_1 and $t_2$are arbitrarily chosen points of time after primary consolidation and ΔGdenotes the increase in shear modulus during the time period t_1 to t_2 .

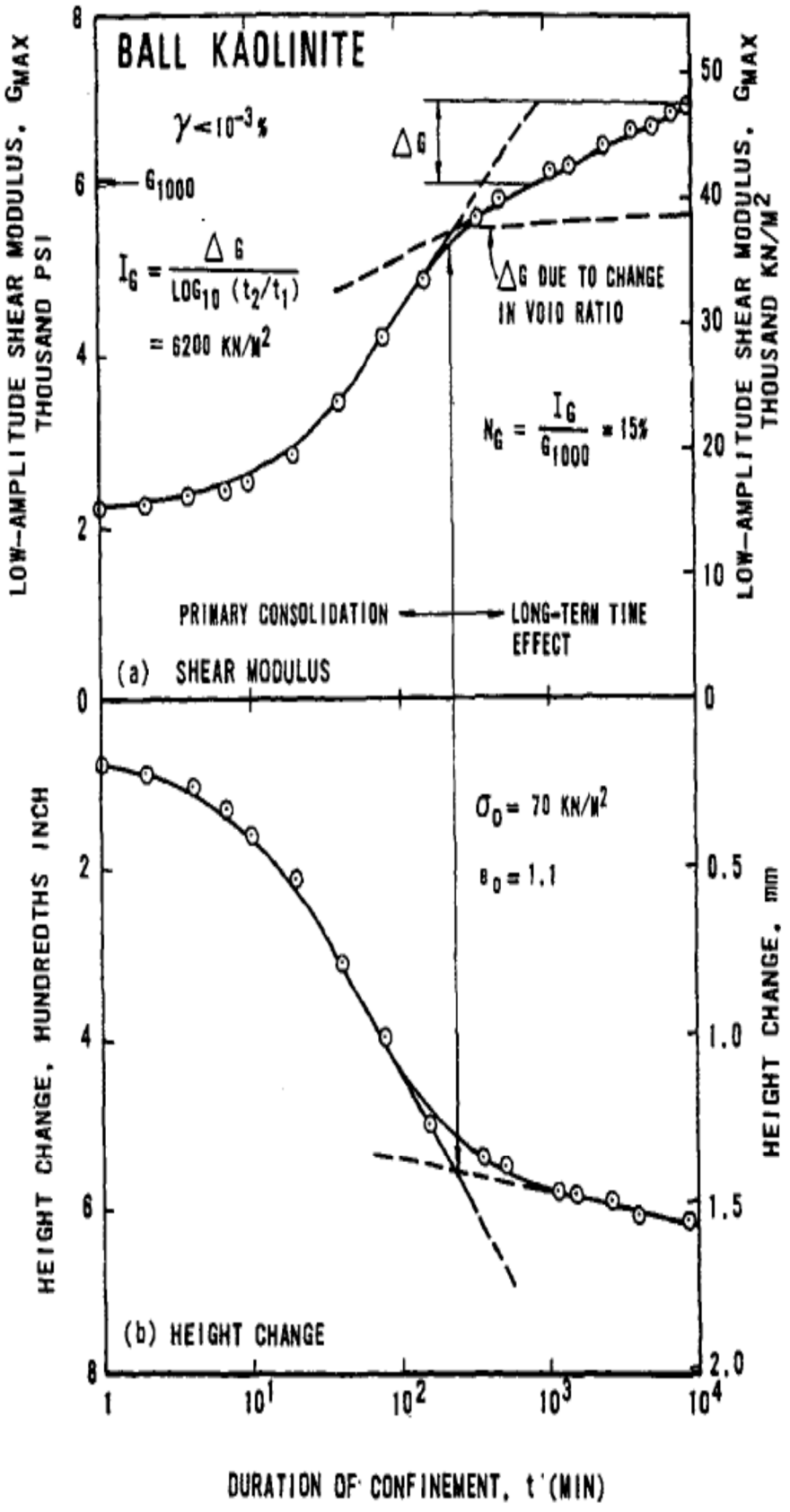


Figure 2.19.Typical modulus and height change with time for clay (Stokoe 1978).

To remove the influence of soil type and confining pressure, Afifi and Richart (1973) also presented the use of a normalized coefficient N_G defined as:

$$N_G = \frac{1}{G_{1000}} \times \frac{\Delta G}{log_{10}(\frac{t_2}{t_1})}, \quad (2.7)$$

where, G_{1000} denotes the shear modulus measured after 1000 minutes of application of constant confining pressure following the primary consolidation. In Figure 2.19a the coefficient of shear modulus increase with time, I_G, is about 900 psi, and the normalized shear modulus increase with time, N_G, is about 15 percent. Afifi and Richart (1973) revealed that the value of N_G tends to decrease with increasing grain size of the soil and Kokusho (1987) showed that the modulus increase ratio $\frac{\Delta G}{G_{1000}}$, increases with respect to plasticity index, I_p shown in Figure 2.20.

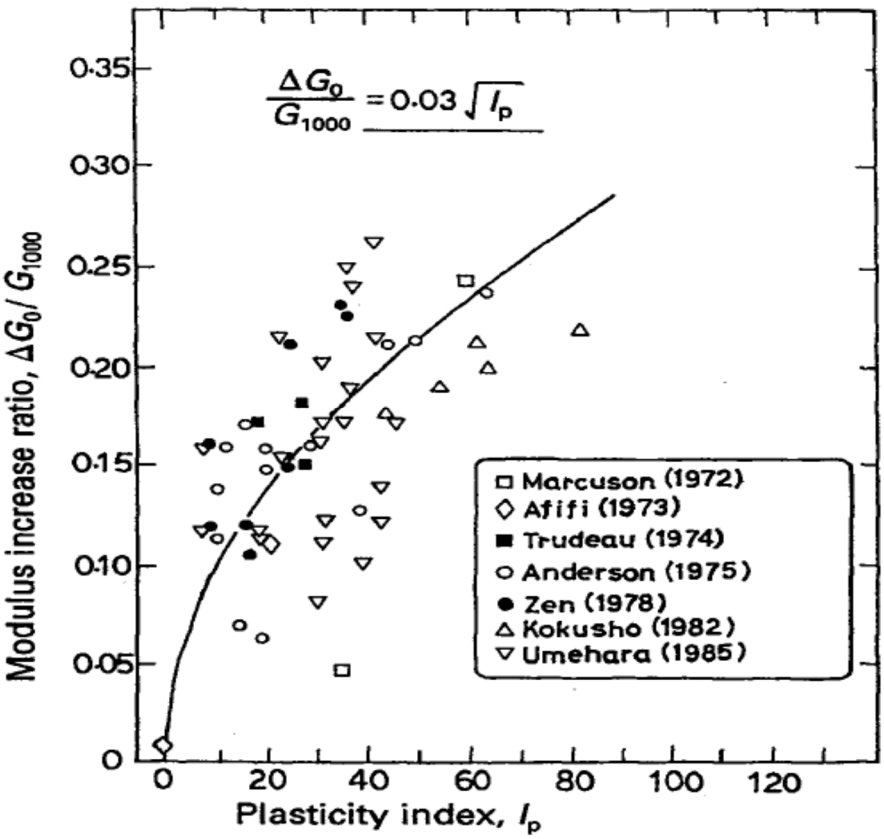


Figure 2.20. Modulus increase ratio versus plasticity index (Kokusho, 1987).

A typical plot of low strain shear modulus vs. time is illustrated in Figure 2.21. As shown in Figure 2.21, the primary time effect due to consolidation is not evident because pore pressure changes and elastic deformations occurred prior to the first measurement (Anderson and Stokoe 1978).

Values of I_G and N_G for the results shown in Figure 2.21 are 250 psi and 1.0 percent,respectively. These values are much smaller than those shown for the clay in Figure 2.19. Stokoe and Richart (1973) also showed similar results using silty sand.

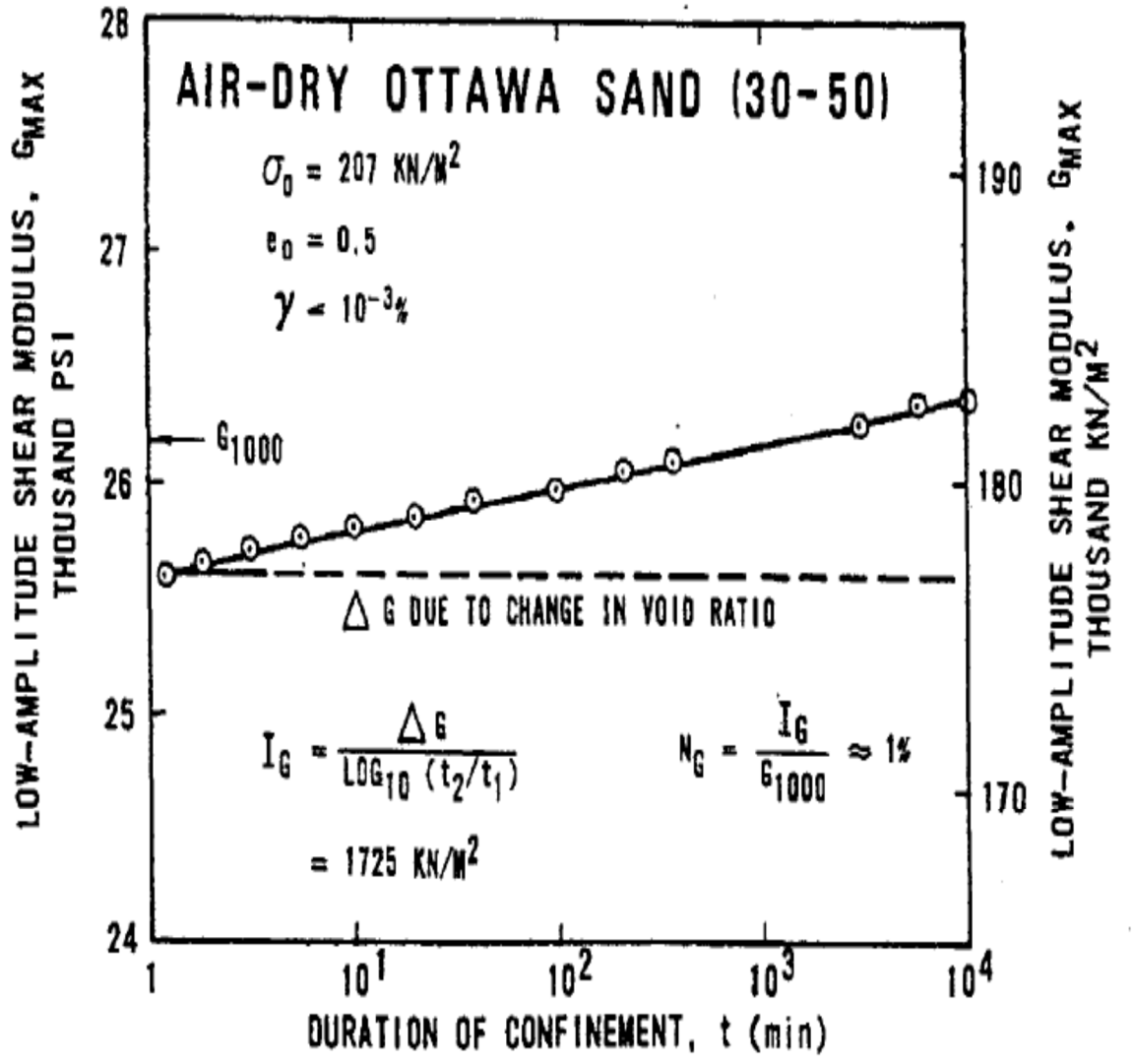


Figure 2.21.Typical modulus change with time for sand (Anderson and Stokoe, 1978).

2.6.2. Strain Dependent Shear Modulus

The small strain range starts from elastic threshold strain to 1% where the shear modulus is highly non-linear and strain dependent.The deformation characteristics of soil are highly nonlinear and vary significantly with amplitude of shear strain under cyclic loading.

Since the decrease of shear modulus with increasing strain amplitude is not the same in all soils, it is common to express the cyclic stress-strain behavior by plots of normalized shear modulus (G/G_{max}) as function of cyclic shear strain (ɣ), which is called a shear modulus reduction curve. Several factors affecting shear modulus reduction curves are presented in this section. Table 2.7 presents the influence of various conditions on the modulus ratio of normally consolidated and moderately overconsolidated clays.

Table 2.7. Effect of Environmental and Loading Conditions on Modulus Ratio (at a given strain level) of Normally Consolidated and Moderately Over-consolidated Soils (Dobry, 1987).

Increasing Factor	Effect on G/G_{max}
Confining pressure, σ'_m	Increase with σ'_m; effect decreases with increasing PI
Void ratio, e	Increase with e
Geologic age, t_g	May increase wit t_g
Cementation, c	May increase with c
Overconsolidation ratio, OCR	Not affected
Plasticity index, PI	Increase with PI
Cyclic strain, γ_c	Decrease with γ_c
Number of loading cycles, N	Decreases after N cycles of large γ_c (Gmax measured before N cycles) for clays; for sands, can increase (under drained conditions) or decrease (under undrained conditions)

3. DIRECT SIMPLE SHEAR TESTING METHODOLOGY

The laboratory testing program for this thesis involved direct simple shear(DSS) tests. Direct simple shear tests allow for the measurement of stress-strain relationship and stiffness of a specimen under drained conditions by maintaining constant vertical stress during shear. In addition to drained shear strength the DSS test allows for collection of consolidation data.

This chapter will provide a detailed description of the experimental program used for this research. This includes details of the equipment, sample preparation, testing procedures and soils tested.

3.1.Testing Equipment

The primary testing system used in this report was a direct simple shear device produced by Geocomp Corporation. The DSS device is Geocomp's Shear Track II system as shown in Figure 2.2. The Sheartrac II system is capable of running fully automated consolidation and shear phases of DSS and additionally can be adjusted to conduct basic direct shear tests. The system consists of a computer controlled unit that uses micro-stepper motors to apply vertical and horizontal loads to the soil specimen. The system allows the tester to modify test parameters at any point during a test, and automatically saves and records data through the use of Geocomp's direct simple shear software (Geocomp, Inc). A detailed schematic view of the test apparatus is shown in Figure 3.1 (Kaveh Hassan Zehtab, 2010).

A soil specimen of diameter 63.5 mm is confined by a rubber membrane supported by Teflon covered aluminum rings instead of conventional reinforced membranes. The load capacity of the device is 4.4 KN. The allowed range of velocity for the load pistons is from 0.00003 to 15 mm/min. The peak displacement allowed for load units (i.e., travel length of load pistons) is 24.45 mm in vertical direction and $\pm$12.5mm in horizontal direction. The

resolution (i.e., step-size) in displacements allowed by micro-stepper motors is 0.0013 mm in both directions.

3.2.Testing Procedure

DSS test in this study consists of three phases: Specimen preparation and setting up the test apparatus, consolidation, and shearing. The phases of DSS, which are consistent with the standard ASTM D 6528-07 , are explained in the following.

3.2.1. Specimen Preparation and Setting Up the Test Apparatus

For a DSS test, the sides of specimen are covered with a rubber membrane(Figure 3.2a), also an air vacuum pump does the air suction between membrane and rings. In order to keep Teflon covered aluminum rings fixed around the specimen, a prism holder was used (Figure 3.2b), and sand is air-pluviated on the porous stone that is mounted on the bottom platen of ShearTrac II-DSS equipment(Figure 3.2c). Top and bottom faces of specimen are covered with filter papers to avoid contact between those faces and the porous stones. The top porous stone is placed on the specimen and fixed by O-rings. Then, the bottom platen is fixed inside the water bath.After placing the sample the Geocomp Sheartrac II is moved horizontally and vertically until the Shear Rod lines up in the center of the sample.

After lining up the sample the rod is tightened to the specimen by holding the top cap firmly while screwing the rod in to it. Finally, all bolts are then tightened on the machine and the vertical LVDT is placed on the top cross bar and then, the vertical load transducer connected to the upper frame is fixed to the top platen in order to complete the test set-up (Figure 3.2d).

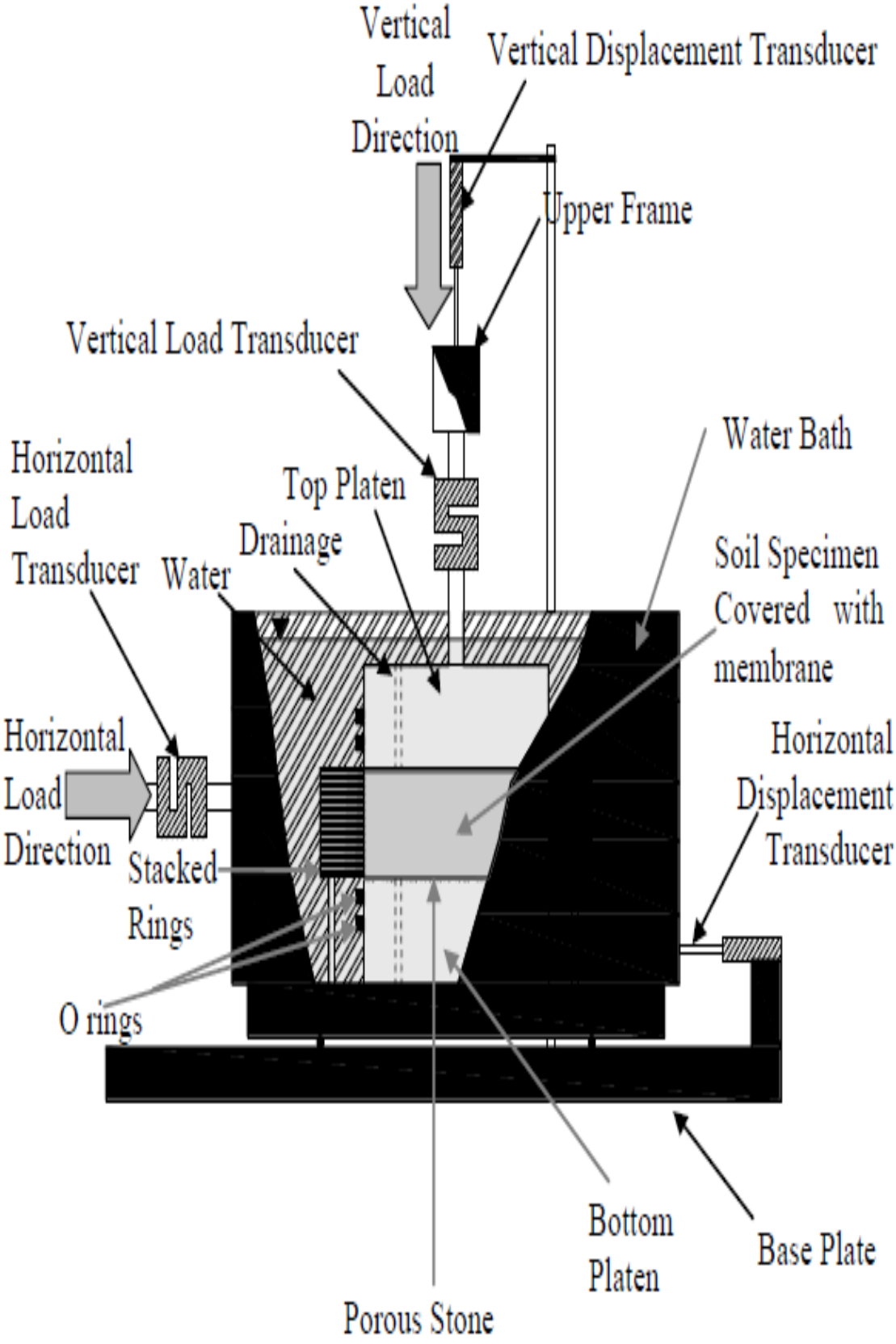
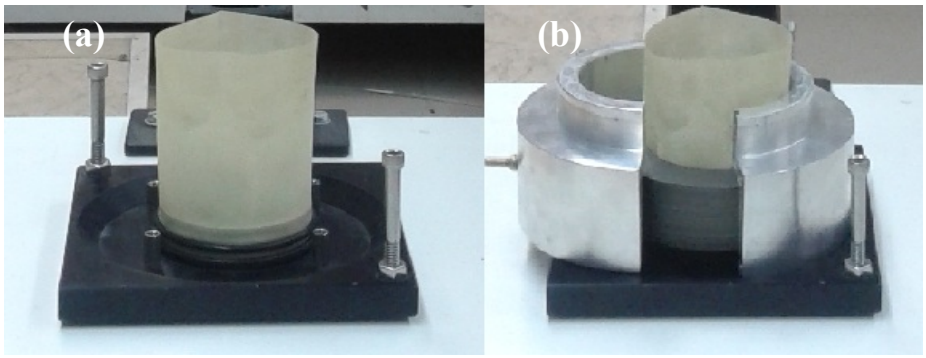
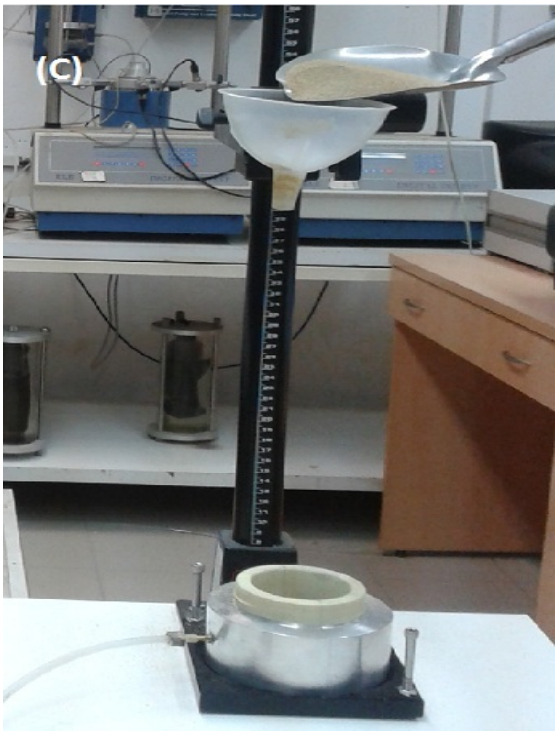


Figure 3.1. Simplified diagram of the DSS device (K. H. Zehtab, 2010).





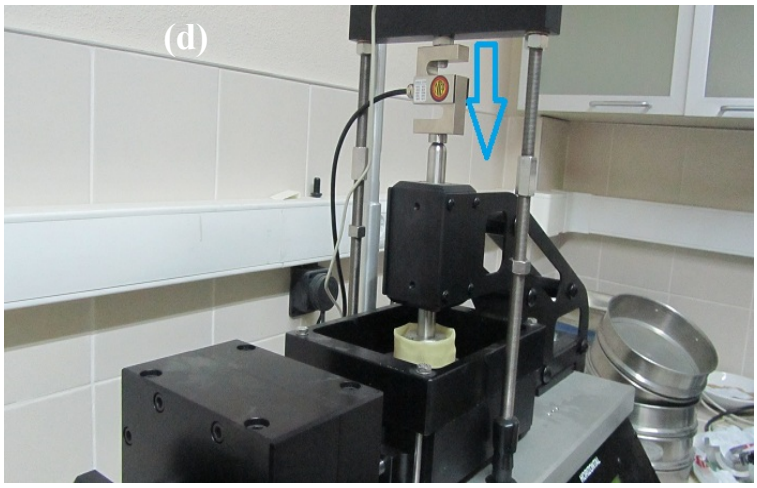


Figure 3.2.Specimen preparation and setting up the test. a)Rubber membrane installation b)Vacuum pump attachment c)Prism holder for aluminum rings d)Air-pluviation of sand from predetermined height e)Vertical load transducer adjusted to the rod.

Air pluviation technique was selected as the sample preparation method in this experimental program. In this method dry sand falls through a funnel from a predetermined height so that the required void ratio for the sand sample could be achieved as shown in Figure 3.3. Funnel moved up as the sand is pluviating to keep the raining height constant and thus to achieve uniformity throughout the sample. According to Kolbuzewsky (1948), density of air-pluviated sample is proportional to the height of the fall.Accordingly a series of air-pluviation tests were performed by (Arshia Abadkon 2012) to define the variation of void ratio with raining height. Obtained relationship as shown in Figure 3.4 can be considered to be linear. Obtained equation is given below:

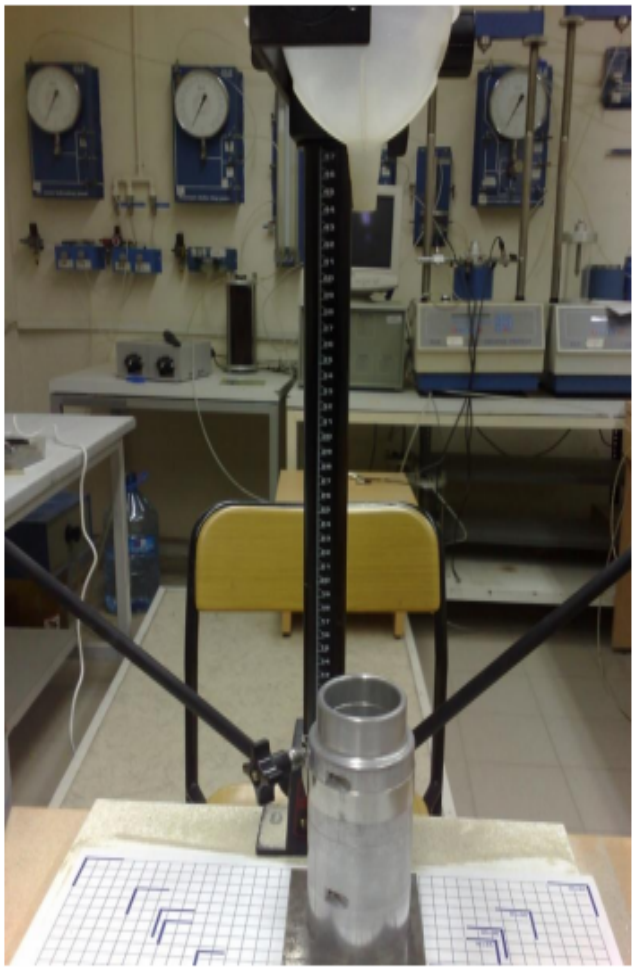


Figure 3.3. Air-pluviation set-up for sample preparation (photo by Arshia Abadkon).

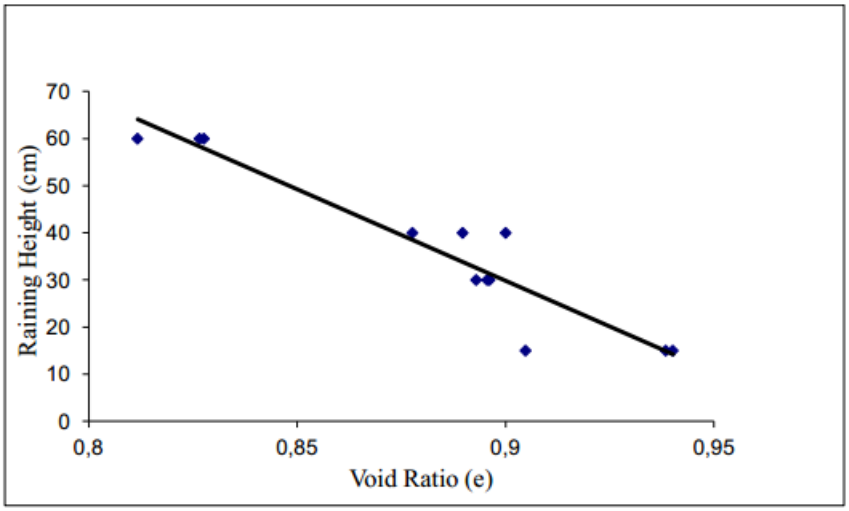


Figure 3.4. Variation of the void ratio with raining height (Arshia Abadkon 2012).

$$h = -388.53e + 379.5 \qquad (3.1)$$

where, h is the raining height in centimeters and e is the void ratio of the sample prepared by pluviation.

3.3.Properties of Soils Tested

Two kinds of sand were used in this study, Well-graded Silivri sand and standard Ottawa graded sand. Properties of each soil are described below.

3.3.1. Silivri Sand

Silivri sand was washed, oven dried and the sieve analysis were done. The grain size distribution of the tested samples is shown in Figure 3.5 and thebasic soil properties are summarized in Table 3.1.

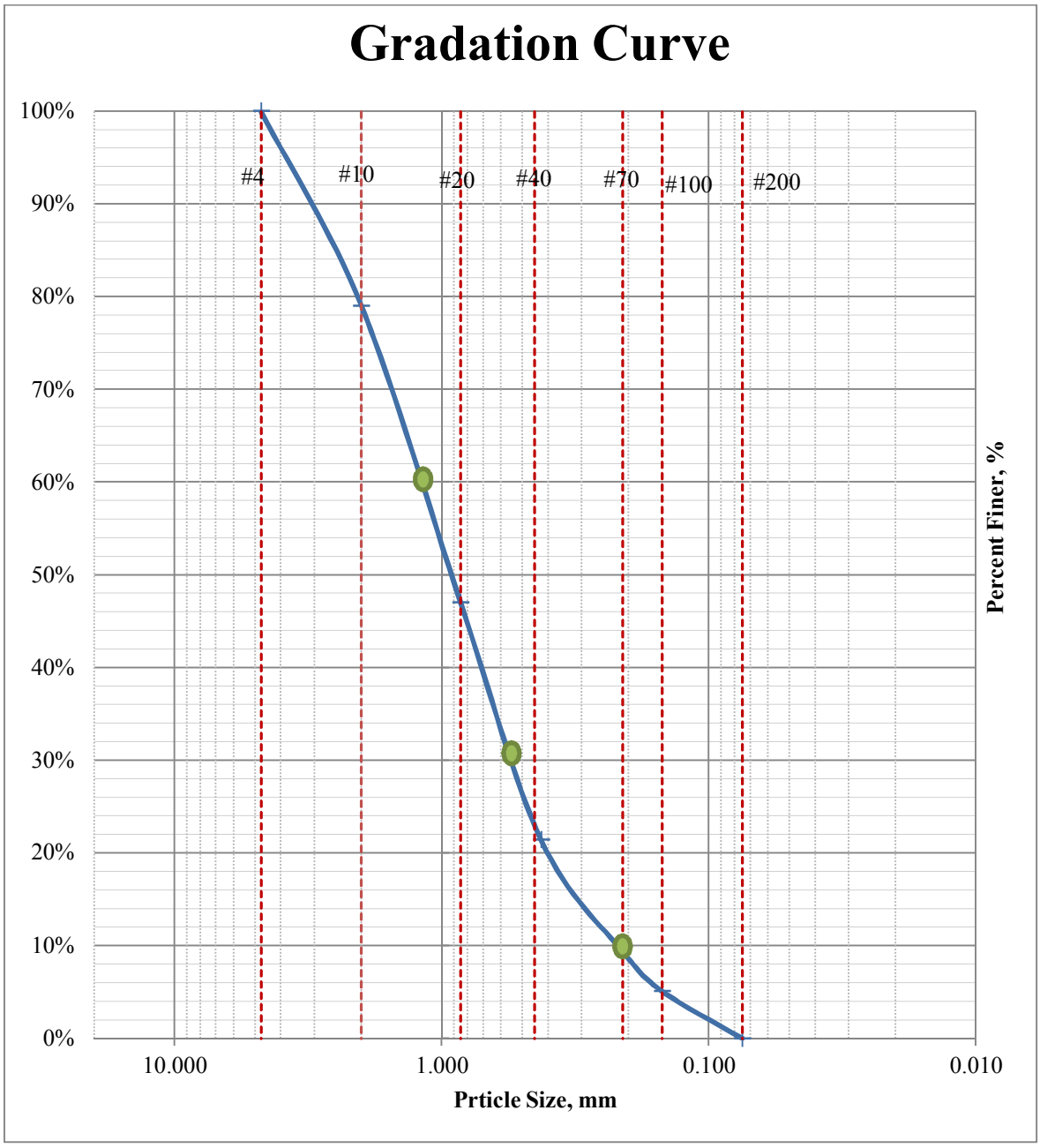


Figure 3.5. Gradation curve for well-graded Silivri sand.

Based on gradation curve, some basic properties of the sand obtained. To be able to figure out uniformity and curvature coefficient, D_{10},D_{30} andD_{60} were marked on the chart, so we have :

$$C_u = \frac{D_{60}}{D_{10}} = \frac{1.3}{0.2} = 6.5 \quad (3.2)$$

$$C_c = \frac{D_{30}^2}{D_{60} \times D_{10}} = \frac{0.53^2}{1.2 \times 0.2} = 1.17 \qquad (3.3)$$

According to Unified Soil Classification System, the sand is classified as well-graded Sand (SW):

$$\begin{cases} Passed\ \#200 < 5\% \\ C_u \geq 6 \\ 1 < C_c < 3 \end{cases}$$

Relative density tests were conducted for determining the maximum and minimum void ratios of the sand sample according to ASTM D-4253and ASTM D-4254 standards, the test apparatus is shown on Figure 3.6. Five specific gravity tests were carried out and an average value of 2.60 was determined according to ASTM D854 – 10, for the sand used in the experimental program.

Table 3.1. Engineering properties summary of Silivri Sand.

Sand type	**Specific gravity**	**Uniformity Coefficient**	**Coefficient of Curvature**	**Minimum Void Ratio (e_{min})**	**Maximum Void Ratio (e_{max})**
Well graded (Silivri sand)	2.60	6	1.17	0.40	0.62



Figure 3.6. Relative density test apparatus.

3.3.2. Standard Ottawa Graded Sand

In order to investigate second objective of this thesis, we choose a type of sand that mineralogy and soil particles distribution was different than well-graded Silivri sand. The chosen sand is from Kavakli. The sand was washed, oven dried and the sieve analysis were done. The grain size distribution of the tested samples is shown in Figure 3.7 and thebasic soil properties are summarized in Table 3.2.

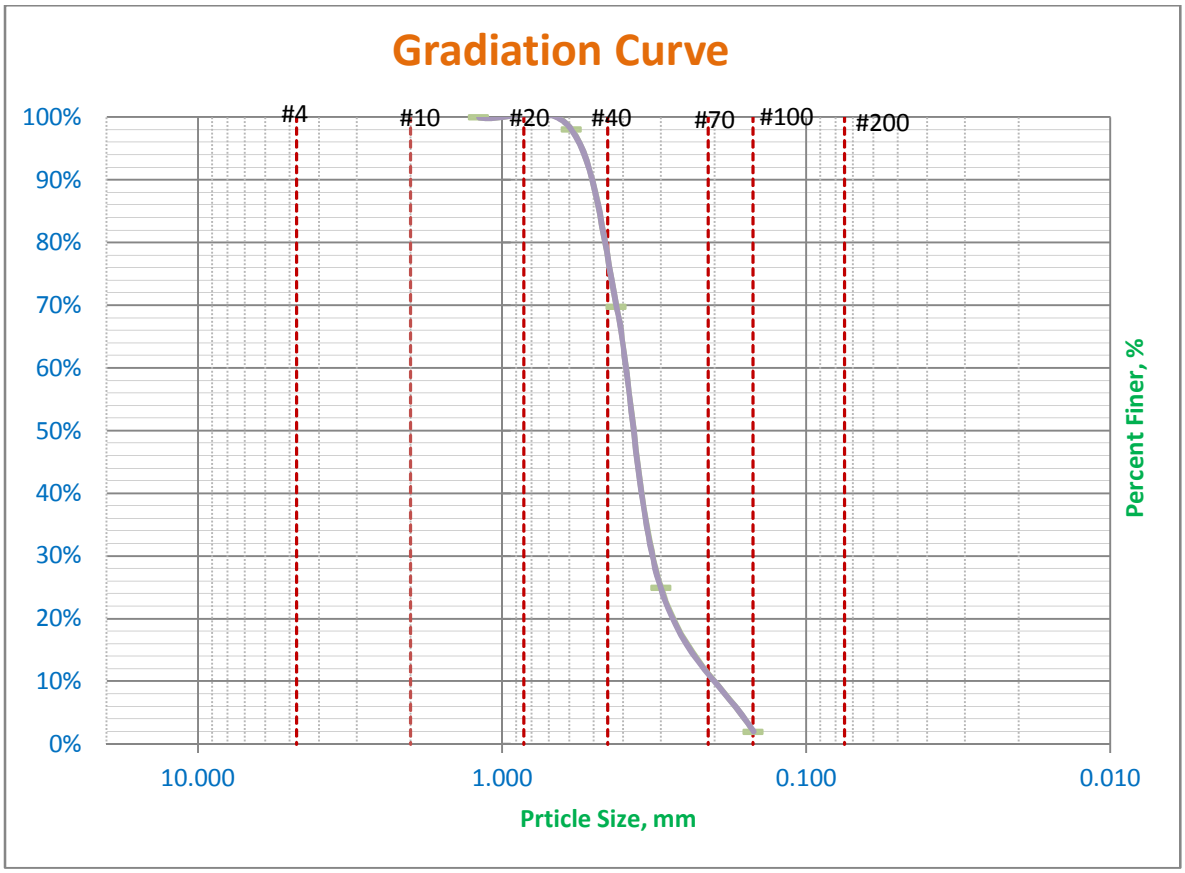


Figure 3.7. Gradation curve for standard Ottawa Silivri sand.

Based on gradation curve, some basic properties of the sand obtained. To be able to figure out uniformity and curvature coefficient, D_{10},D_{30} andD_{60} were marked on the chart, so we have :

$$C_u = \frac{D_{60}}{D_{10}} = \frac{0.4}{0.21} = 1.90 \qquad (3.2)$$

$$C_c = \frac{D_{30}^2}{D_{60} \times D_{10}} = \frac{0.33^2}{0.4 \times 0.2} = 1.36 \qquad (3.3)$$

According to Unified Soil Classification System, the sand is classified as will be named as well-graded Sand (SP).

Table 3.2. Engineering properties summary of Standard Ottawa graded Sand.

Sand Type	Specific Gravity	Uniformity Coefficient	Coefficient of Curvature	Minimum Void Ratio (e_{min})	Maximum Void Ratio (e_{max})
Standard Ottawa graded (Kavakli sand)	2.67	1.90	1.36	0.56	0.96

3.4.Geocomp DSS SoftwareProportional Integral-Derivative Settings

The Geocomp software allows for flexibility when inputting test parameters. Full control of consolidation load steps, duration, and percentage can be specified for manual or automated control. Shear rate speed and maximum strain can also be set.

In the options menu of the DSS Software is a field called PID. PID stands for Proportional Integral-Derivative controller, which is a common feedback loop control system used in automated testing. This field controls the PID settings for both the horizontal and vertical phases of the DSS test. The entry fields are shown in Figure 3.8.

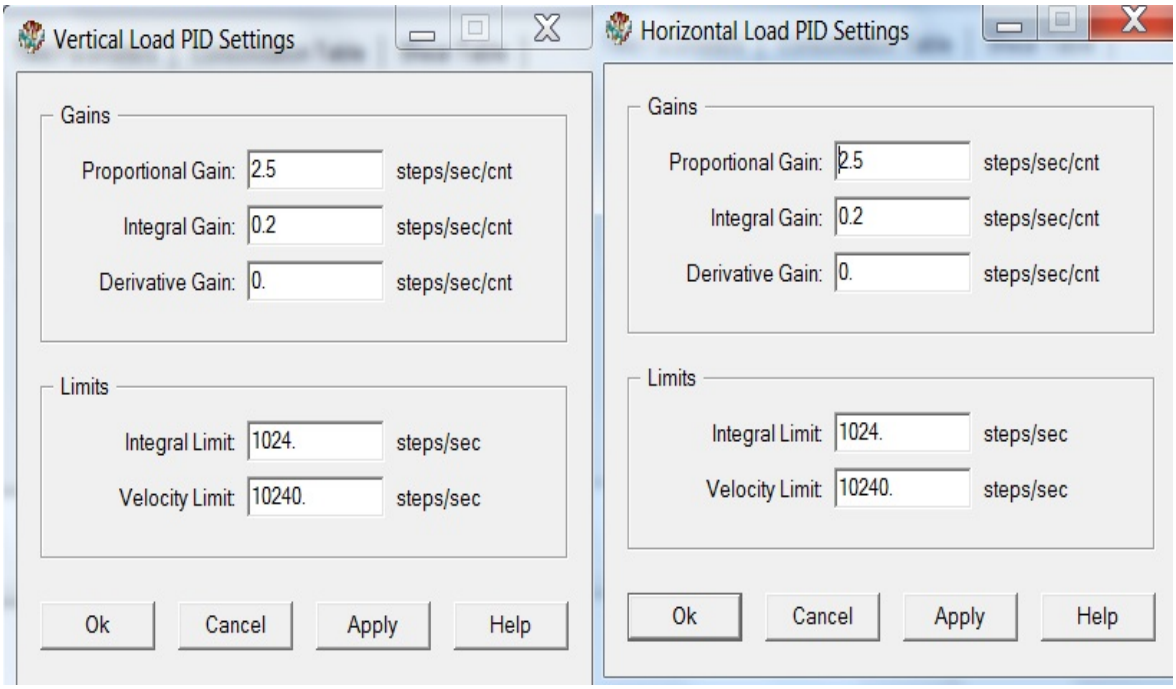


Figure 3.8. PID Input Manual Geocomp Software (Geocomp, Inc, 1985-2005).

These values affect the smoothness of the measured data and must be varied to match the stiffness of the samples being tested. The PID Settings control the timing of the change in force in both directions. During the shear phase of the DSS tests, the vertical stress was varied to maintain the constant volume conditions of the test. However, the data was notsmooth because of the feedback control system, and the PID settings were varied over several tests to reduce this effect. Ultimately the variability in the vertical stress data was not reduced to an acceptable level and it was decided to maintain constant volume conditions for all tests by locking the vertical force to the value it reads at the end of consolidation phase while monitoring axial strain making sure it never exceeded 0.5 %. This procedure is an acceptable method by ASTM for maintaining constant sample volume during shear. PID settings were left at P = 2.5, I = 0.2, and D = 0. These are the Geocomp recommended values. For extremely soft soil P could be increased. P would be decreased for very hard soils.

3.5.Consolidation Test

Consolidation data was run in accordance with ASTM D2435 (constant rate of strain test). After setting up the test, the consolidation phase of the test is initiated. The normal stress for consolidation (σ_v) is set to a pre-selected value.

During the consolidation phase of a DSS test, the normal consolidation pressure is increased to the target value in steps. Then, the specimens are left to consolidate until T100 (end of primary consolidation) reached.

In theory, it will take an infinite amount of time to reach 100% consolidation.However, we can approximate a finite value for T100 by extrapolating the linear middleportion of the curve until it hits the asymptote of 100 Percent of consolidation(U=100%), as shown onFigure 3.9.

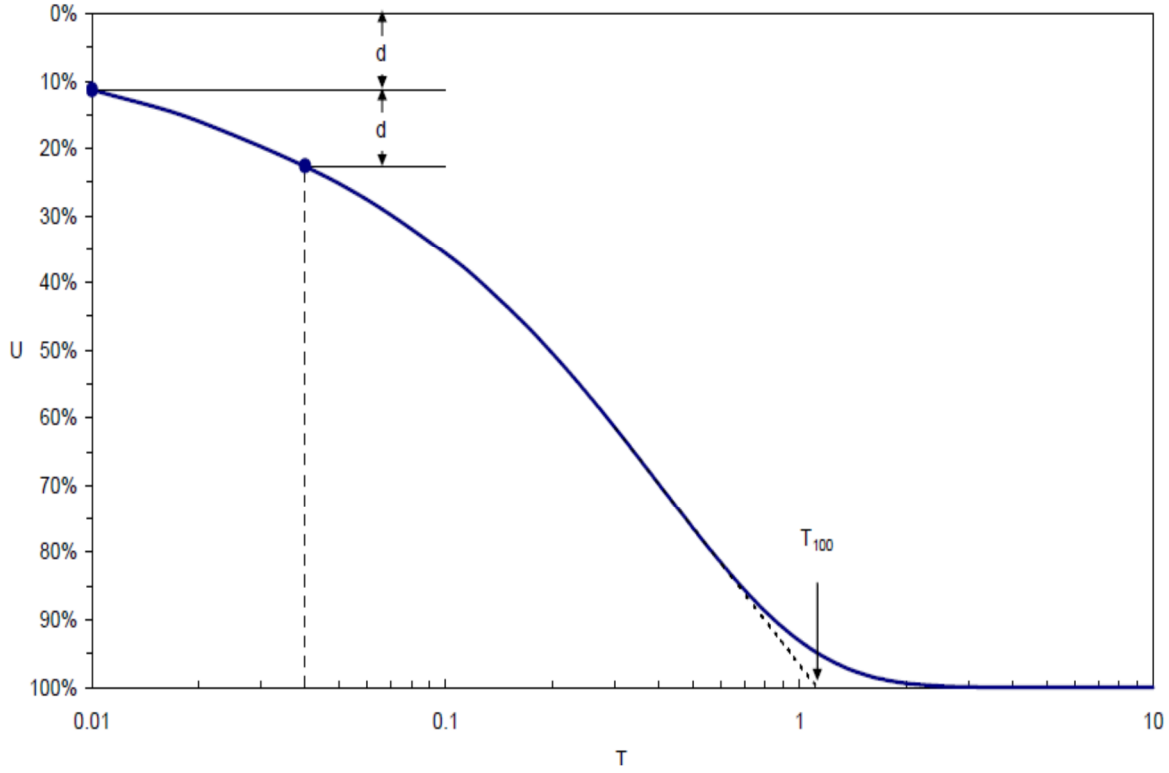


Figure 3.9. Consolidation test result, interpretation of t100 parameter (Advanced Soil Mechanics lecture by Roger W. Meier, University of Memphis).

4. EVALUATION OF DIRECT SIMPLE SHEAR TEST RESULTS

DSS test results have been evaluated to achieve the following objectives :

(i) Quantify the shear modulus of Silivri sand in large strains as a function of vertical effective stress and relative density and propose an equation;

(ii) evaluate proposed equation for another type of sand, a standard Ottawa graded sand.

After an extensive literature review and by analyzing DSS test results, two main parameters controlling the function $G = f(\gamma)$ of clean cohesionless soils were found to be a) relative density (R_D) and b) vertical effective stress (σ_v').

For investigating and quantifying the influence of $R_D$and σ_v',a DSS testing program was prepared in which samples were tested at different combination of relative densities and vertical effective stresses. All tests started with an initial phase of consolidation and followed by shearing.

The tests were conducted at different combinations ofvertical effective stresses and relative densities, in order to formulate a mathematical model for shear modulus.

4.1. Silivri Sand DSS Test Results

Table 4.1 lists the details of the DSS tests conducted during the experimental program. In this table, vertical effective stress during both consolidation and shear phases, void ratios and also relative densities of the samples are shown.

Table 4.1. Details of DSS tests conducted on Silivri sand.

vertical Effective Stress, σ_v' Kpa	Void Ratio, e	Relative Density, R_D %
10 Kpa	0.57	19.7
	0.52	42.4
	0.48	61.0
	0.43	85.3
	0.57	18.8
	0.52	41.8
	0.47	63.9
	0.51	45.5
	0.56	25.1
	0.46	69.6
	0.50	52.7
	0.50	56.1
20 Kpa	0.53	41.6
	0.55	32.8
	0.50	56.1
	0.48	65.0
	0.45	76.6
	0.55	32.8
	0.48	64.0
	0.44	83.0
	0.58	18.9
	0.52	46.4
	0.47	68.9
30 Kpa	0.58	18.9
	0.51	47.8
	0.51	49.3
	0.43	87.8
	0.58	18.3
	0.49	61.1
	0.43	85.1
	0.54	34.7
	0.53	42.4
	0.50	53.1
	0.52	44.8
50 Kpa	0.47	67.9
	0.59	14.9
	0.46	73.7
	0.55	33.6
	0.49	60.3
	0.49	60.7
	0.54	37.6
	0.54	36.9
	0.47	69.7
	0.51	47.9

Table 4.1. Details of DSS test (cont.).

	0.55	33.6
70 Kpa	0.49	58.3
	0.59	14.4
	0.53	41.7
	0.57	23.2
	0.52	43.2
	0.40	98.9
	0.53	40.8
	0.44	81.8
	0.54	36.0
	0.53	42.8
	0.48	61.9
	0.54	35.9

4.1.1. Effect of Relative Density on Shear Modulus of Silivri Sand

Relative density is one of the properties of the soil that rules its shear strength, calculated using following equation :

$$R_D = \frac{e_{max} - e}{e_{max} - e_{min}} \quad (4.1)$$

In this experimental program, the vertical effective stress is kept constant and the variation of shear modulus with shear strain is monitored. For each selected σ_v', the shear strain is defined between 0.1 and 10 %. To obtain unit-less coefficients, G is normalized with atmospheric pressure (in the case of this testing program, since G is measured in kPa, so $P_a = 100Kpa$). The results are shown in Figures 4.2 to 4.5.

Shear modulus can be determined from the stress-strain curve. The inclination of the curve depends on the stiffness of the soil, which can be described at any point during loading process by the tangent shear modulus (G_{tan}), as shown on Figure 4.1, that varies throughout the loading.

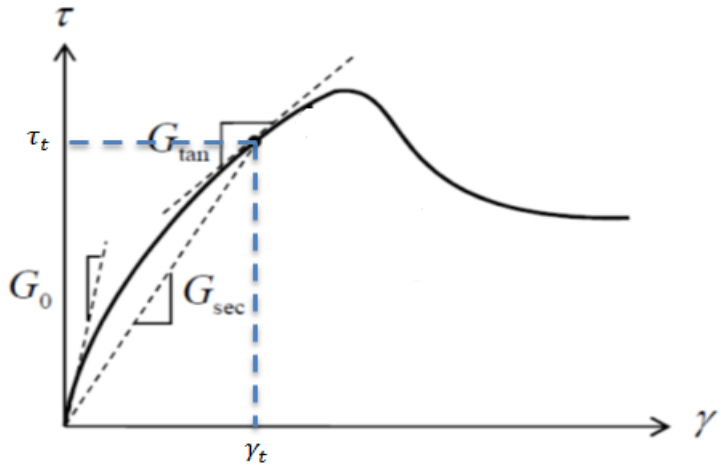
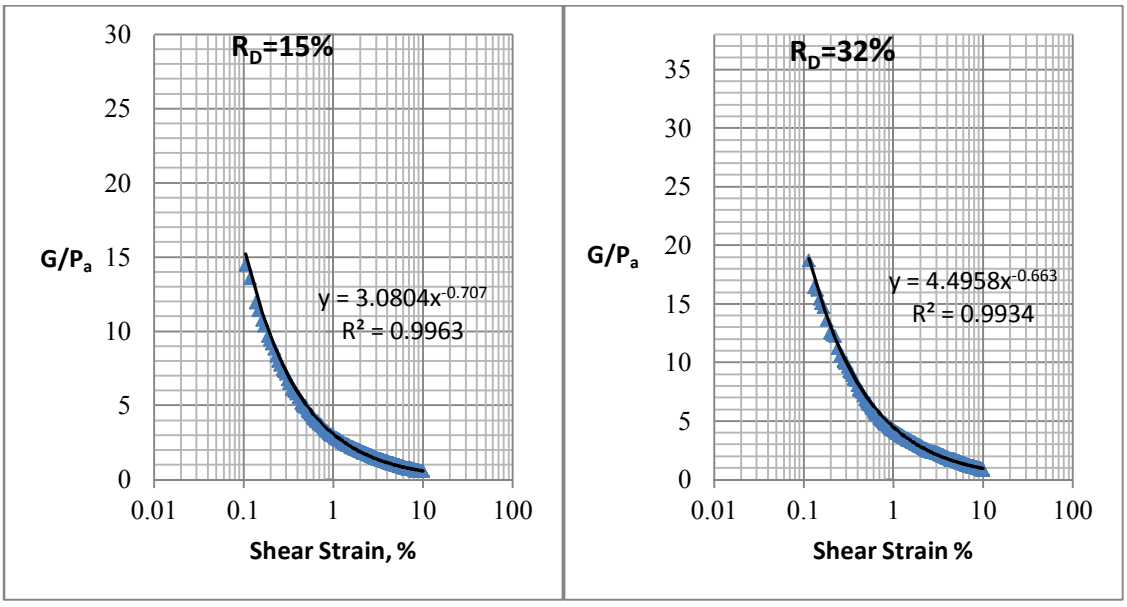


Figure 4.1. Stress-strain curve of soil and G_{tan} determination.

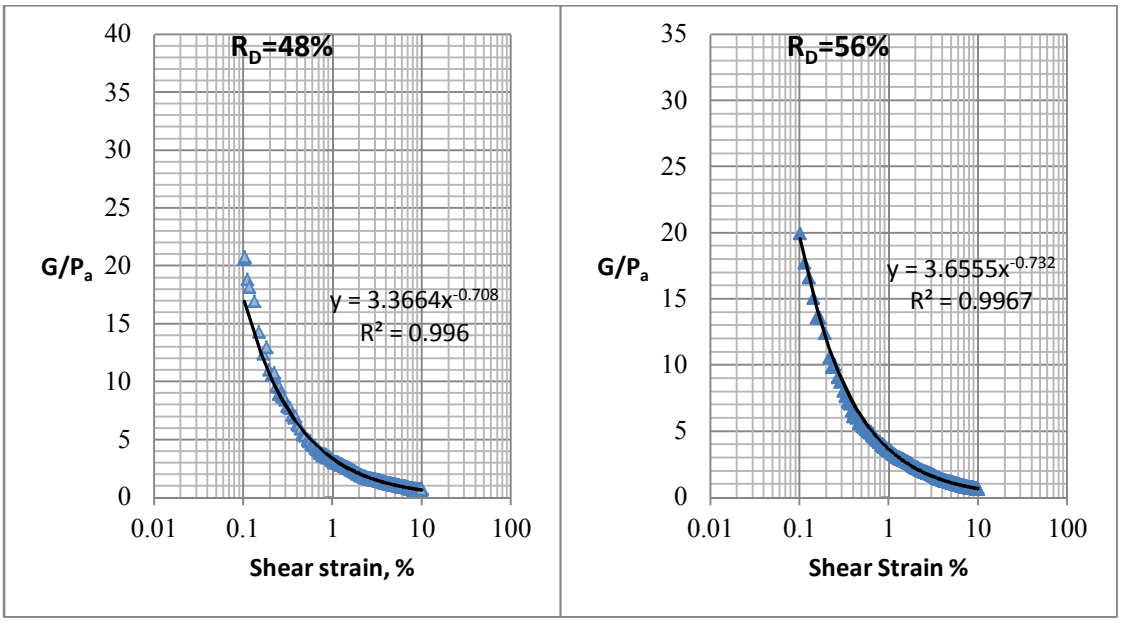
The value of the tangent shear modulus can be calculated by Equation 4.2:

$$G_{tan} = \frac{\tau_t}{\gamma_t}. \quad (4.2)$$

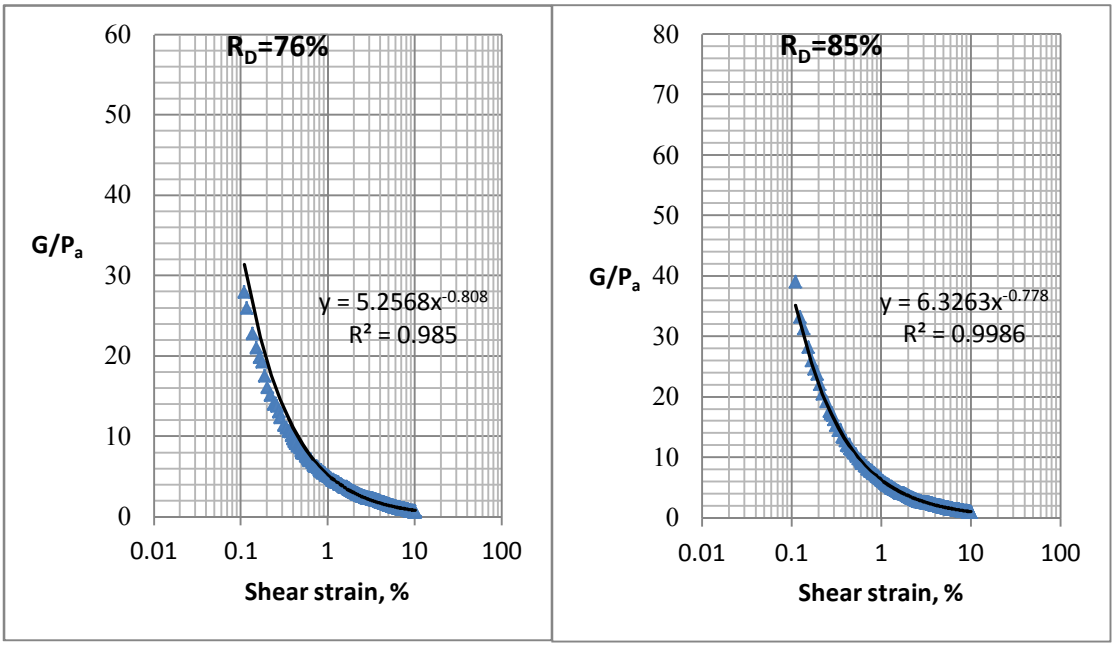


(a) (b)

Figure 4.2. Shear modulus variation with shear strain between 0.1 to 10 % for $\sigma'_v = 10\ Kpa$ a)$R_D = 15$ b)$R_D = 32$.

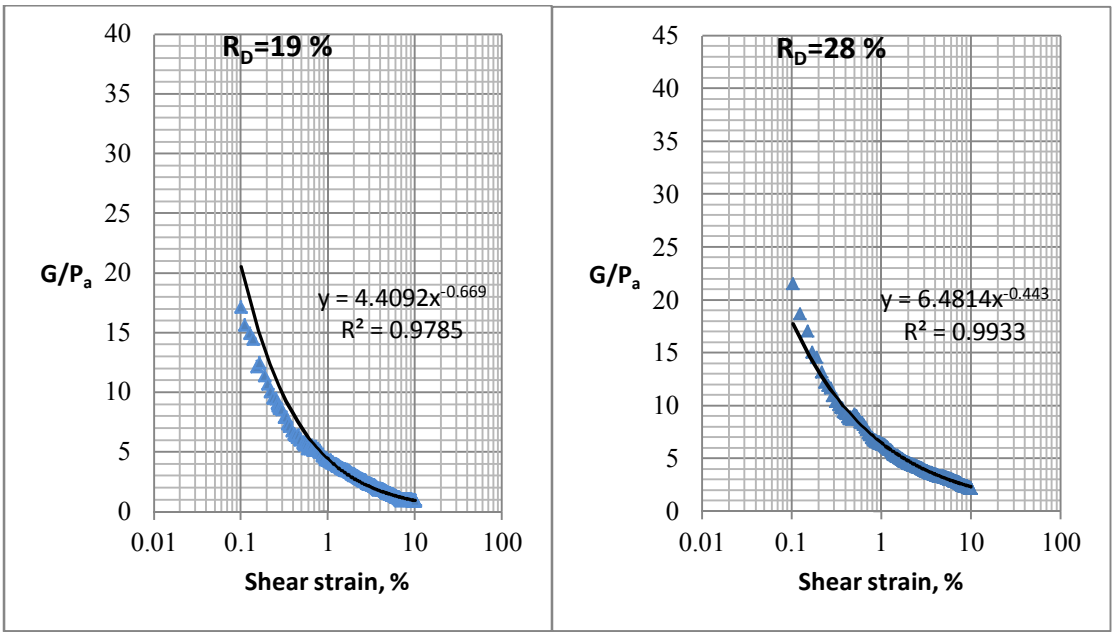


(c) (d)

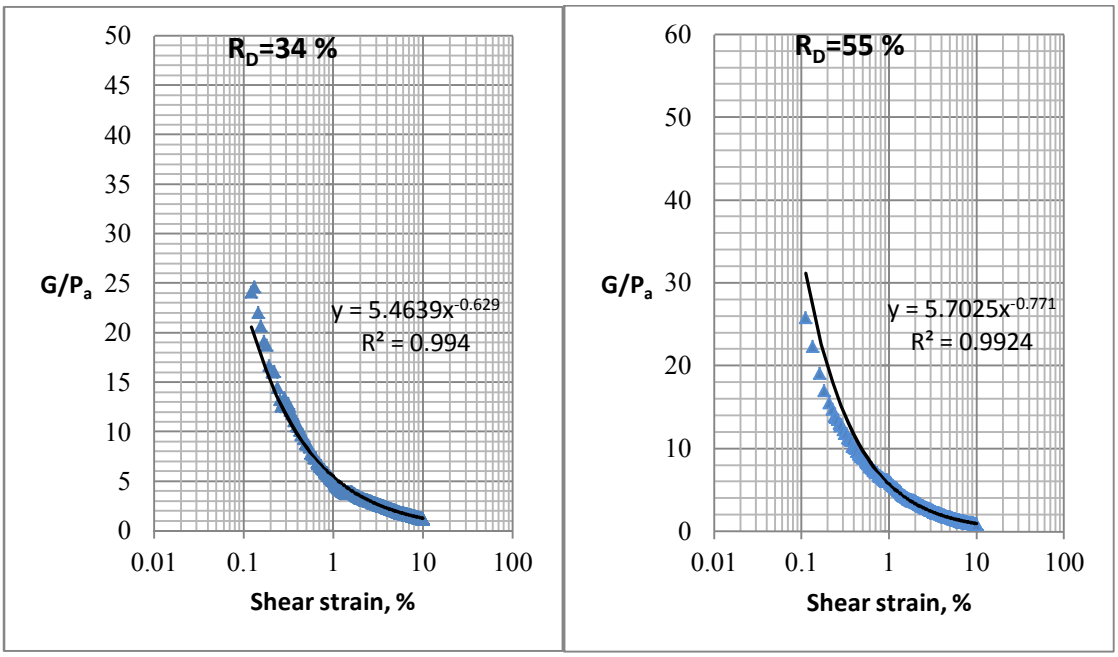


(e) (f)

Figure 4.2. Shear modulus variation with shear strain between 0.1 to 10 % forσ'_v = 10 Kpac)$R_D = 48$ d)$R_D = 56$ e)$R_D = 76$ f)$R_D = 85$ (Cont.).

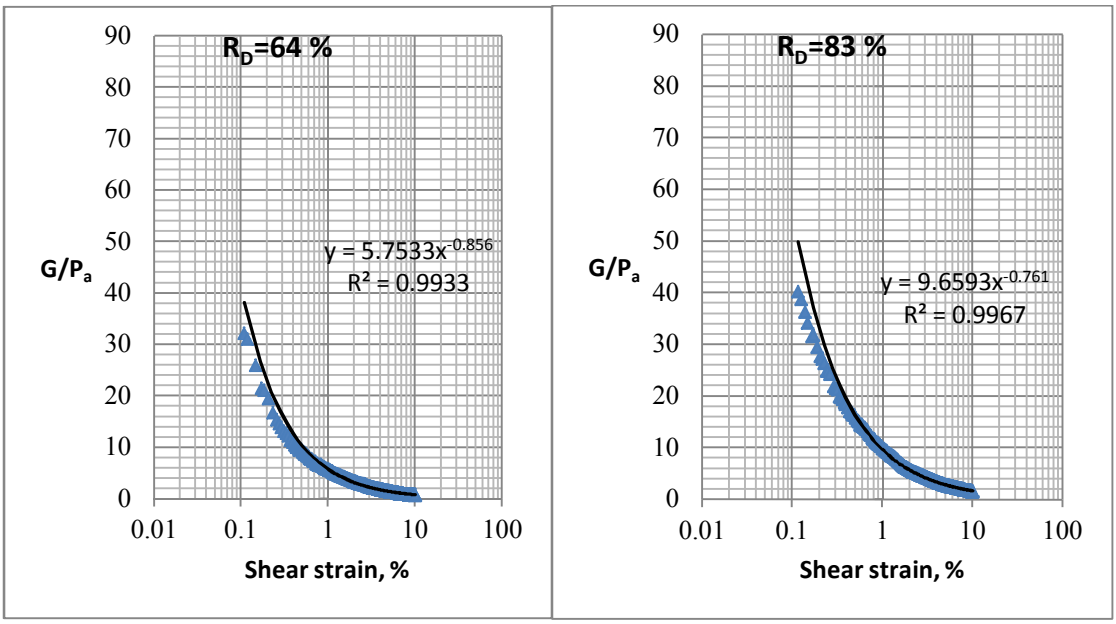


(a) (b)



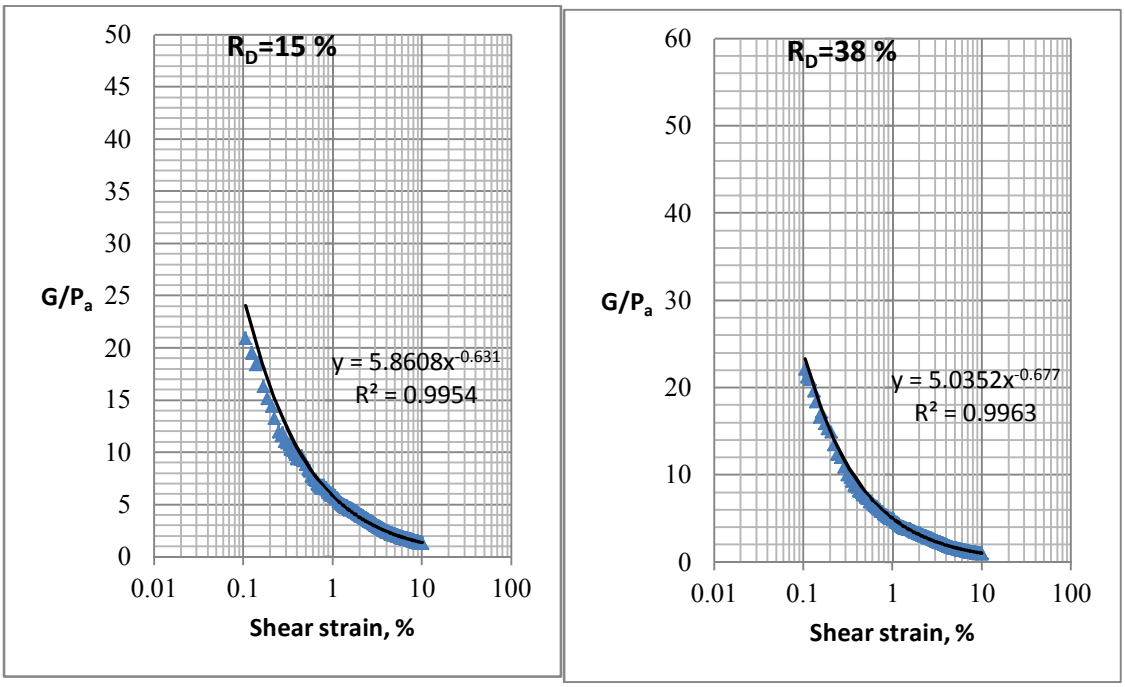
(c) (d)

Figure 4.3. Shear modulus variation with shear strain between 0.1 to 10 % for $\sigma'_v = 20\ Kpa$ a)$R_D = 19$ b)$R_D = 28$ c)$R_D = 34$ d)$R_D = 55$.



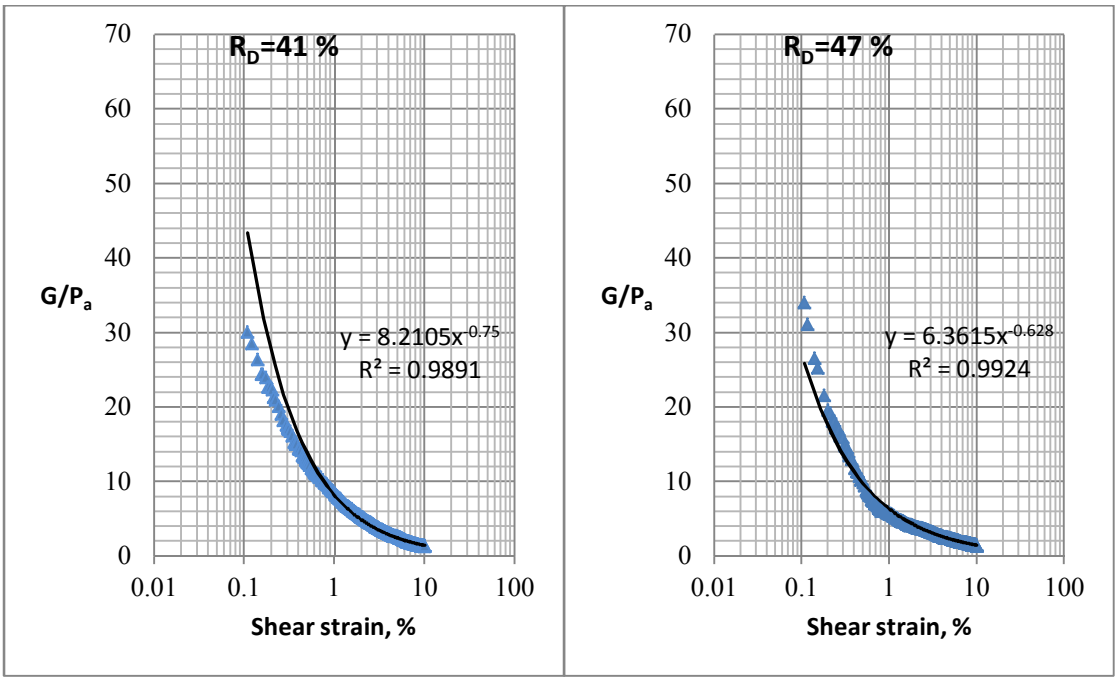
(e) (f)

Figure 4.3. Shear modulus variation with shear strain between 0.1 to 10 % for $\sigma'_v = 20\ Kpa$e)$R_D = 64$ f)$R_D = 83$ (Cont.).

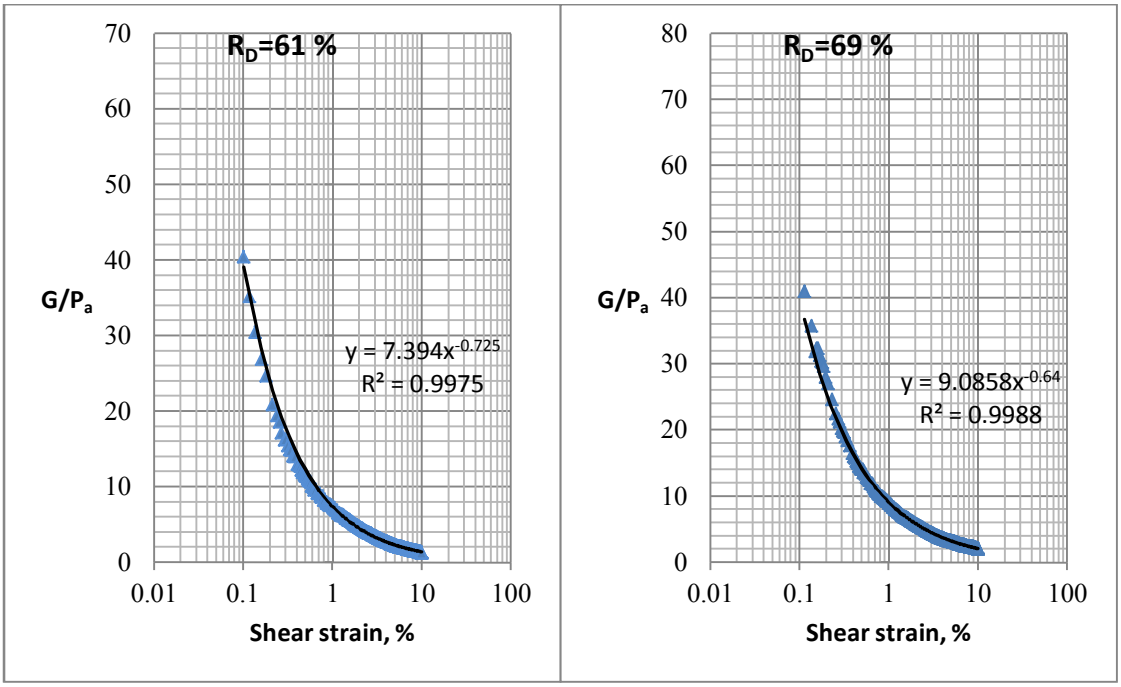


(a) (b)

Figure 4.4. Shear modulus variation with shear strain between 0.1 to 10 % for $\sigma'_v = 30\ Kpa$ a)$R_D = 15$ b)$R_D = 38$.

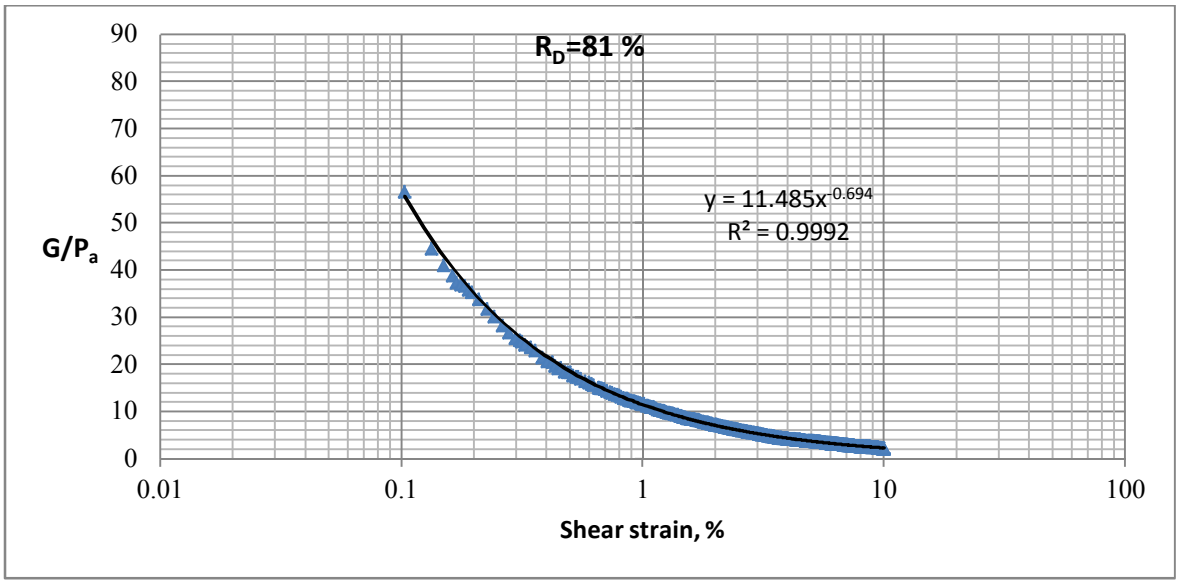


(b) (d)



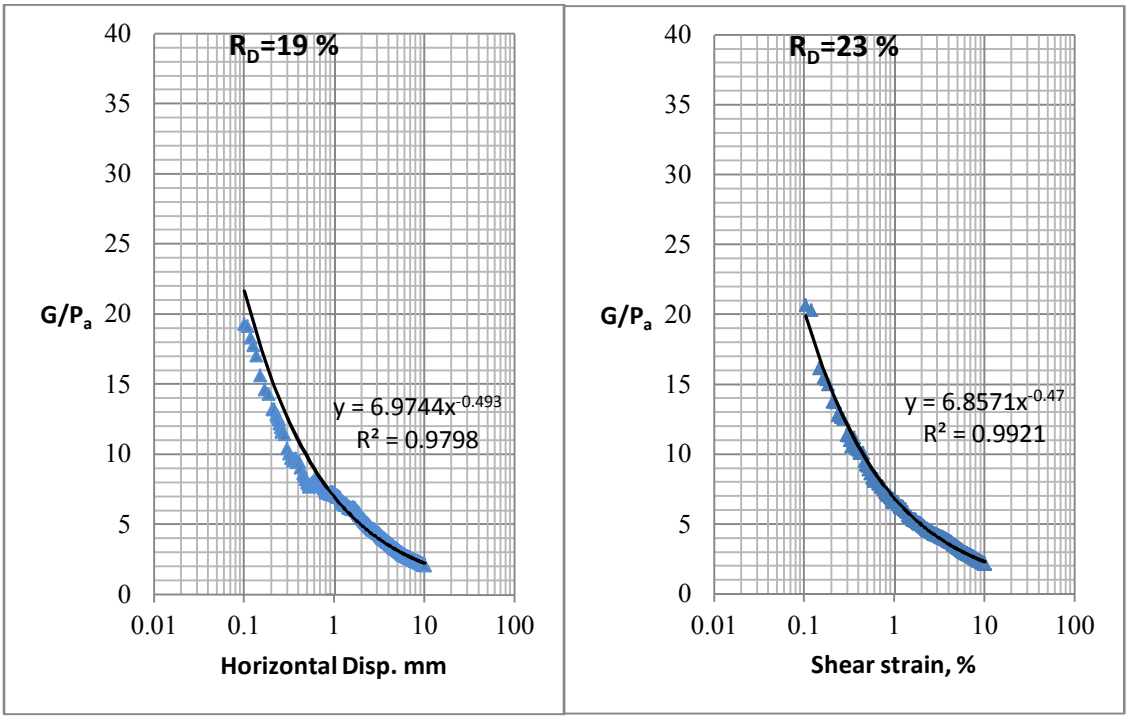
(e) (f)

Figure 4.4. Shear modulus variation with shear strain between 0.1 to 10 % forσ'_v = 30 Kpac)$R_D = 41$ d)$R_D = 47$ e)$R_D = 61$ f)$R_D = 69$ (Cont.).



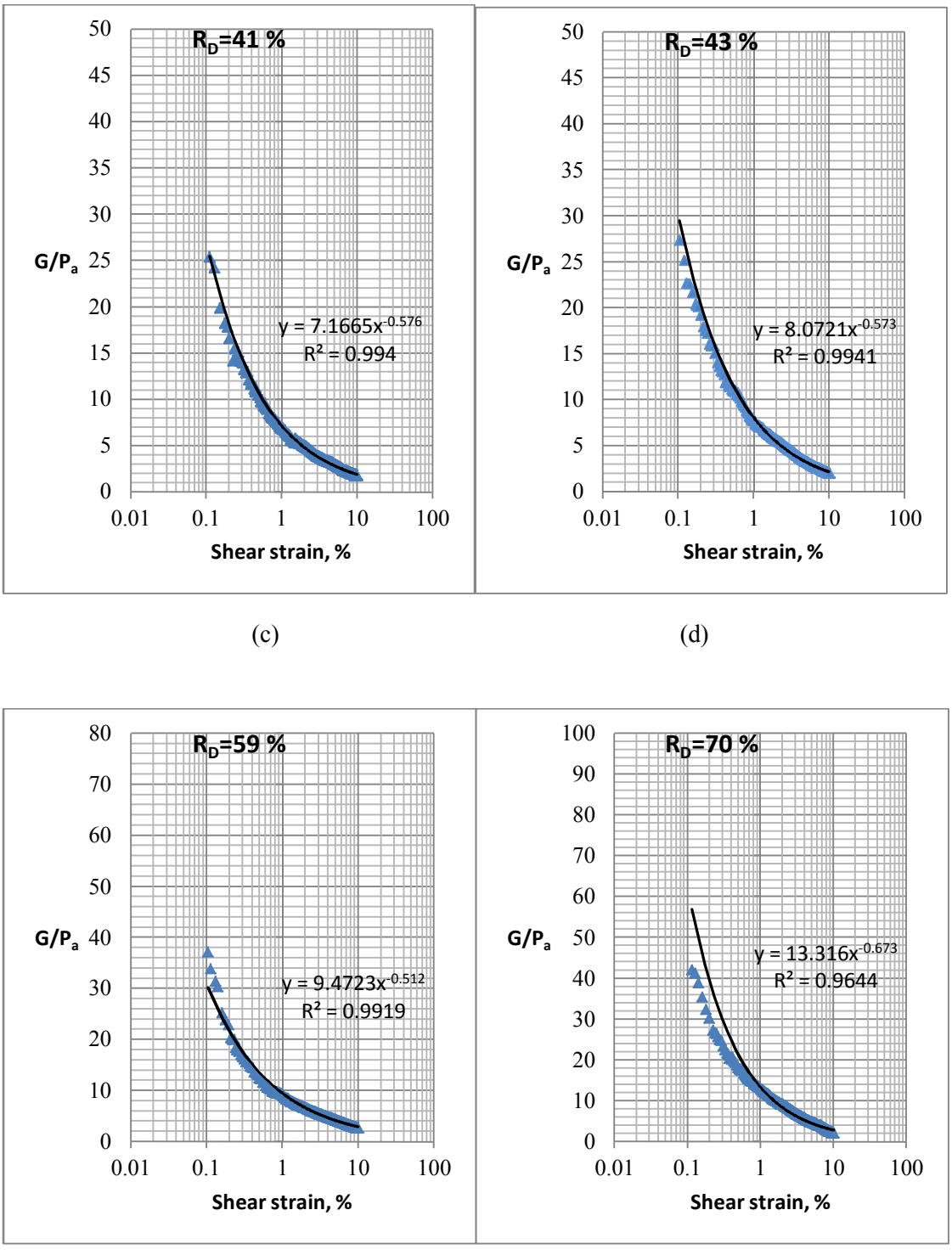
(g)

Figure 4.4. Shear modulus variation with shear strain between 0.1 to 10 % for $\sigma'_v = 30\ Kpag) R_D = 81$ (Cont.).



(a) (b)

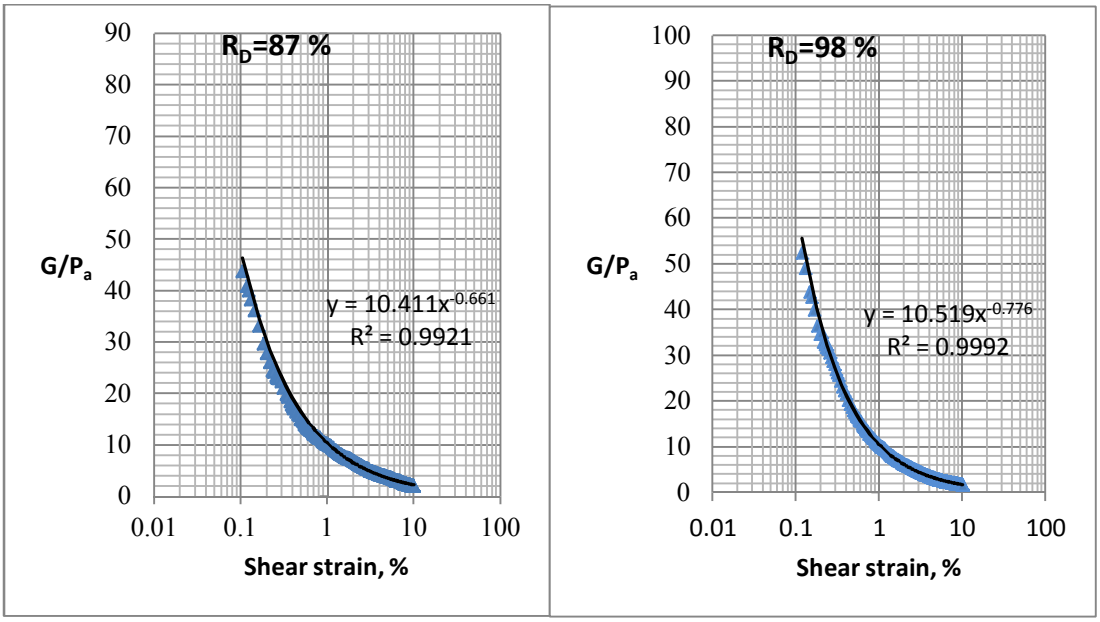
Figure 4.5. Shear modulus variation with shear strain between 0.1 to 10 % for$\sigma'_v = 50\ Kpa$ a)$R_D = 19$ b)$R_D = 23$.



(c) (d)

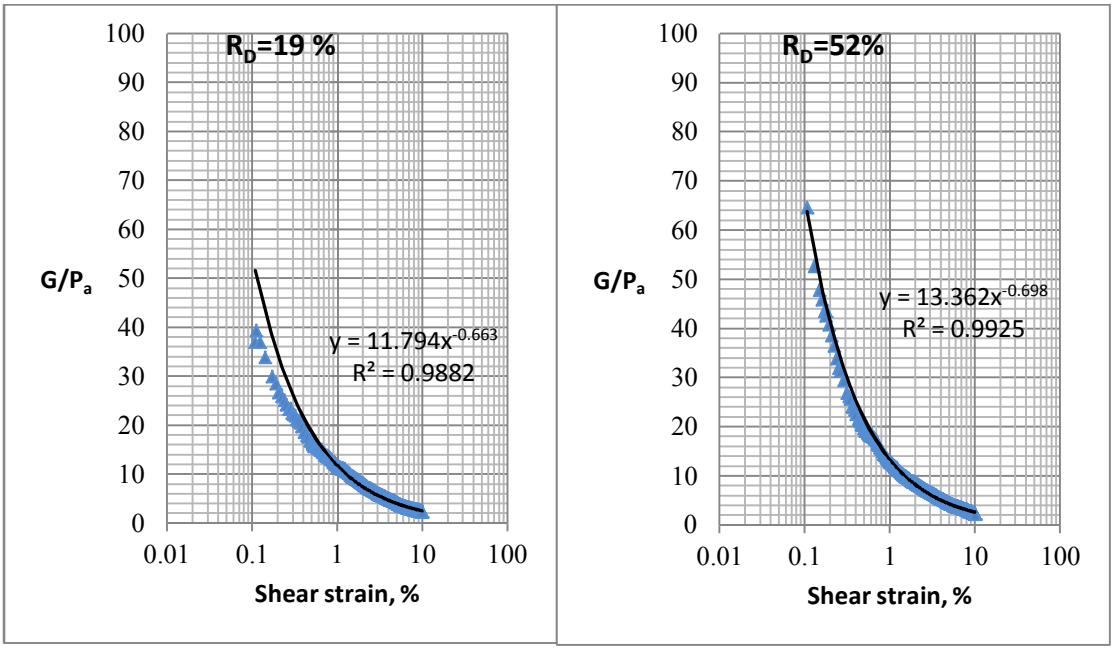
(e) (f)

Figure 4.5. Shear modulus variation with shear strain between 0.1 to 10 % for $\sigma'_v = 50\ Kpac) R_D = 41$ d)$R_D = 43$ e)$R_D = 59$ f)$R_D = 70$ (Cont.).



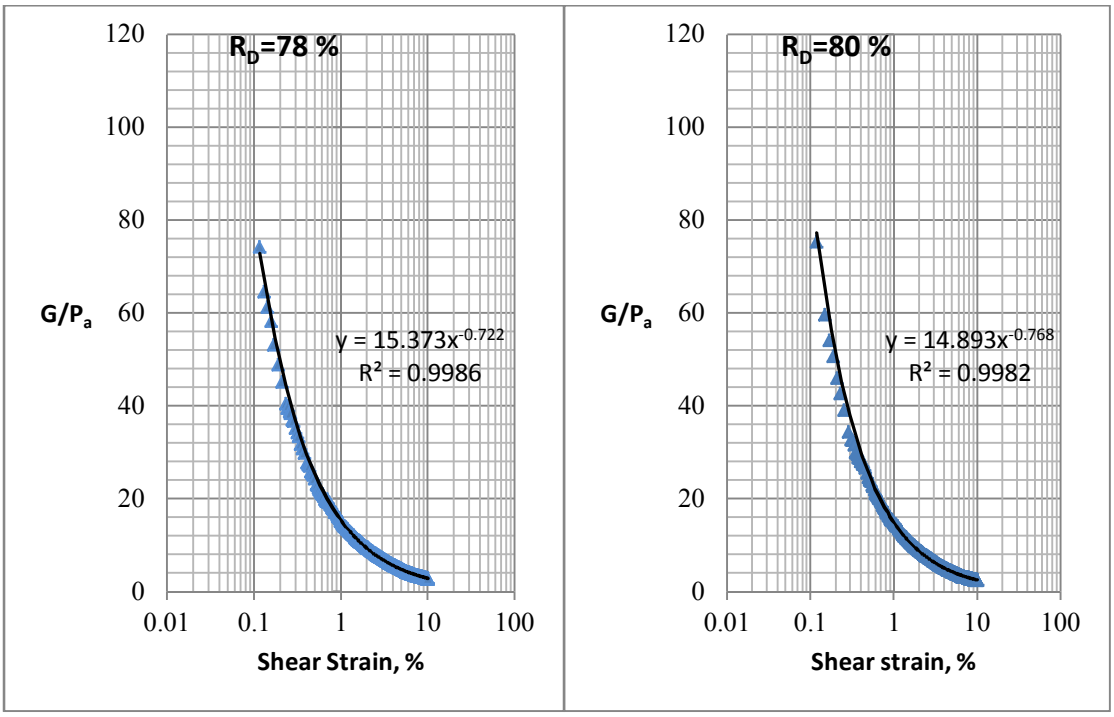
(g) (h)

Figure 4.5. Shear modulus variation with shear strain between 0.1 to 10 % for $\sigma'_v = 50\ Kpa$ g)$R_D = 87$ h) $R_D = 98$ (Cont.).

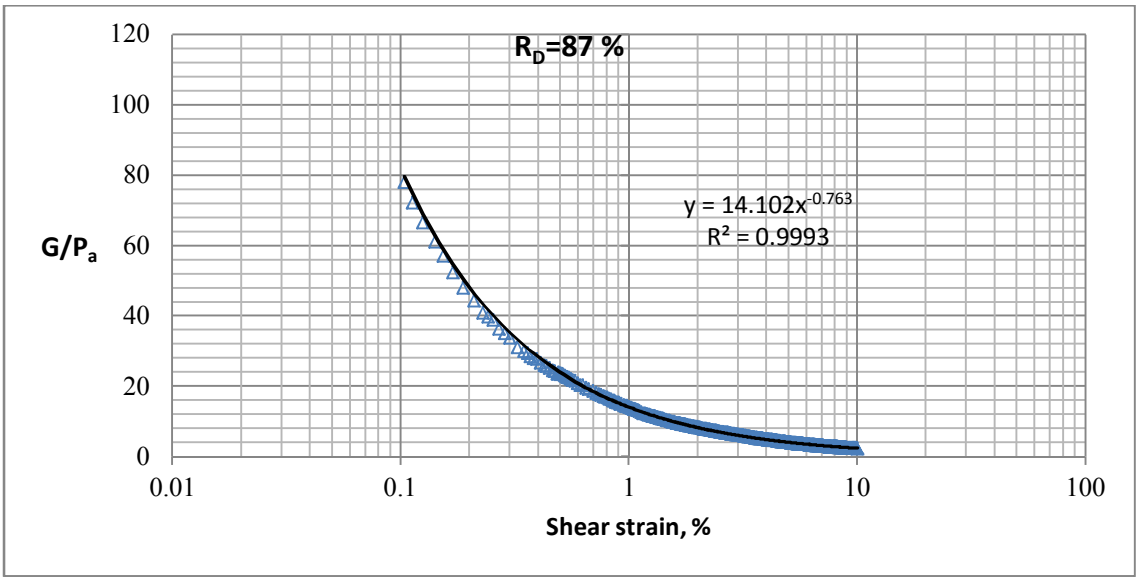


(a) (b)

Figure 4.6. Shear modulus variation with shear strain between 0.1 to 10 % for$\sigma'_v = 70\ Kpa$ a)$R_D = 19$ b)$R_D = 59$.



(c) (d)



(e)

Figure 4.6. Shear modulus variation with shear strain between 0.1 to 10 % for $\sigma'_v = 70\ Kpac)R_D = 78$ d)$R_D = 80$ e)$R_D = 87$ (Cont.).

Figure 4.2 shows the results obtained from DSS test on Silivri sand under a constant vertical stress of 10 Kpa. The relative density varies between15 to 85 % and the behavior of normalized shear modulus of the sand is plotted with respect to shear strain increment. Although σ_v' is constant during shearing for each test, since the R_D increases from test to test, the soil gains shear stiffness and so a higher G is observed. Respectively, the results of G/p_a vs. γ are plotted for $\sigma_v' = 20, \sigma_v' = 30, \sigma_v' = 50$ and $\sigma_v' = 70kpa$, which are shown in Figures 4.3, 4.4, 4.5 and 4.6. A similar behavior can be seen for these results.

4.1.2. Quantifying G As a Function of σ_v', R_D and γ for Silivri Sand

In plots above, a general curve shape can be observed, so the corresponding trend-line as a power function was plotted for each. Table 4.2 is a summary of the equations for each individual σ'_v and $R_D$and also R^2 values.

It is essential to statistically investigate how closely a certain function fits our experimental data. In this experiment program, we have relied on coefficient of determination which is shown as R^2.This values is computed in Excel to see how closely our data conform to a power function. R^2 values varybetween 0 and 1, with 1 representing an absolute fit between the data and the line drawn through them, and 0 representing no statistical correlation between the data and the line. The R^2 value is computed as follows:

$$R^2 = 1 - \frac{\sum(Y_i - Y_i')^2}{\sum(Y_i - \overline{Y})^2} \qquad (4.3)$$

where, Y_i is an individual data point value, Y_i' is value obtained when the independent coordinate of this data point is input into the best-fit function (represents the values of the data points projected onto the line of best fit) and $\overline{Y}$ is average of the Y_i values.

Table 4.2. Summary of power functions of trend-lines and R^2 values.

σ'_v	R_D %	Power Function	R^2
10 Kpa	15	$y = 3.0804x^{-0.707}$	$R^2 = 0.9963$
	32	$y = 4.4958x^{-0.663}$	$R^2 = 0.9934$
	48	$y = 3.3664x^{-0.708}$	$R^2 = 0.996$
	56	$y = 3.6555x^{-0.732}$	$R^2 = 0.9967$
	76	$y = 5.2568x^{-0.808}$	$R^2 = 0.985$
20 Kpa	34	$y = 4.138x^{-0.568}$	$R^2 = 0.994$
	40	$y = 4.492x^{-0.573}$	$R^2 = 0.9898$
	55	$y = 4.639x^{-0.602}$	$R^2 = 0.9924$
	83	$y = 5.237x^{-0.647}$	$R^2 = 0.9967$
30 Kpa	15	$y = 5.8608x^{-0.631}$	$R^2 = 0.9954$
	38	$y = 5.0352x^{-0.677}$	$R^2 = 0.9963$
	41	$y = 8.2105x^{-0.75}$	$R^2 = 0.9891$
	47	$y = 6.3615x^{-0.628}$	$R^2 = 0.9924$
	61	$y = 7.394x^{-0.725}$	$R^2 = 0.9975$
	69	$y = 9.0858x^{-0.64}$	$R^2 = 0.9988$
	81	$y = 11.485x^{-0.694}$	$R^2 = 0.9992$
50 Kpa	19	$y = 6.9744x^{-0.493}$	$R^2 = 0.9798$
	23	$y = 6.8571x^{-0.47}$	$R^2 = 0.9921$
	41	$y = 7.1665x^{-0.576}$	$R^2 = 0.994$
	43	$y = 8.0721x^{-0.573}$	$R^2 = 0.9941$
	59	$y = 9.4723x^{-0.512}$	$R^2 = 0.9919$
	70	$y = 13.316x^{-0.673}$	$R^2 = 0.9644$
	87	$y = 10.411x^{-0.661}$	$R^2 = 0.9921$
	98	$y = 10.519x^{-0.776}$	$R^2 = 0.9992$
70 Kpa	19	$y = 11.794x^{-0.663}$	$R^2 = 0.9882$
	42	$y = 13.362x^{-0.698}$	$R^2 = 0.9925$
	78	$y = 15.373x^{-0.722}$	$R^2 = 0.9986$
	80	$y = 14.893x^{-0.768}$	$R^2 = 0.9982$
	87	$y = 14.102x^{-0.763}$	$R^2 = 0.9993$

It is vivid from Table 4.2 that a power function with a general form of Equation 4.4 can be used to quantify G as a function of σ'_v and R_D :

$$\frac{G}{P_a} = \zeta * \gamma^{\eta} \quad (4.4)$$

where, ζ and η are unit-independent fitting parameters, and the value of γ varies between 0.1 to 10 %.

Initially, we took σ'_vas a constant and plotted the variations between (ζ vs. R_D) and (η vs. R_D). Figures 4.7 to 4.11show variation of dependent variables (ζ and η) with respect to relative density. The trend-line of these data are computed so we have a general linear function for predicting ζ and η as :

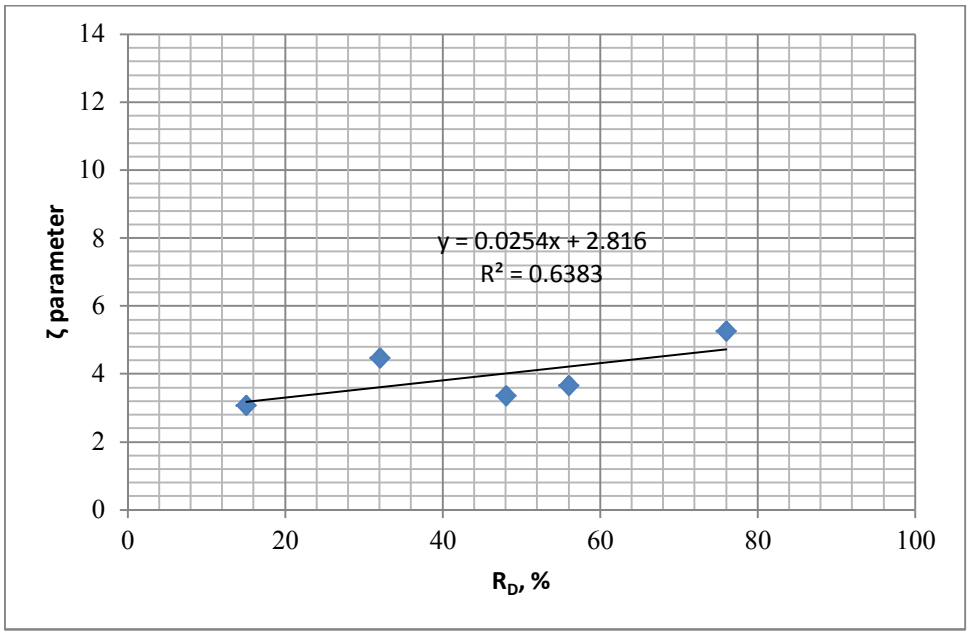
$$\zeta = \alpha_\zeta R_D + \beta_\zeta \quad (4.5)$$

$$\eta = \alpha_\eta R_D + \beta_\eta \quad (4.6)$$

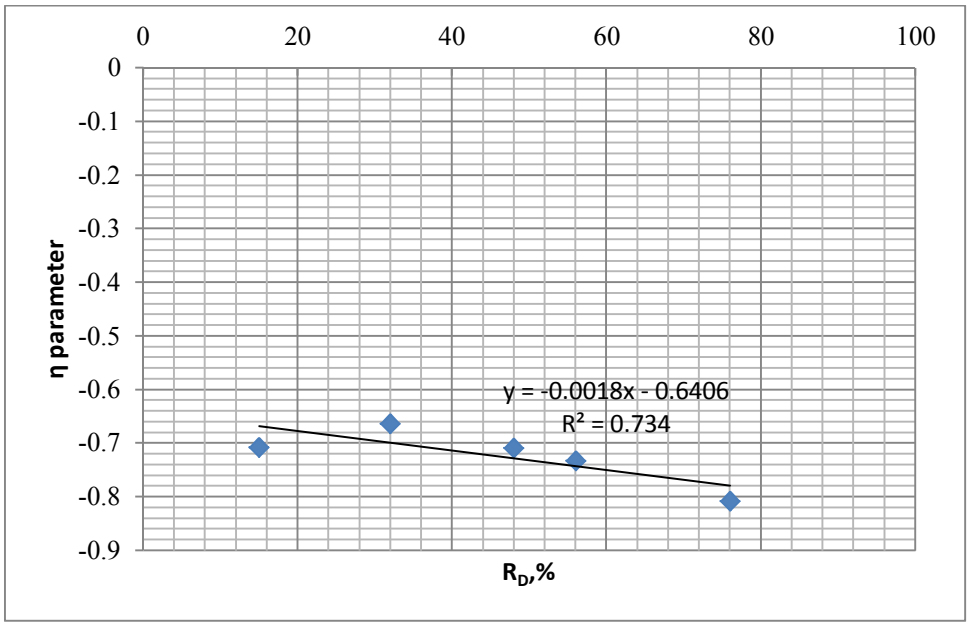
α_ζ , β_ζ , α_η and β_η are unit-independent fitting parameters.

Inserting Equation 4.5 and 4.6 into Equation4.4, we have :

$$\frac{G}{P_a} = (\alpha_\zeta R_D + \beta_\zeta)\gamma^{\alpha_\eta R_D + \beta_\eta} \quad (4.7)$$

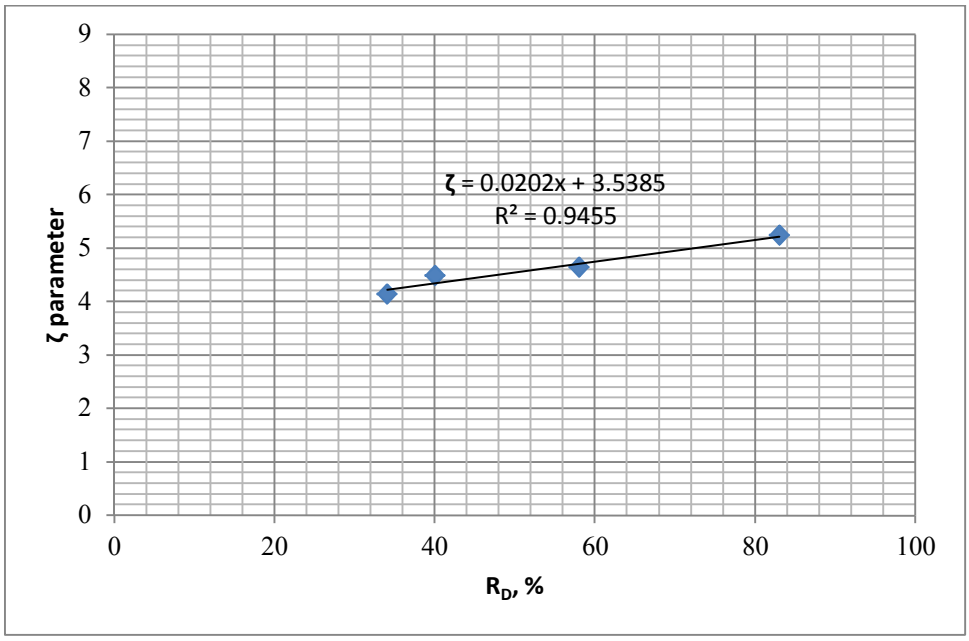


(a)

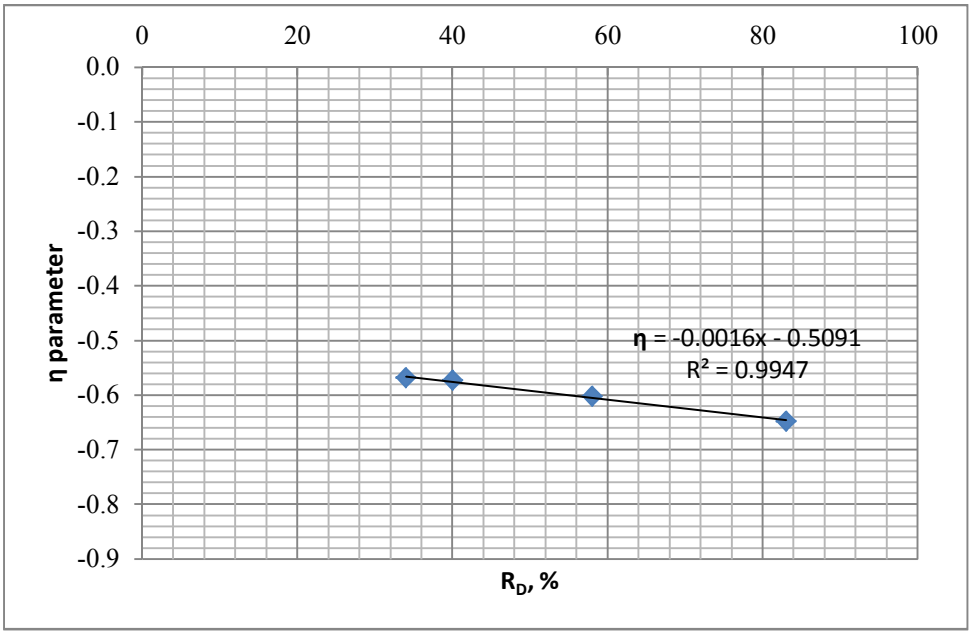


(b)

Figure 4.7. Variation of fitting parameters with R_D , for $\sigma'_v = 10\ Kpa$ a)ζparameter b) η parameter.

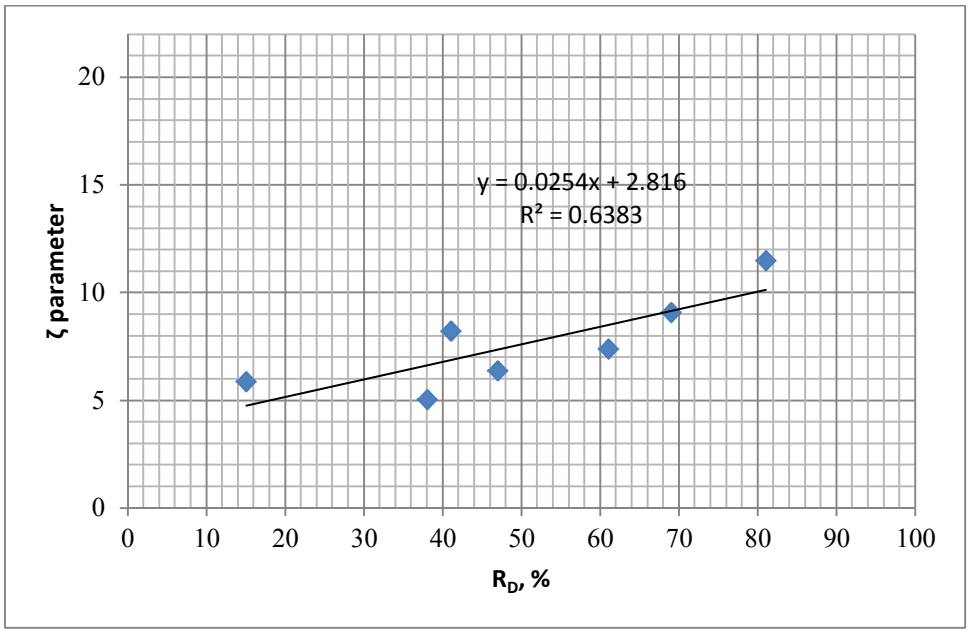


(a)

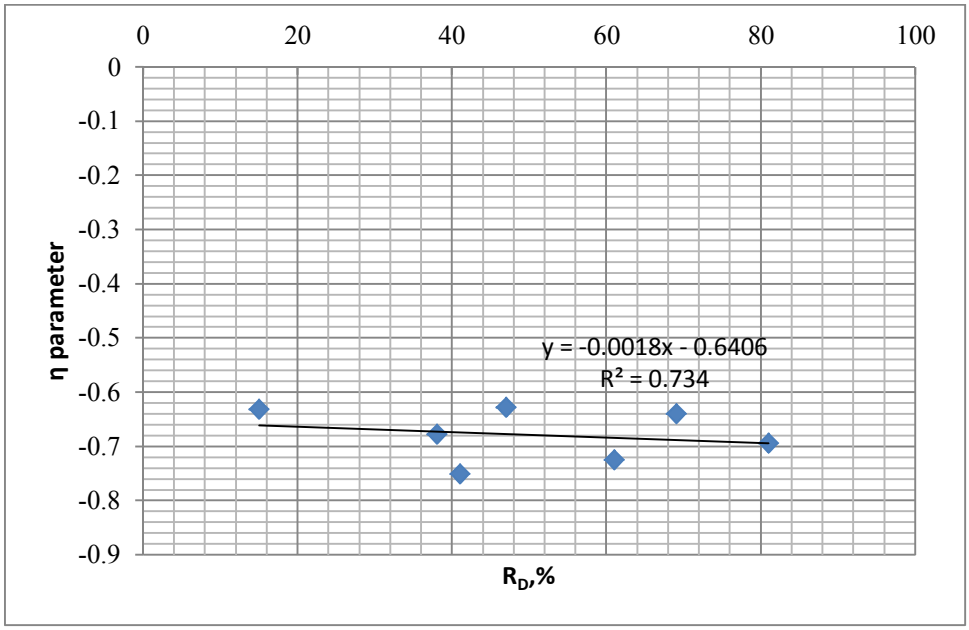


(b)

Figure 4.8. Variation of fitting parameters with R_D , for $\sigma'_v = 20\ Kpa$ a)ζparameter b) η parameter.

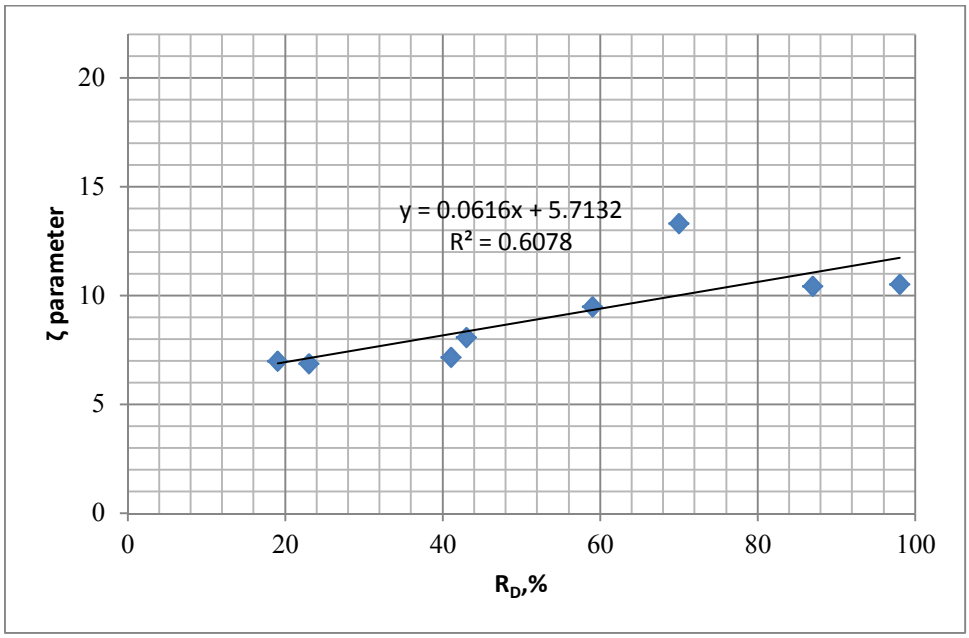


(a)

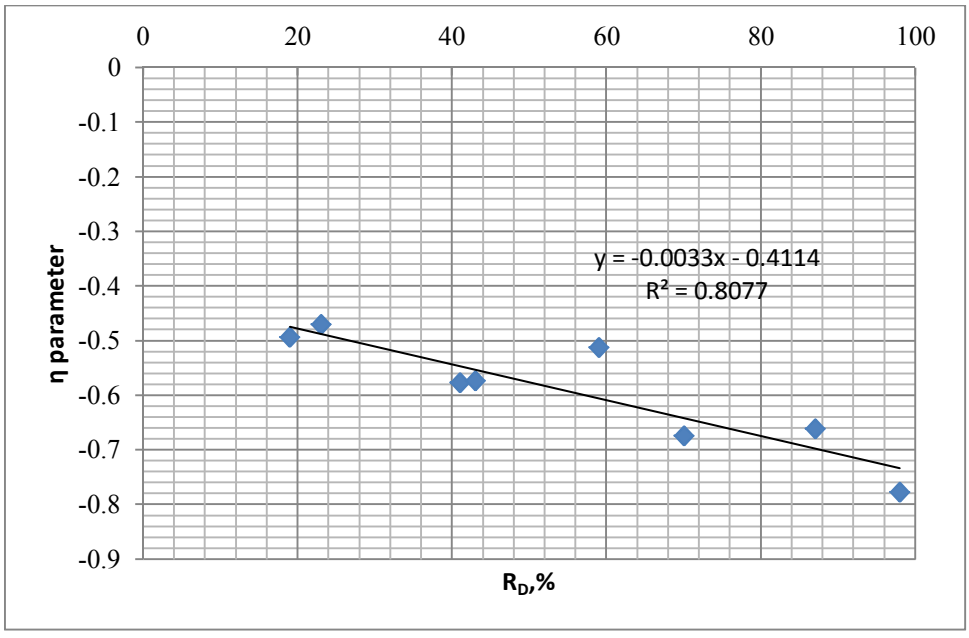


(b)

Figure 4.9. Variation of fitting parameters with R_D , for $\sigma'_v = 30\ Kpa$ a)ζparameter b) η parameter.

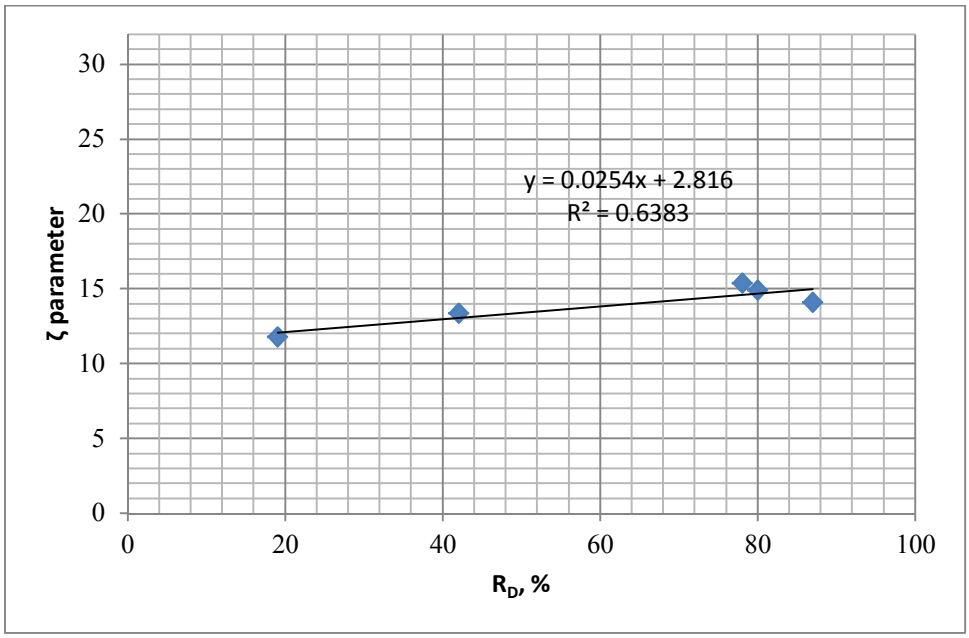


(a)

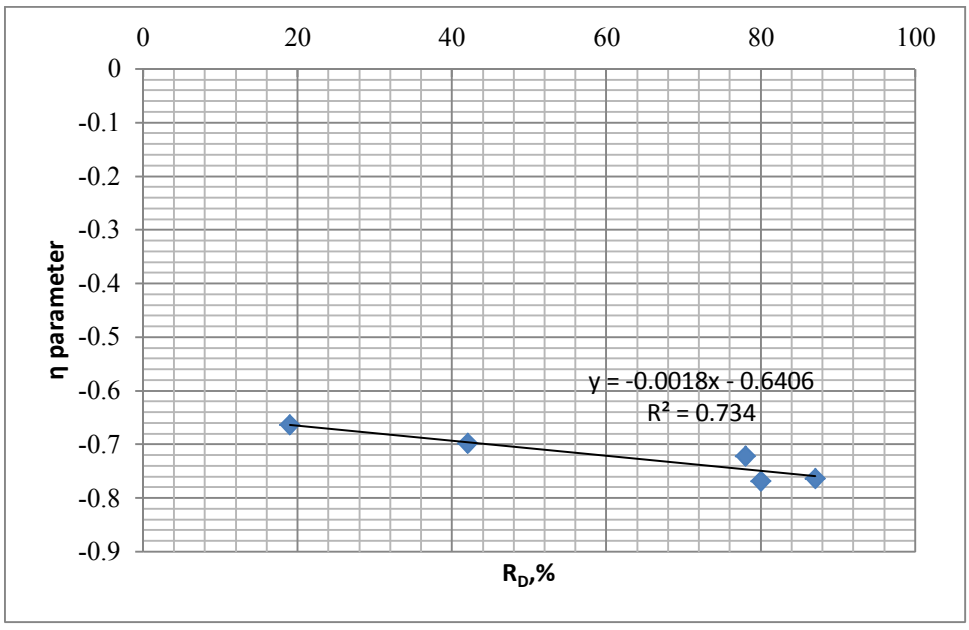


(b)

Figure 4.10. Variation of fitting parameters with R_D , for $\sigma'_v = 50\ Kpa$ a)ζparameter b) η parameter.



(a)



(b)

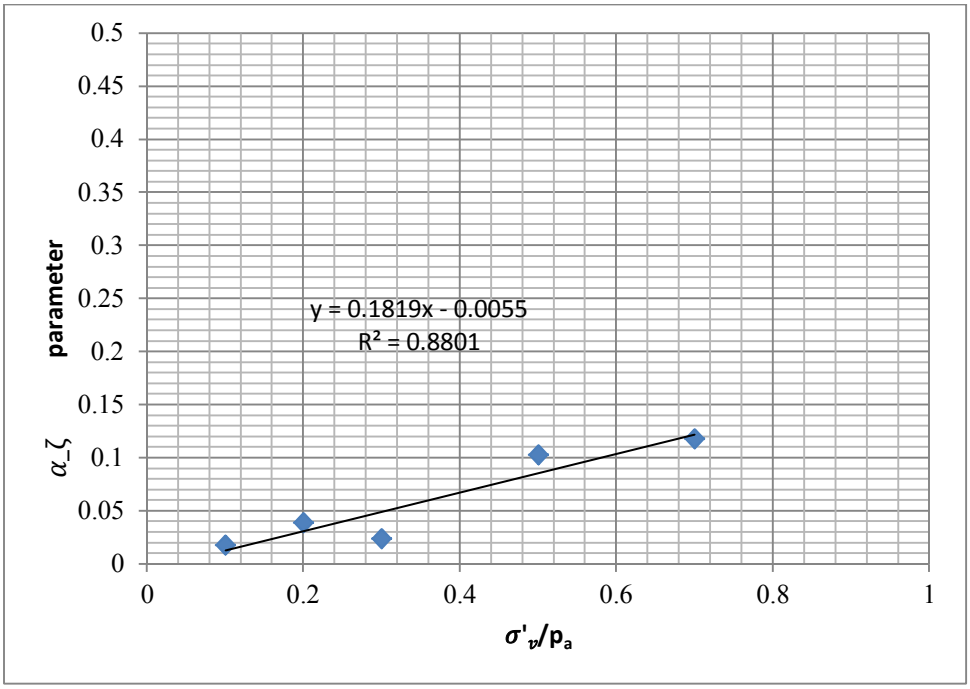
Figure 4.11. Variation of fitting parameters with R_D , for $\sigma'_v = 70\ Kpa$ a)ζparameter b) η parameter.

Table 4.3 is summary of the equations corresponding and R^2 value of trend-lines for ζ and η parameters. Since Equation 4.4 is dependent both on σ'_v and R_D , so, this time, to

consider the effect of σ'_v on G function, we need to monitor variations of α_ζ , β_ζ , α_η and β_η with respect to normalized vertical effective stress(σ'_v/P_a), as shown on Figure 4.12. Values of α_ζ , β_ζ , α_η and $\beta_\eta$are available at Table 4.4.

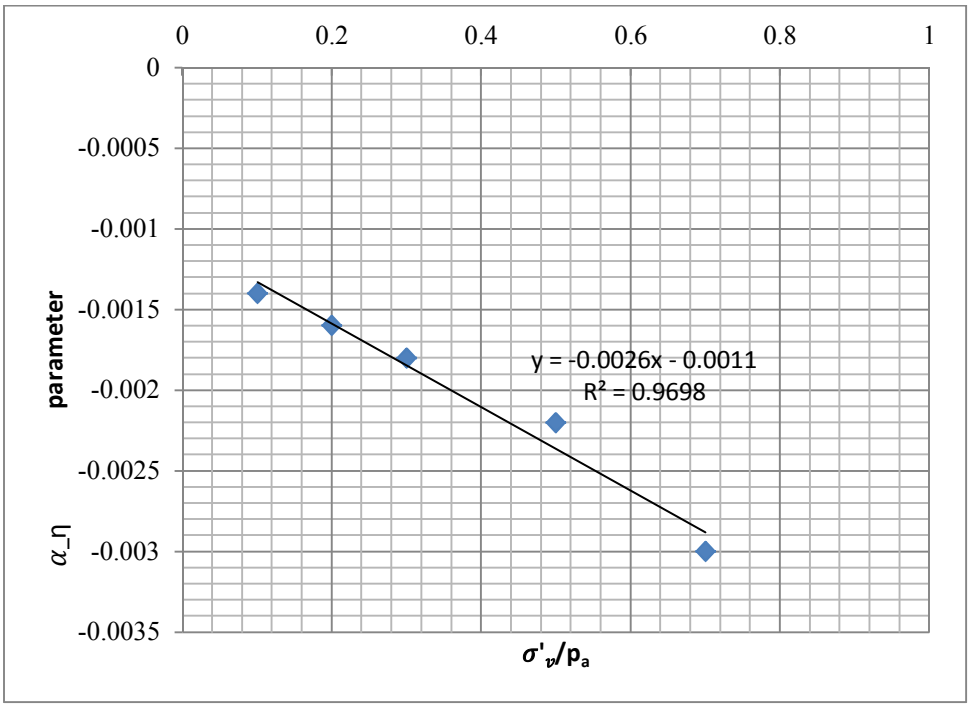
Table 4.3.Summary of the equations corresponding to trend-lines for ζ and η parameters.

σ'_v, Kpa	Equation forζ parameter	R^2	Equation for η parameter	R^2
10	ζ = 0.0254x + 2.816	0.6383	η = -0.0018x - 0.6406	0.734
20	ζ = 0.0202x + 3.5385	0.9455	η = -0.0016x - 0.5091	0.9947
30	ζ = 0.0254x + 2.816	0.6383	η = -0.0018x - 0.6406	0.734
50	ζ = 0.0616x + 5.7132	0.6078	η = -0.0033x - 0.4114	0.8077
70	ζ = 0.0954x + 2.816	0.6383	η = -0.0018x - 0.6406	0.734

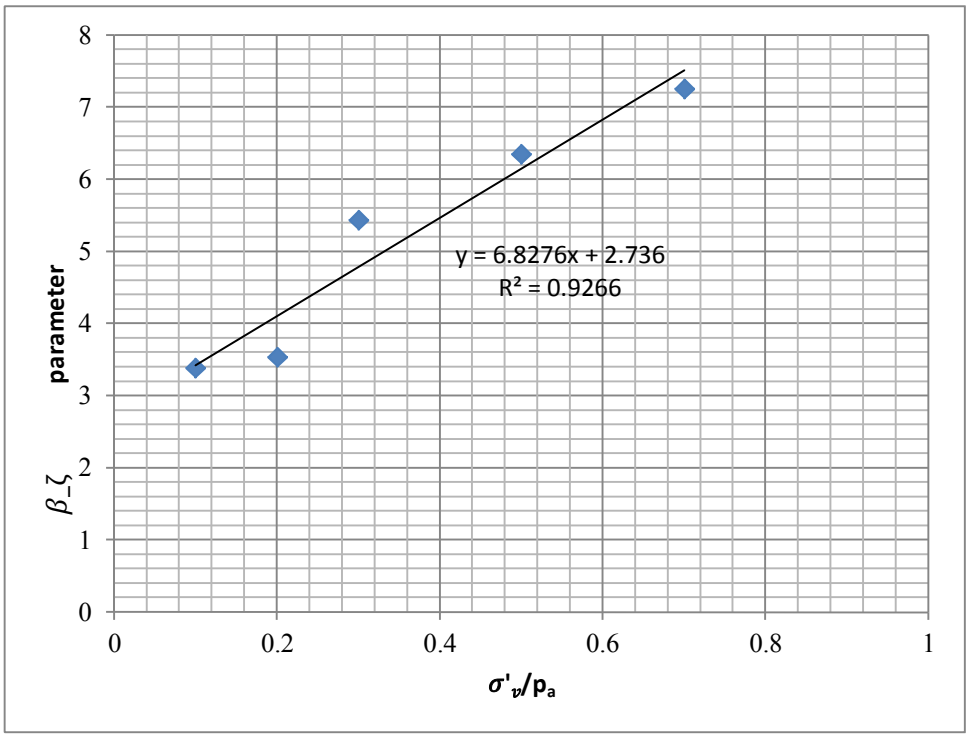


(a)

Figure 4.12. Fitting parameters variation with σ'_va)$\alpha_\zeta - \sigma'_v/p_a$.

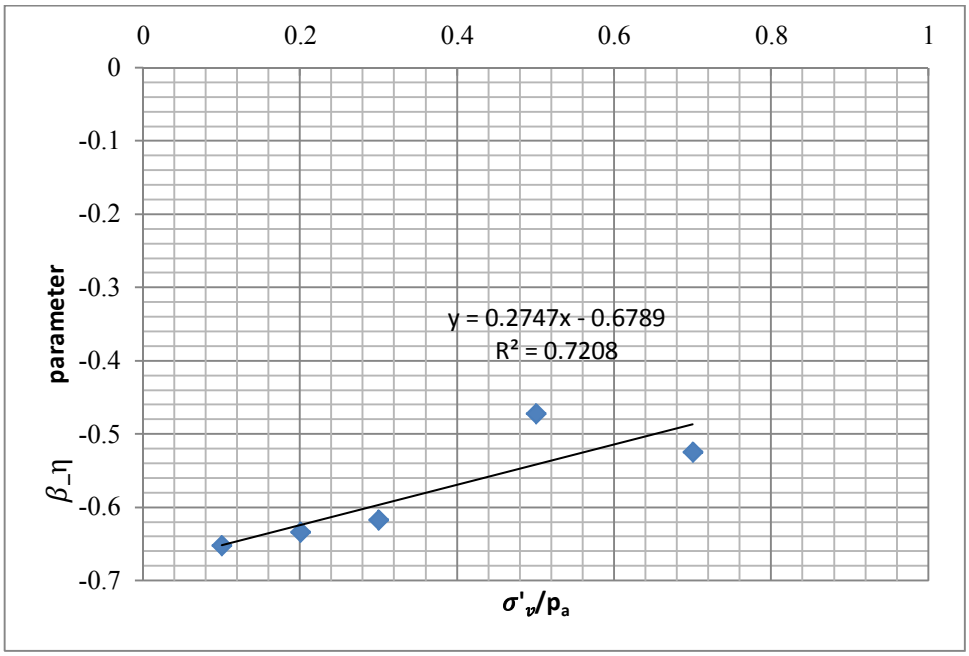


(b)



(c)

Figure 4.12. Fitting parameters variation with σ'b) $\alpha_\eta - \sigma'_v/p_a$ and c) $\beta_\zeta - \sigma'_v/p_a$ (Cont.).



(d)

Figure 4.12. Fitting parameters variation with σ', d) $\beta_\eta - \sigma'_v/p_a$(Cont.).

Table 4.4. Fitting parameters variation with σ'_v.

σ'_v, Kpa	α_ζ	β_ζ	α_η	β_η
10	1.7477	3.383	-0.0014	-0.6525
20	3.8933	3.5385	-0.0016	-0.634
30	2.3506	5.4418	-0.0018	-0.6172
50	10.241	6.34935	-0.0022	-0.4721
70	11.778	7.2569	-0.003	-0.5244

As it can be seen on Figure 4.12, a general linear equation can be defined for the fitting parameters:

$$\alpha_\zeta = k_1 \frac{\sigma'_v}{P_a} + k_2 \qquad (4.8)$$

$$\alpha_\eta = k_3 \frac{\sigma'_v}{P_a} + k_4 \qquad (4.9)$$

$$\beta_\zeta = k_5 \frac{\sigma'_v}{P_a} + k_6 \qquad (4.10)$$

$$\beta_\eta = k_7 \frac{\sigma'_v}{P_a} + k_8, \qquad (4.11)$$

where, $k_{1,\ldots,8}$ are fitting parameters of α_ζ , β_ζ , α_η and β_η for values are summarized in table 4.5.

Table 4.6gives a summary of the parameters of the equations and the corresponding R^2 values of the trend-lines for α_ζ , β_ζ , α_η and β_η parameters. Inserting the unit-independent parameters into Equation 4.6, our mathematical equation for variation of G with respect to σ'_v , R_D and γ can be computed. Equation 4.12 is a power function that let us to have shear modulus in any shear strain between 0.1 to 10 % :

$$\frac{G}{P_a} = \left[\left(k_1\left(\frac{\sigma'_v}{P_a}\right) + k_2\right)R_D + k_3\left(\frac{\sigma'_v}{P_a}\right) + k_4\right] * \gamma^{\left[\left(k_5\left(\frac{\sigma'_v}{P_a}\right)+k_6\right)R_D + k_7\left(\frac{\sigma'_v}{P_a}\right)+k_8\right]} \qquad (4.12)$$

Table 4.5. Summary of $k_{1,\ldots,8}$ values of trend-lines for α_ζ , β_ζ , α_η and β_η parameters.

k_1	k_2	k_3	k_4	k_5	k_6	k_7	k_8
0.1819	- 0.0055	6.8276	2.736	-0.0026	- 0.0011	0.2747	- 0.6789

Table 4.6. Summary of fitting constants and corresponding R^2 value of trend-lines for α_ζ , β_ζ , α_η and β_η parameters.

Unit-independent parameter	Corresponding linear equation	R^2
α_ζ	α_ζ= 0.1819x - 0.0055	0.8801
α_η	α_η= -0.0026x - 0.0011	0.9698
β_ζ	β_ζ= 6.8276x + 2.736	0.9266
β_η	β_η= 0.2747x - 0.6789	0.7208

4.2.Standard Ottawa graded sand DSS test results

Table 4.7 gives the details of the DSS tests conducted during the experimental program for standard Ottawa graded sand. In this table, vertical effective stress during both

consolidation and shear phases, void ration and also relative density of the samples are shown.

Table 4.7. Details of DSS tests conducted on standard Ottawa graded sand.

vertical Effective Stress, σ_v' Kpa	Void Ratio, e	Relative Density, %
10	0.73	58.0
10	0.67	73.5
10	0.56	99.9
10	0.64	79.5
50	0.65	76.3
50	0.71	61.8
50	0.74	54.5
50	0.67	73.0
70	0.71	61.4
70	0.70	66.0
70	0.61	87.0
70	0.77	47.3
70	0.58	94.7
70	0.64	79.5
70	0.74	54.4
90	0.77	47.4
90	0.73	57.1
90	0.74	55.1
90	0.60	89.4
90	0.72	60.4
90	0.63	81.3
90	0.58	94.9
90	0.70	65.6
90	0.63	82.5
90	0.62	85.8
90	0.58	94.8
110	0.72	60.1
110	0.74	56.2
110	0.61	86.3
110	0.74	54.1
110	0.66	74.7
110	0.65	77.4
110	0.57	96.3
110	0.57	98.3
110	0.68	70.0
110	0.72	59.0
110	0.62	84.7
130	0.77	47.3

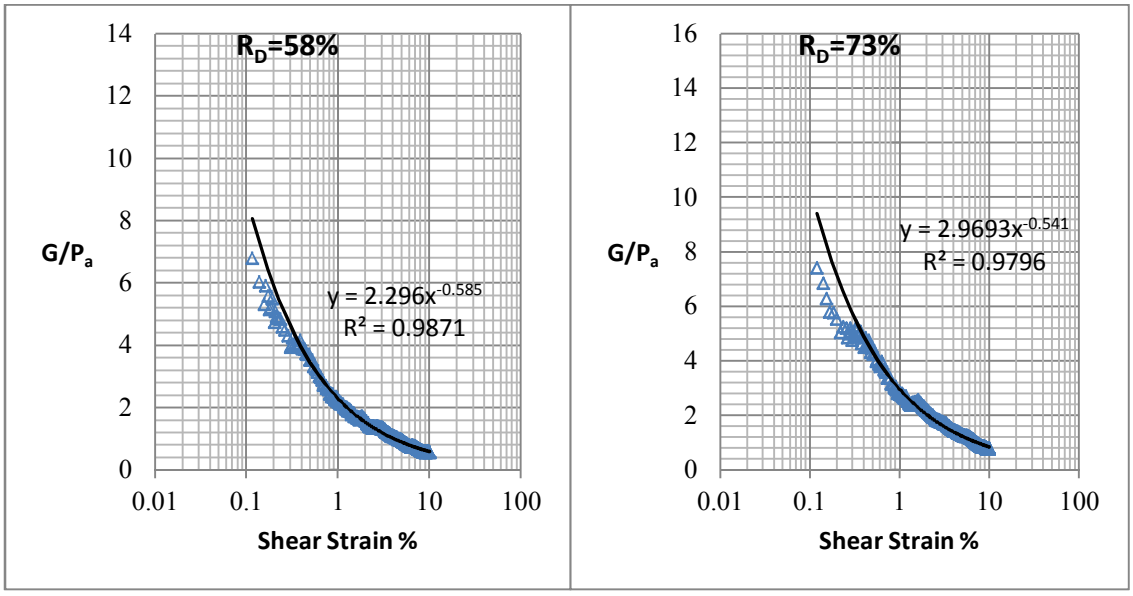
Table 4.6 Details of DSS tests conducted on standard Ottawa graded sand (cont.).

130	0.68	69.4
130	0.72	60.5
130	0.69	67.6
130	0.63	82.0
130	0.72	59.7
130	0.68	68.8
130	0.58	95.5
130	0.57	97.3
130	0.66	74.4
130	0.61	87.8
130	0.64	80.1
130	0.70	65.1
130	0.58	95.8
160	0.77	48.6
160	0.76	51.1
160	0.70	65.0
160	0.64	81.1
160	0.73	57.5
160	0.70	64.4
160	0.56	100.0
160	0.67	72.0
160	0.73	58.7
160	0.74	55.3
160	0.66	74.7
160	0.63	83.6
160	0.58	94.6
160	0.71	61.2
160	0.65	76.6
160	0.62	85.7
200	0.79	42.4
200	0.75	52.5
200	0.70	64.2
200	0.67	71.8
200	0.61	86.6
200	0.76	50.9
200	0.59	93.0
200	0.67	71.2
200	0.61	87.2
200	0.58	94.7
200	0.73	57.1

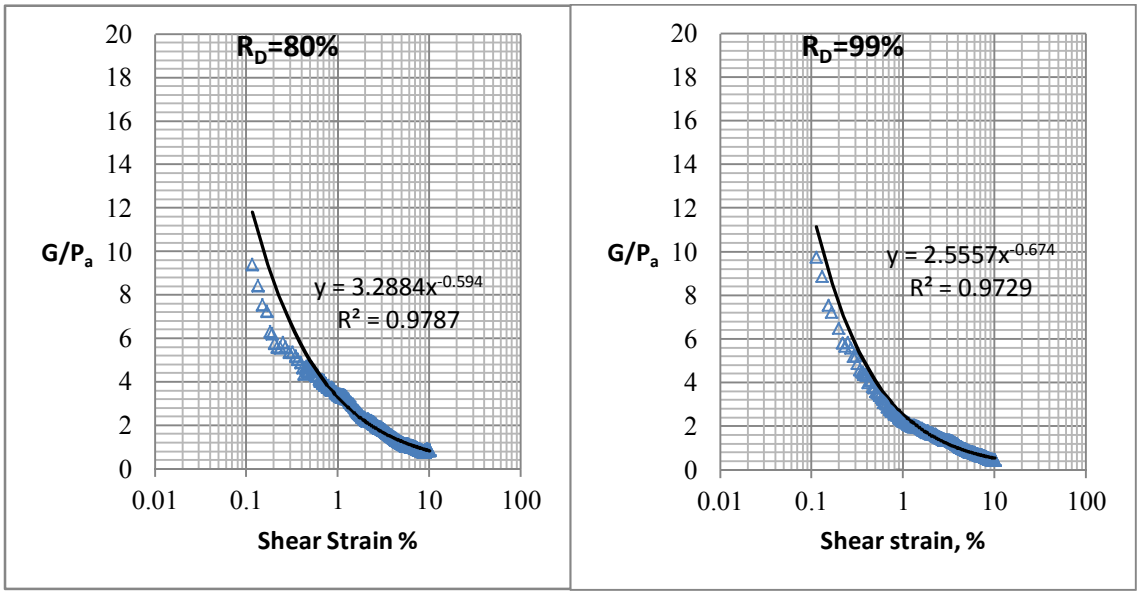
4.2.1. Effect of Relative Density on Shear Modulus of Standard Ottawa Graded Sand

As for the Silivri sand, tests were conducted on Ottawa graded sand (OGS) with constant vertical effective stress during consolidation and shear phases in order to monitor the variation of shear modulus with shear strain. Also, for each selected σ_v', the range

forshear strain boundary is defined between 0.1 and 10 %. It was mentioned in the previous section that, for obtaining unit-less coefficients, G is normalized with the atmospheric pressure ($P_a = 100Kpa$). The results are shown in Figures 4.13 to 4.20.

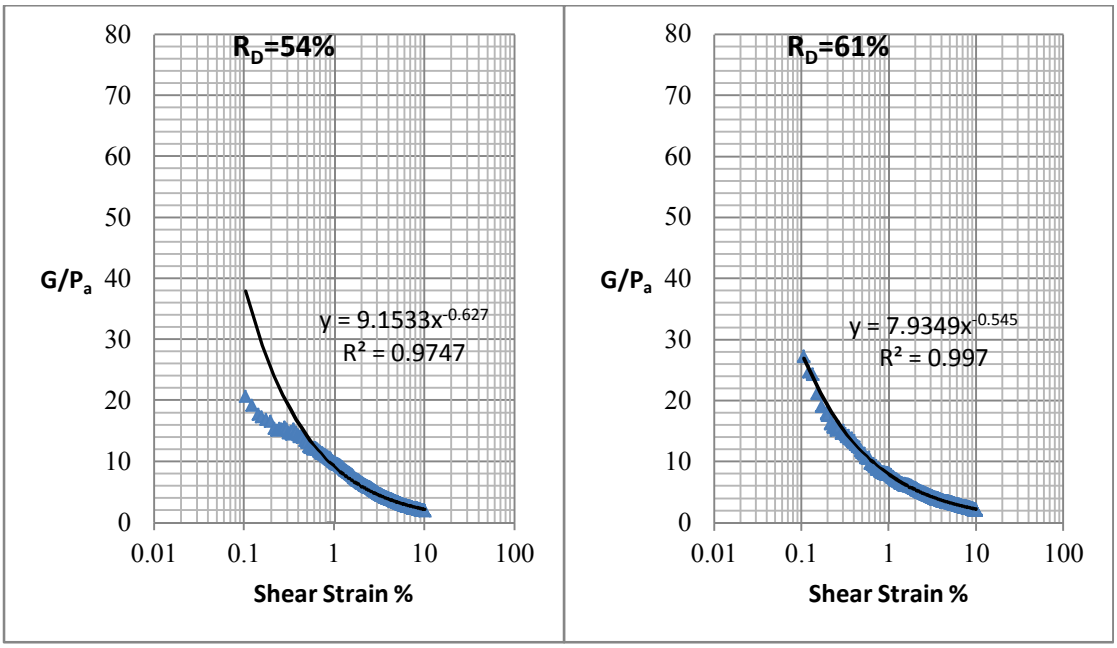


(a) (b)

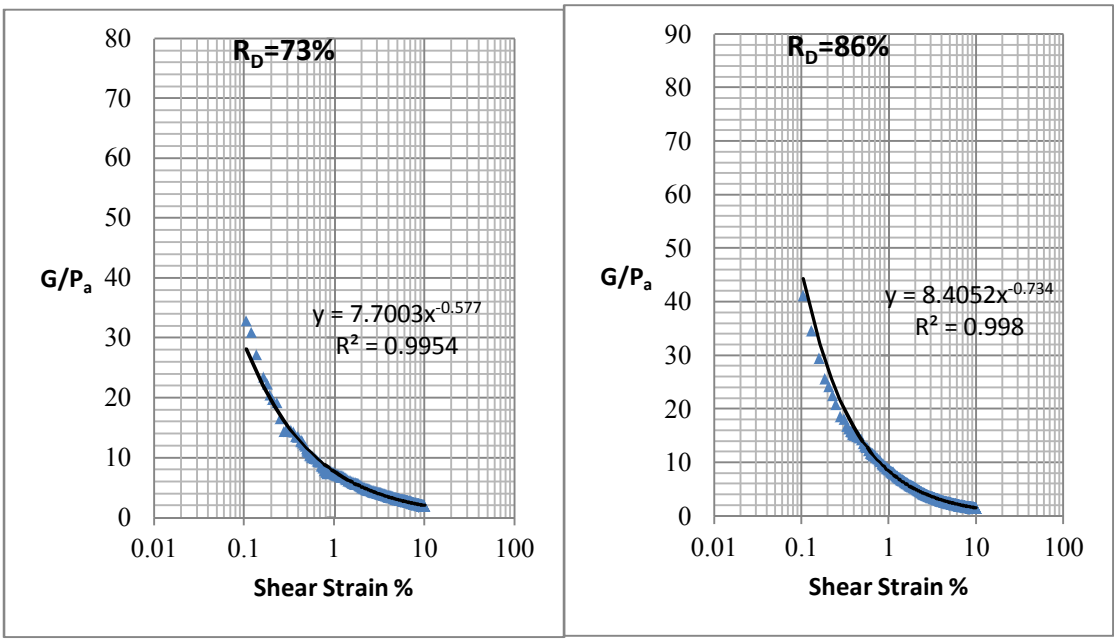


(c) (d)

Figure 4.13. Shear modulus variation with shear strain between 0.1 to 10 % for $\sigma'_v = 10\ Kpa$ a)$R_D = 58$ b)$R_D = 73$ c)$R_D = 80$ d)$R_D = 99$.

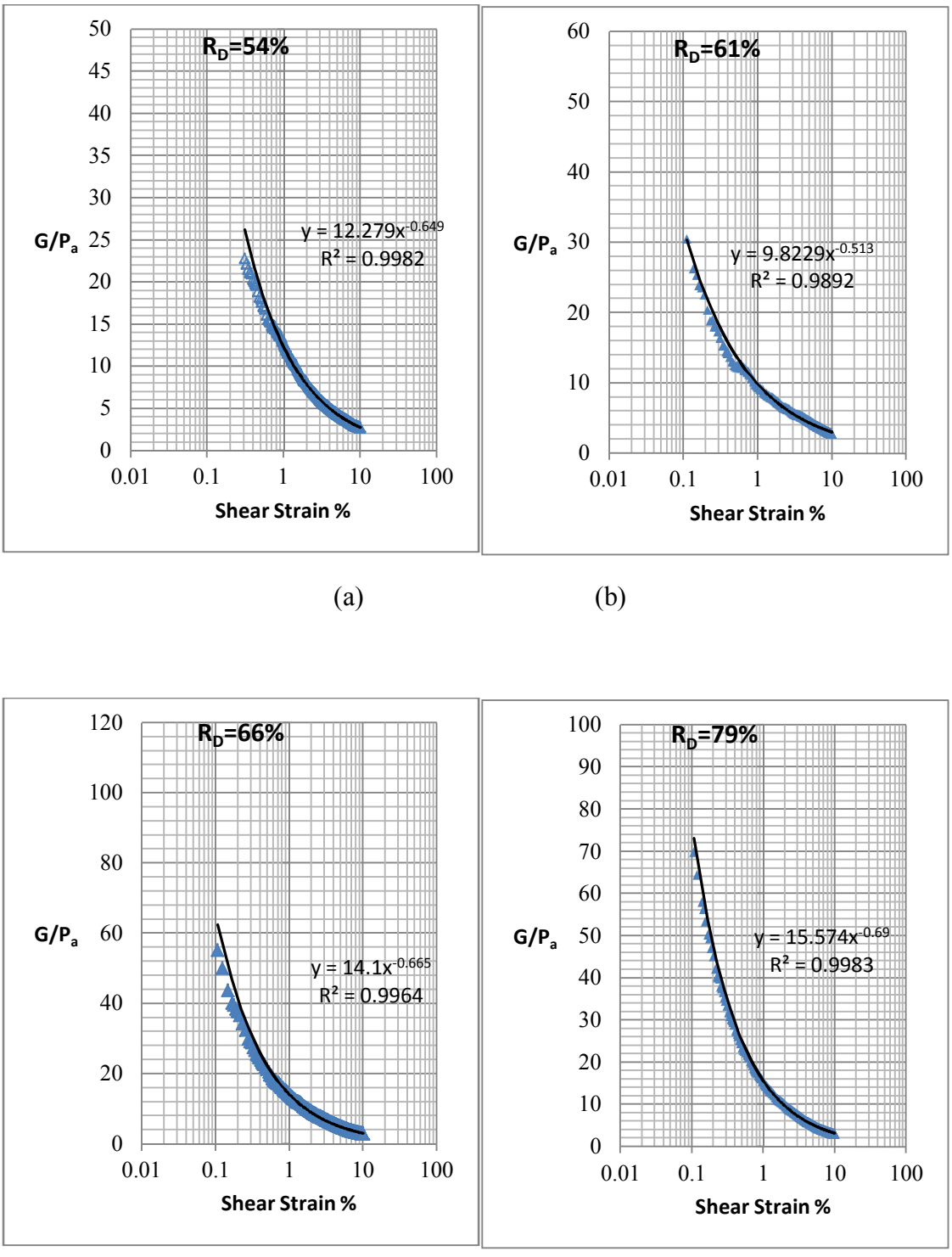


(a) (b)



(c) (d)

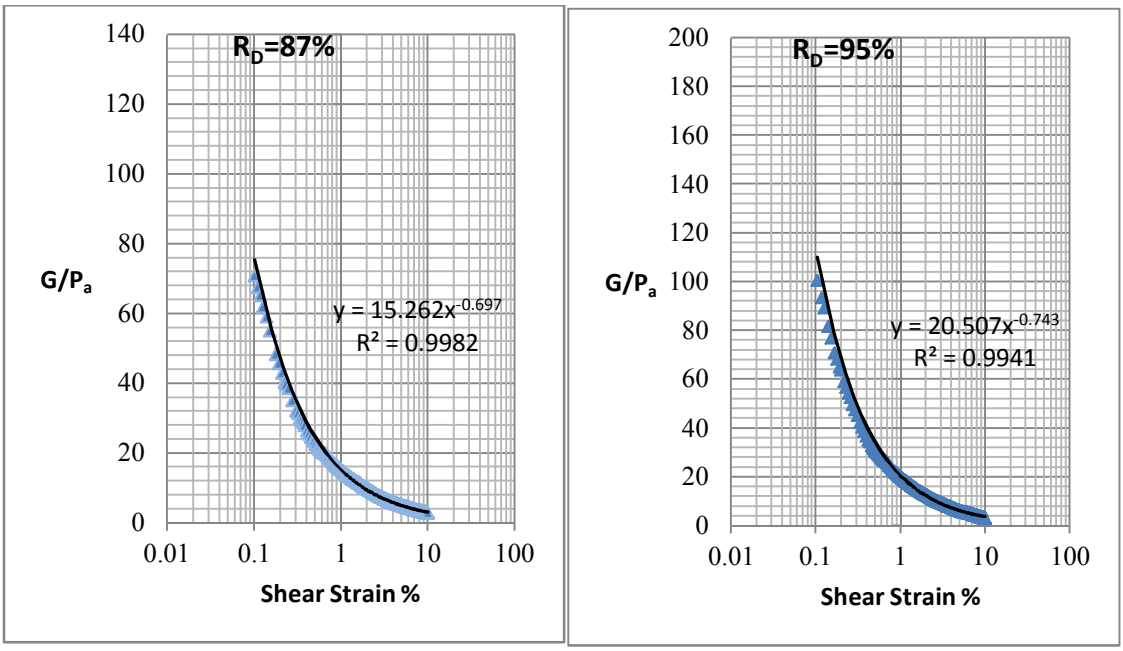
Figure 4.14. Shear modulus variation with shear strain between 0.1 to 10 % for$\sigma'_v = 50\ Kpa$ a)$R_D = 54$ b)$R_D = 61$ c)$R_D = 73$ d)$R_D = 86$.



(a) (b)

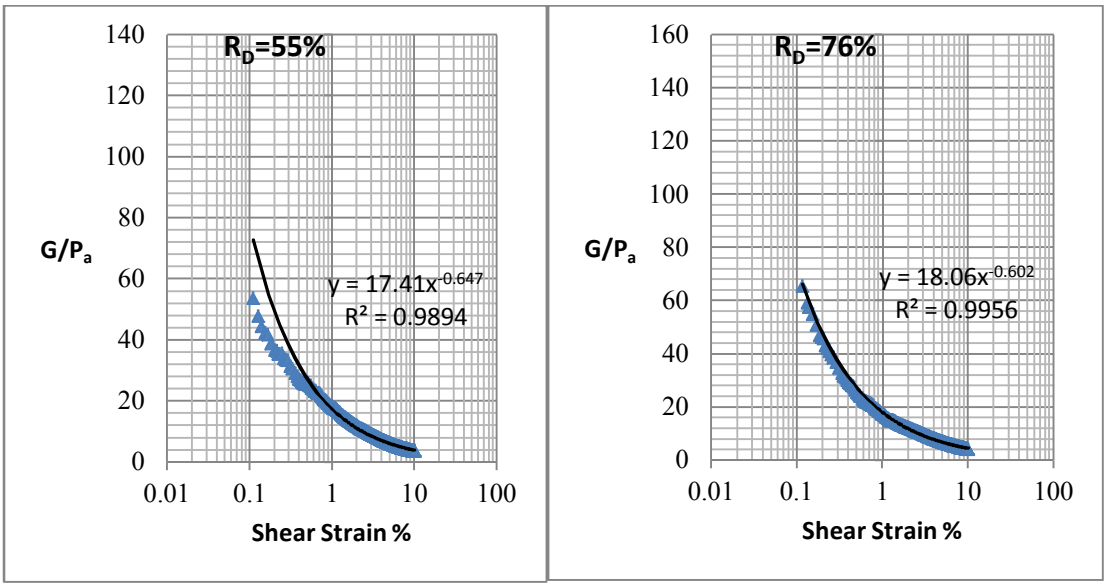
(c) (d)

Figure 4.15. Shear modulus variation with shear strain between 0.1 to 10 % for$\sigma'_v = 70\ Kpa$ a)$R_D = 54$ b)$R_D = 61$ c)$R_D = 66$ d)$R_D = 79$.



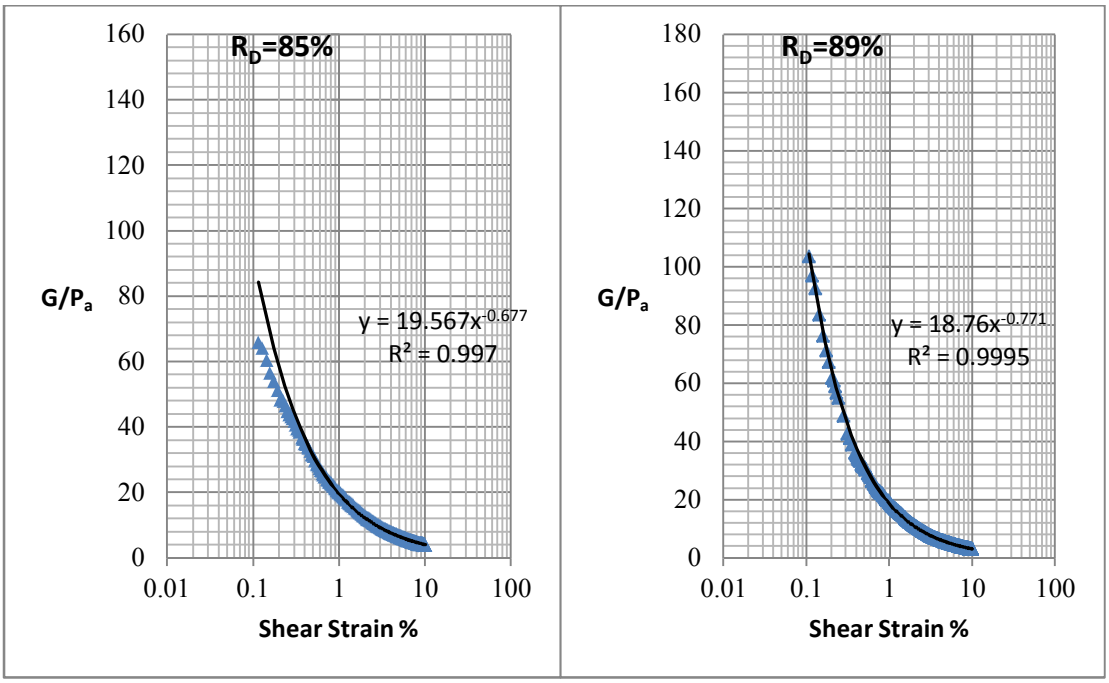
(e) (f)

Figure 4.15. Shear modulus variation with shear strain between 0.1 to 10 % for$\sigma'_v = 70\ Kpa$e)$R_D = 87$ f)$R_D = 95$ (Cont.).

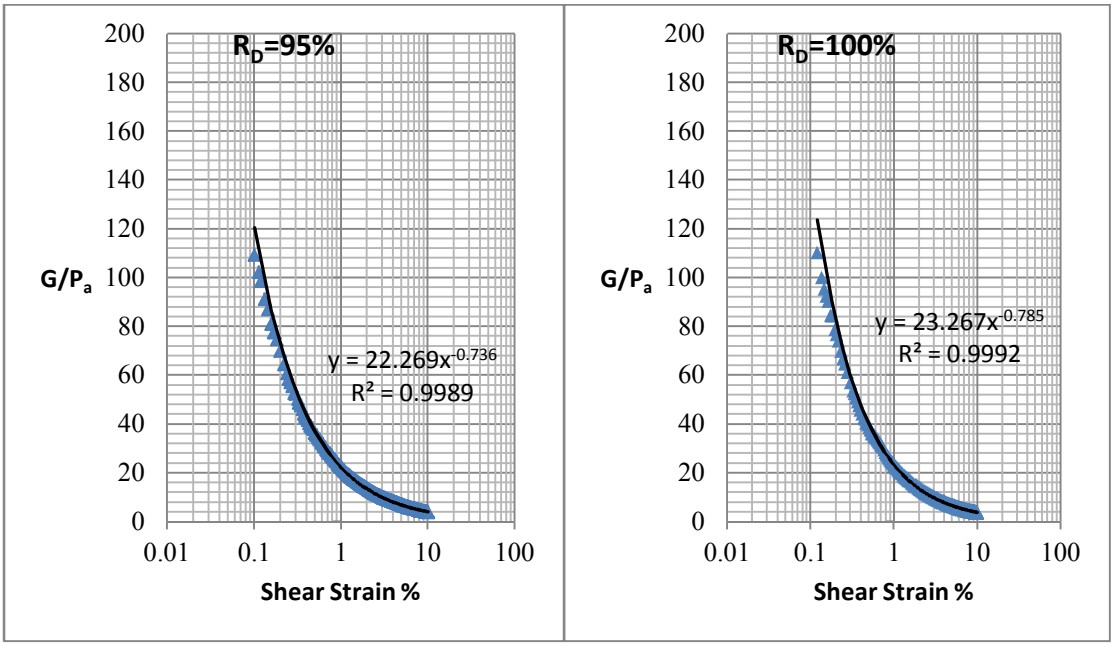


(a) (b)

Figure 4.16. Shear modulus variation with shear strain between 0.1 to 10 % for$\sigma'_v = 90\ Kpa$ a)$R_D = 55$ b)$R_D = 76$.

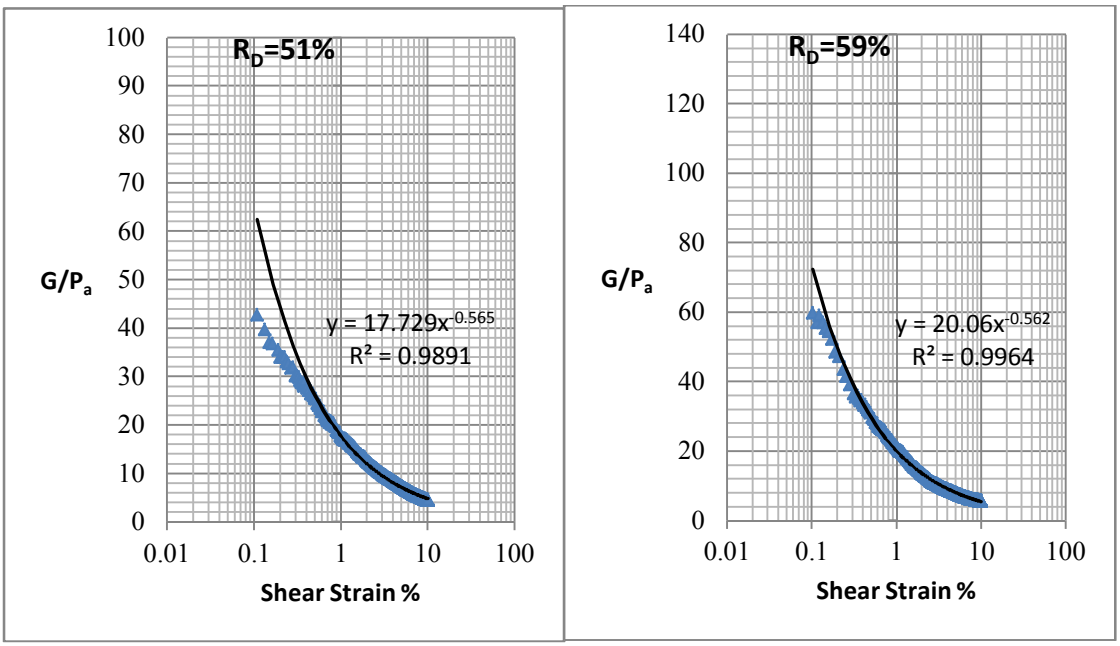


(c) (d)

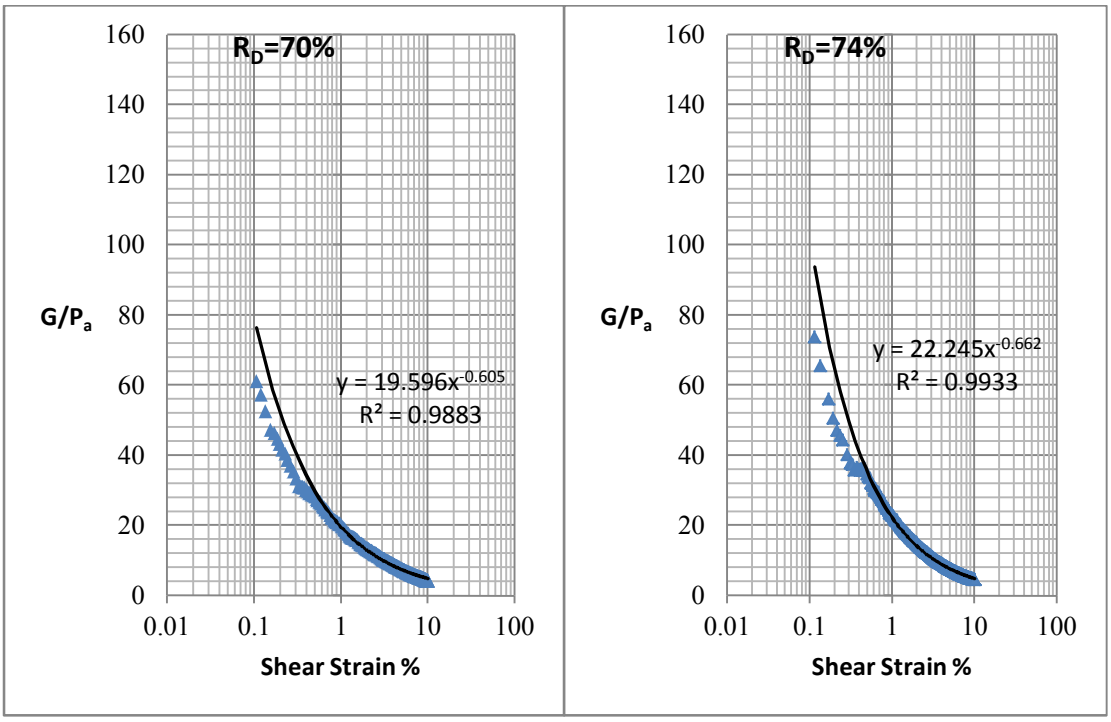


(e) (f)

Figure 4.16. Shear modulus variation with shear strain between 0.1 to 10 % for $\sigma'_v = 90\ Kpa$c)$R_D = 85$ d)$R_D = 89$ e)$R_D = 95$ f)$R_D = 100$ (Cont.).

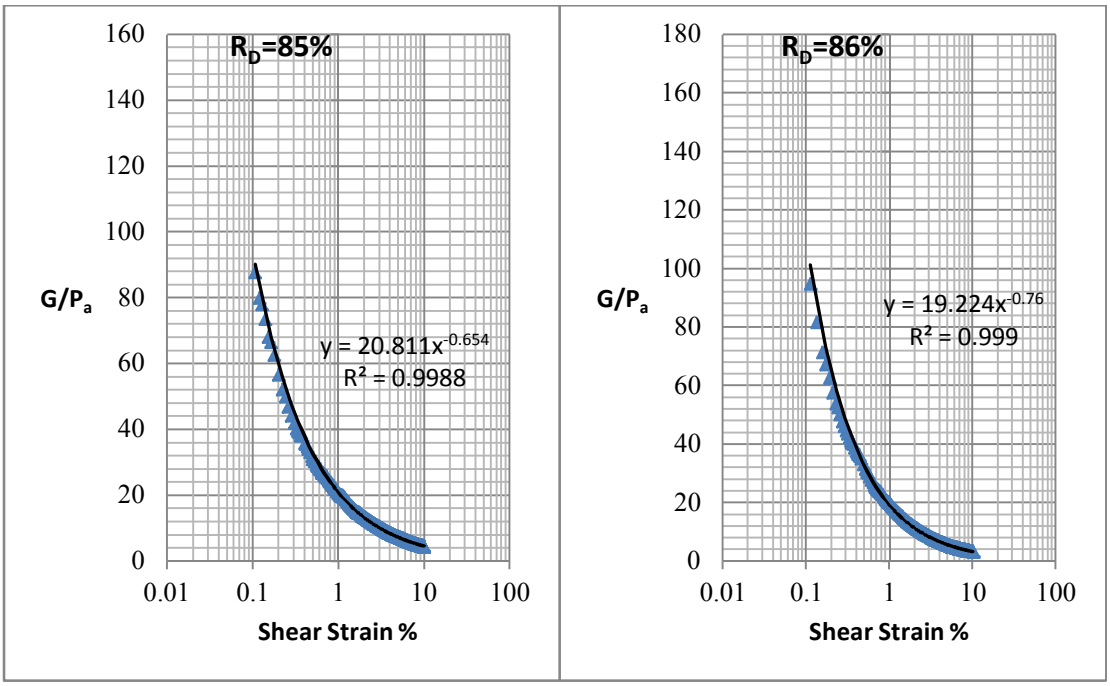


(a) (b)

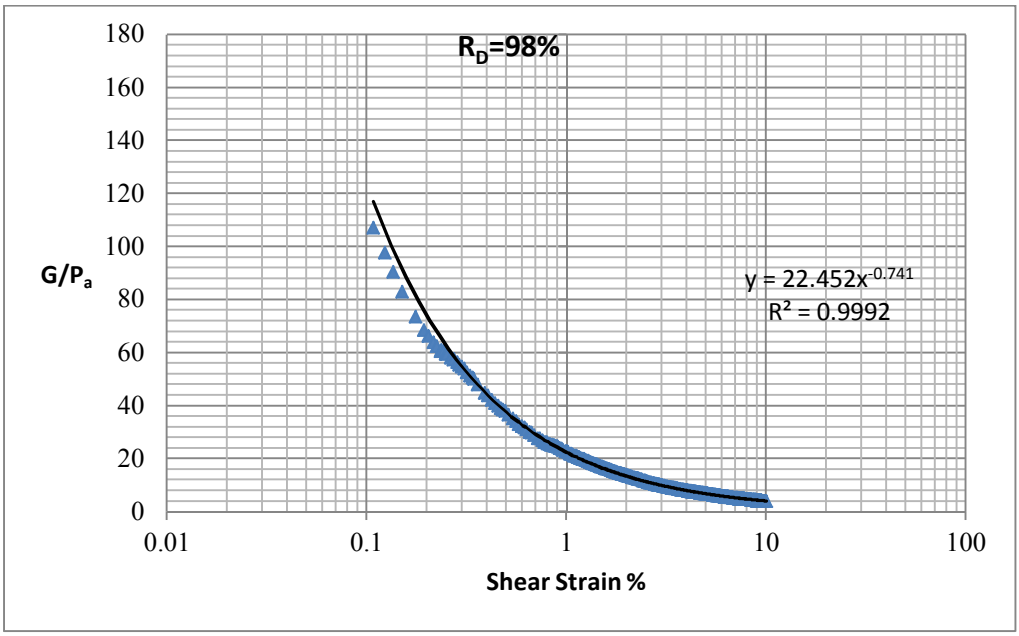


(c) (d)

Figure 4.17. Shear modulus variation with shear strain between 0.1 to 10 % for $\sigma'_v = 110\ Kpa$ a)$R_D = 51$ b)$R_D = 59$ c)$R_D = 70$ d)$R_D = 74$.

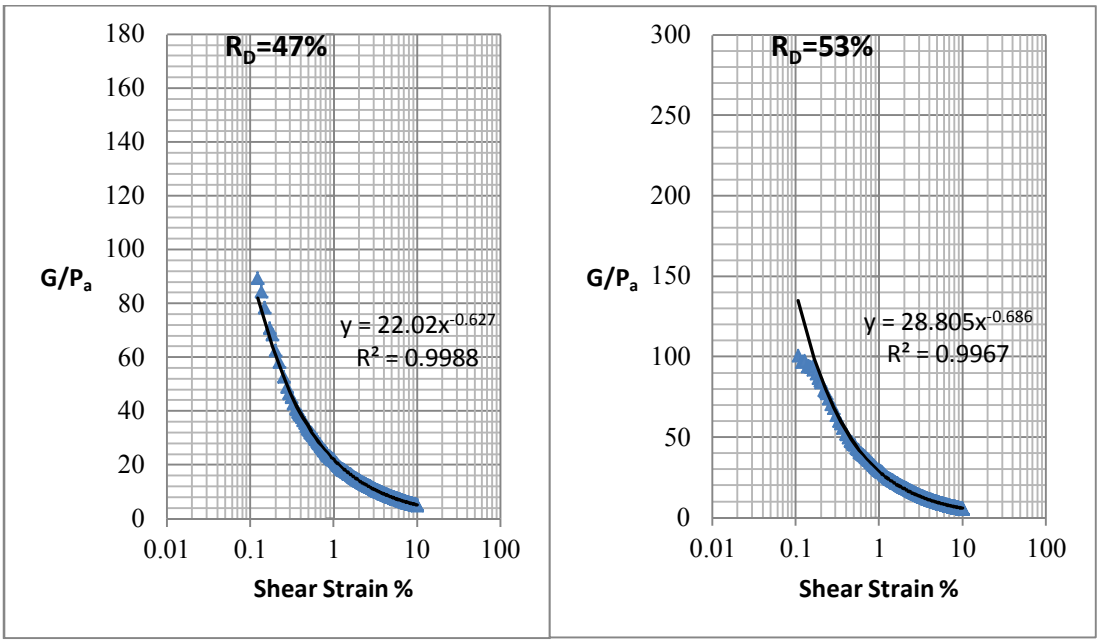


(e) (f)

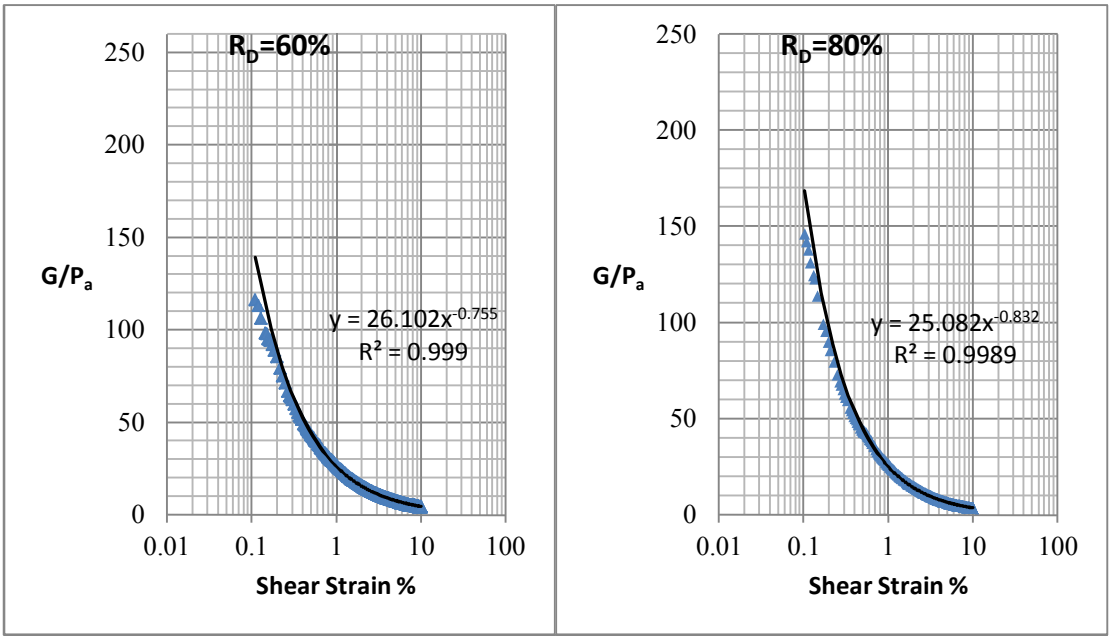


(g)

Figure 4.17. Shear modulus variation with shear strain between 0.1 to 10 % for $\sigma'_v = 110\ Kpa$e)$R_D = 85$ f)$R_D = 86$ g)$R_D = 98$ (Cont.).

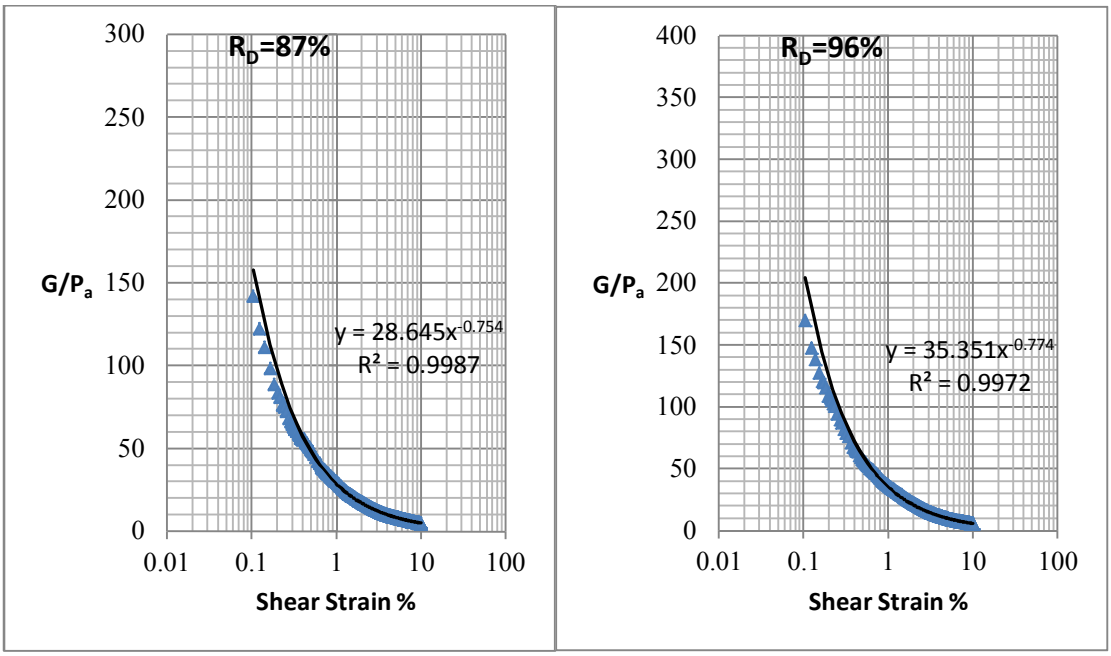


(a) (b)



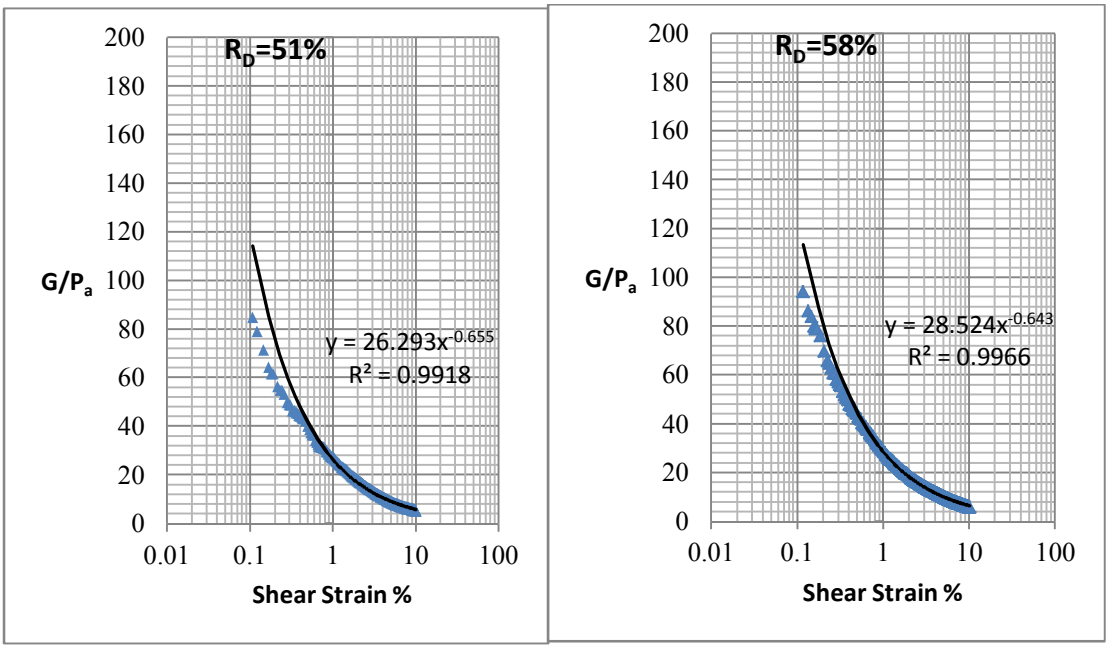
(c) (d)

Figure 4.18. Shear modulus variation with shear strain between 0.1 to 10 % for$\sigma'_v = 130\ Kpa$ a)$R_D = 47$ b)$R_D = 53$ c)$R_D = 60$ d)$R_D = 80$.



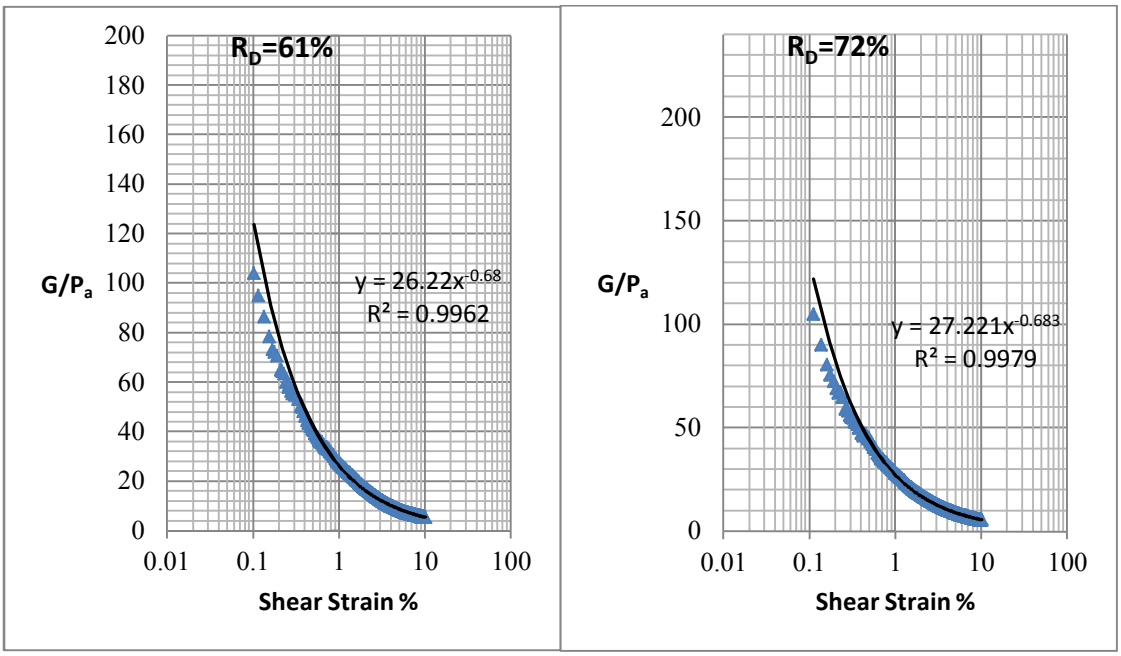
(e) (f)

Figure 4.18. Shear modulus variation with shear strain between 0.1 to 10 % for $\sigma'_v = 130\ Kpa$ e)$R_D = 87$ f)$R_D = 96$ (Cont.).

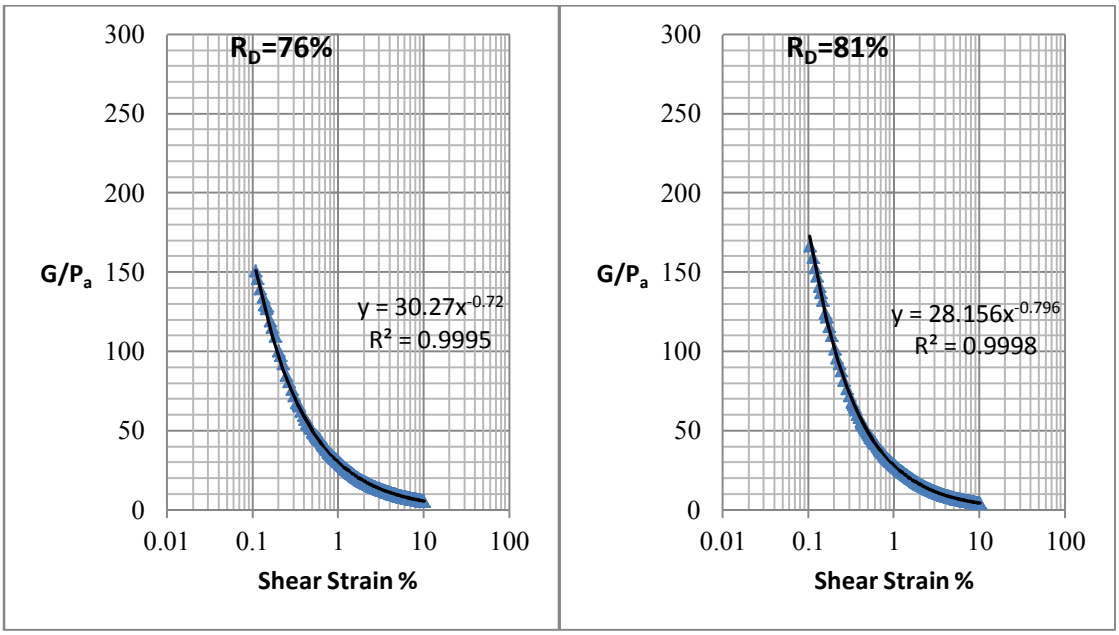


(a) (b)

Figure 4.19. Shear modulus variation with shear strain between 0.1 to 10 % for $\sigma'_v = 160\ Kpa$ a)$R_D = 51$ b)$R_D = 58$.

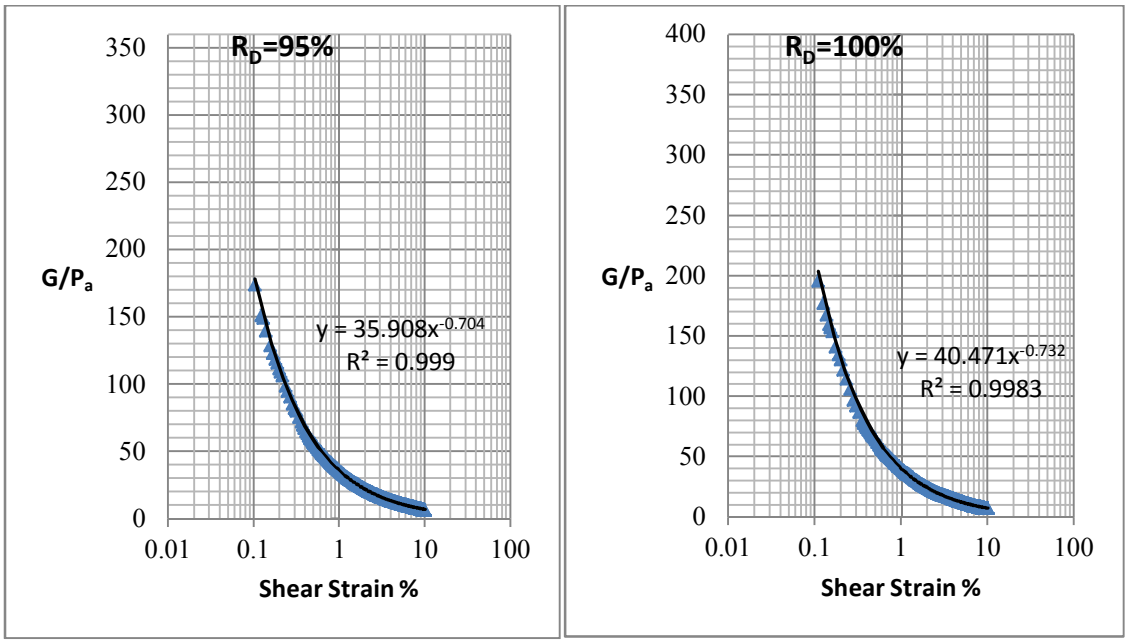


(b) (d)



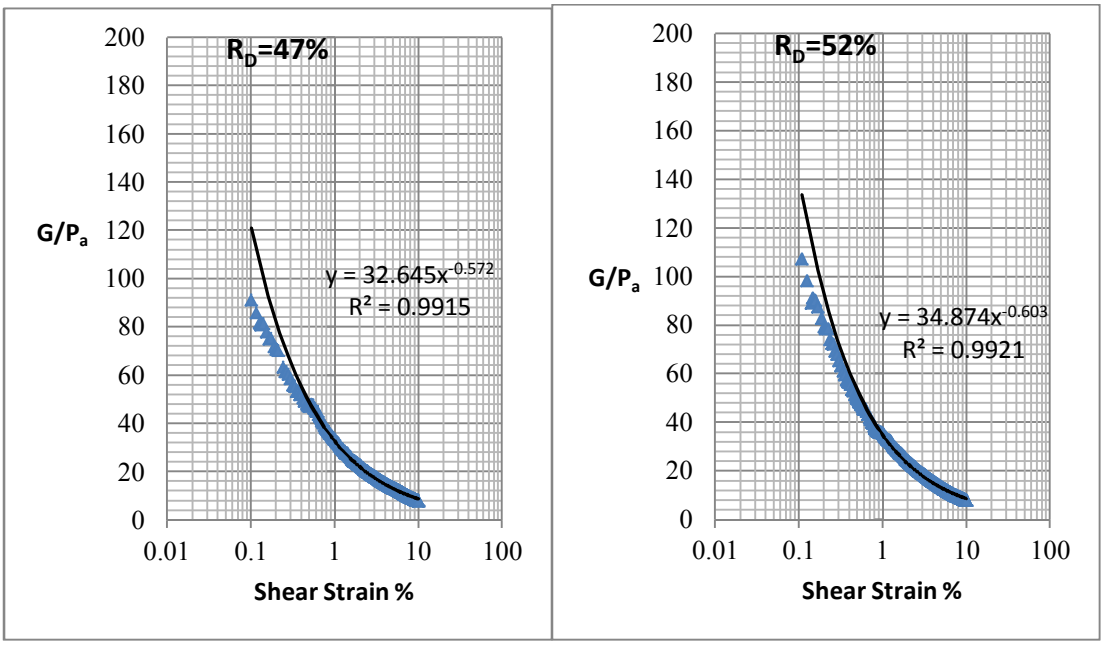
(e) (f)

Figure 4.19. Shear modulus variation with shear strain between 0.1 to 10 % for $\sigma'_v = 160\ Kpa$c)$R_D = 61$ d)$R_D = 72$ e)$R_D = 76$ f)$R_D = 81$ (Cont.).



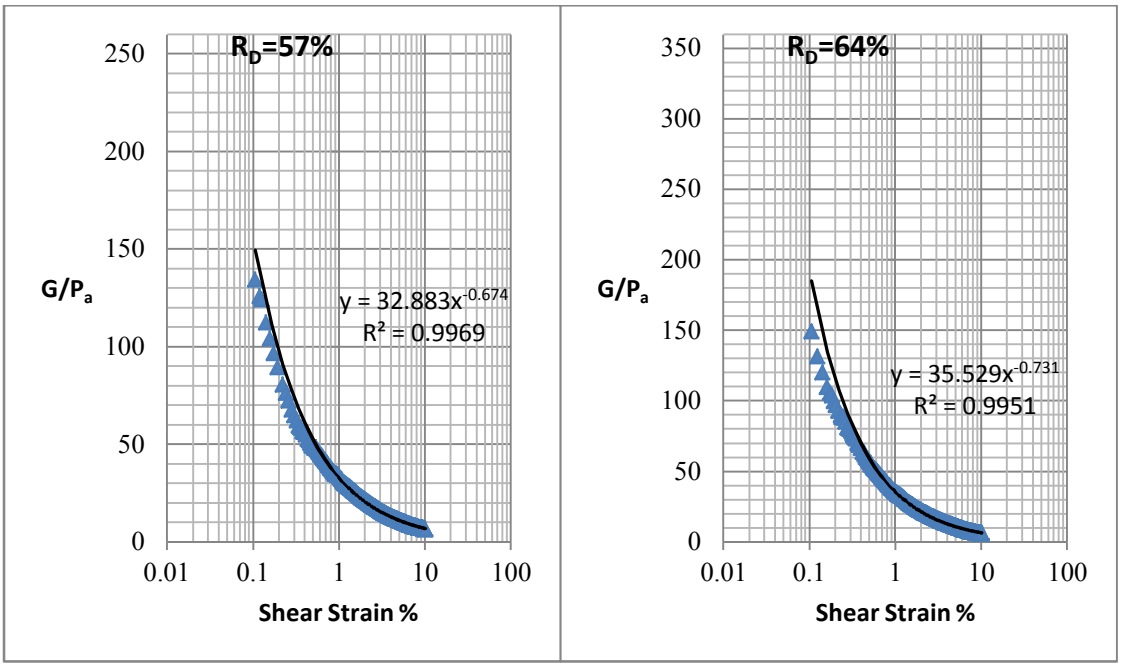
(g) (h)

Figure 4.19. Shear modulus variation with shear strain between 0.1 to 10 % for $\sigma'_v = 160\ Kpa$ g)$R_D = 95$ h)$R_D = 100$ (Cont.).

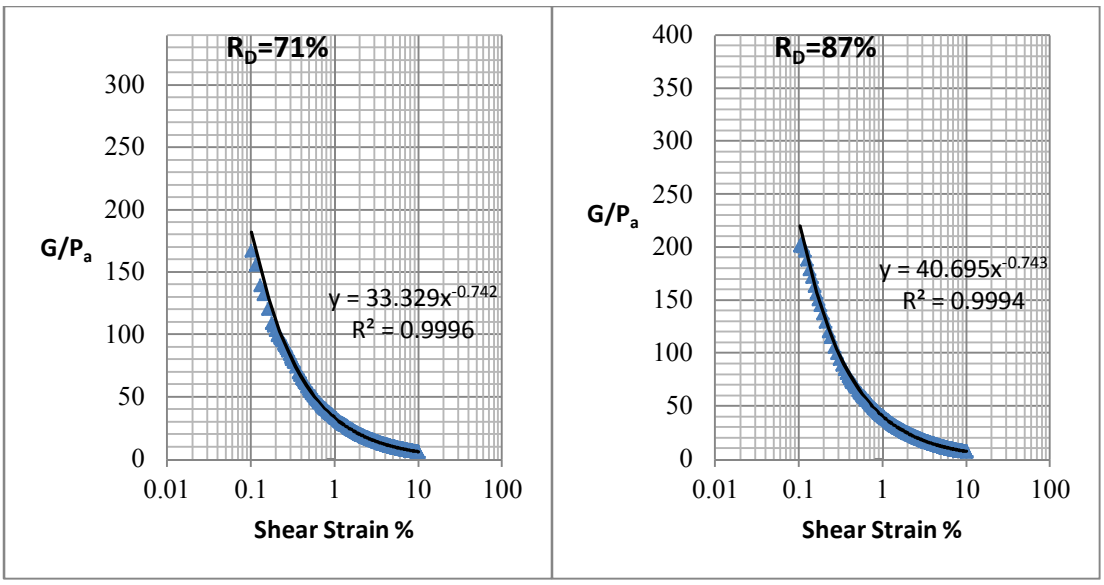


(a) (b)

Figure 4.20. Shear modulus variation with shear strain between 0.1 to 10 % for$\sigma'_v = 200\ Kpa$ a)$R_D = 47$ b)$R_D = 52$.

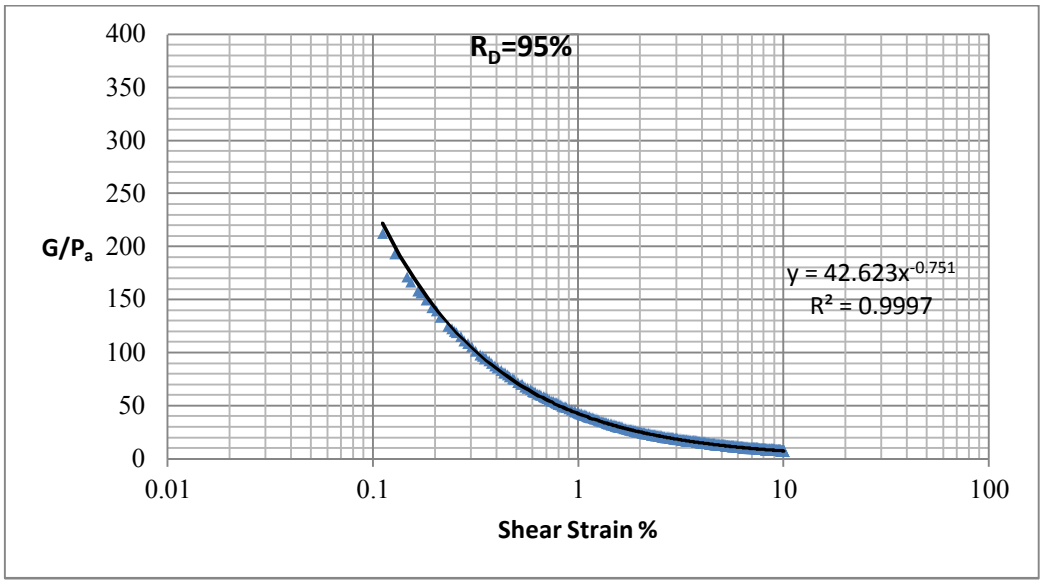


(b) (d)



(e) (f)

Figure 4.20. Shear modulus variation with shear strain between 0.1 to 10 % for $\sigma'_v = 200\ Kpa$c)$R_D = 57$ d)$R_D = 64$ e)$R_D = 71$ f)$R_D = 87$(Cont.).



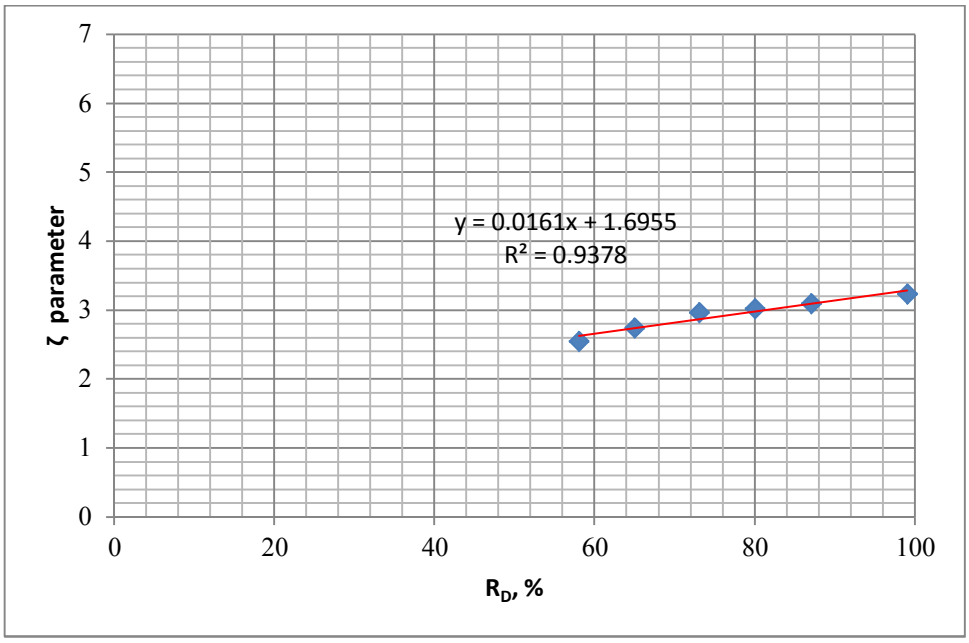
(g)

Figure 4.20. Shear modulus variation with shear strain between 0.1 to 10 % for $\sigma'_v = 200\ Kpag) R_D = 95$ (Cont.).

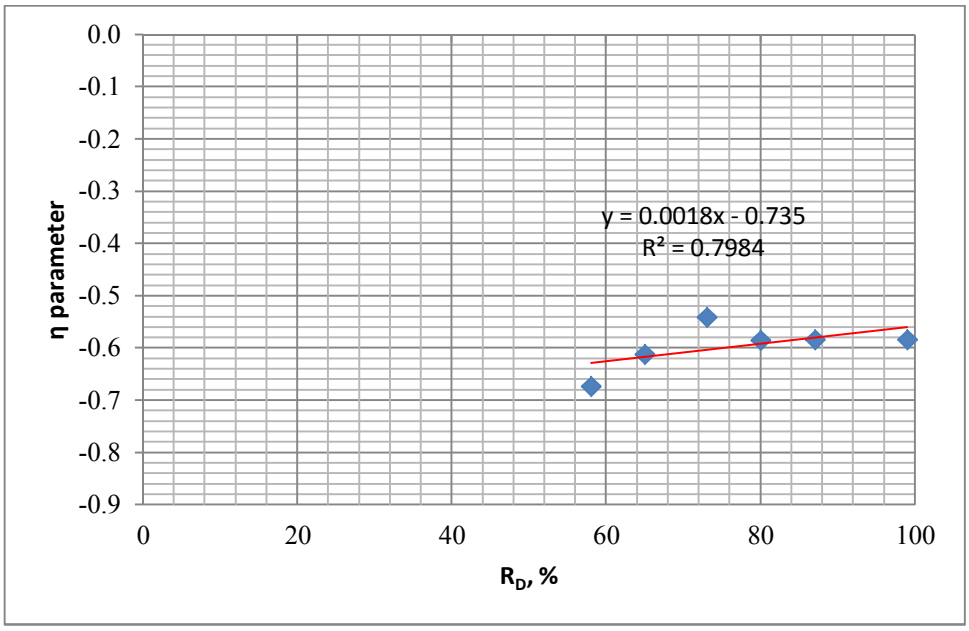
Figure 4.13 shows the results obtained from DSS test on standard Ottawa graded sand under a constant vertical stress of 10 Kpa. The relative density varies between58 and 99 % and the behavior of normalized shear modulus of the sand is plotted with respect to shear strain increment. Although σ_v' is constant during shearing for each test, since the R_D increases, the soil gains shear stiffness increases too, and so a higher G is observed. Respectively, the results of G/p_a vs. γ are plotted for $\sigma_v' = 50, \sigma_v' = 70, \sigma_v' = 90, \sigma_v' = 110,\ \sigma_v' = 130, \sigma_v' = 160\ and\ \sigma_v' = 200kpa$ as shown in Figures 4.14, 4.15, 4.16, 4.17, 4.18 , 4.19 and 4.20. A similar behavior was observed for the above mentioned vertical effective stresses.

4.2.2. Quantifying G As a Function of $\sigma'_v, R_D\ and\ \gamma$ for Standard Ottawa Graded Sand

Section 4.1.2 explained the method of relating unit-less fitting parameters (ζ and η) to relative density.$\sigma'_v$was kept as a constant and the variations of the unit-less parameters were plotted with respect to R_D, (ζ vs. R_D and η vs. R_D). Figures 4.21 to 4.28show variations of dependent variables (ζ and η) with respect to relative density.

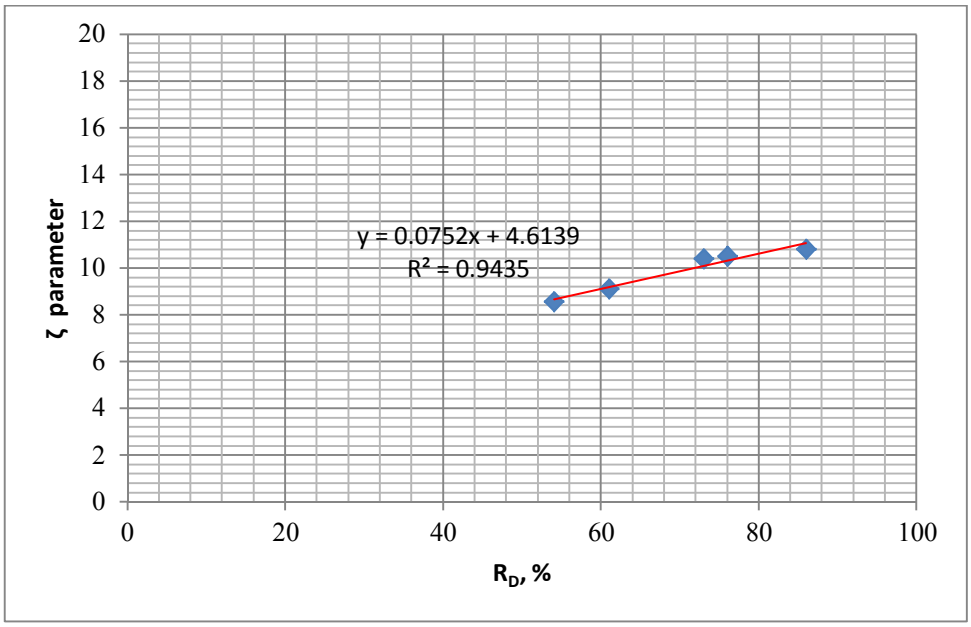


(a)

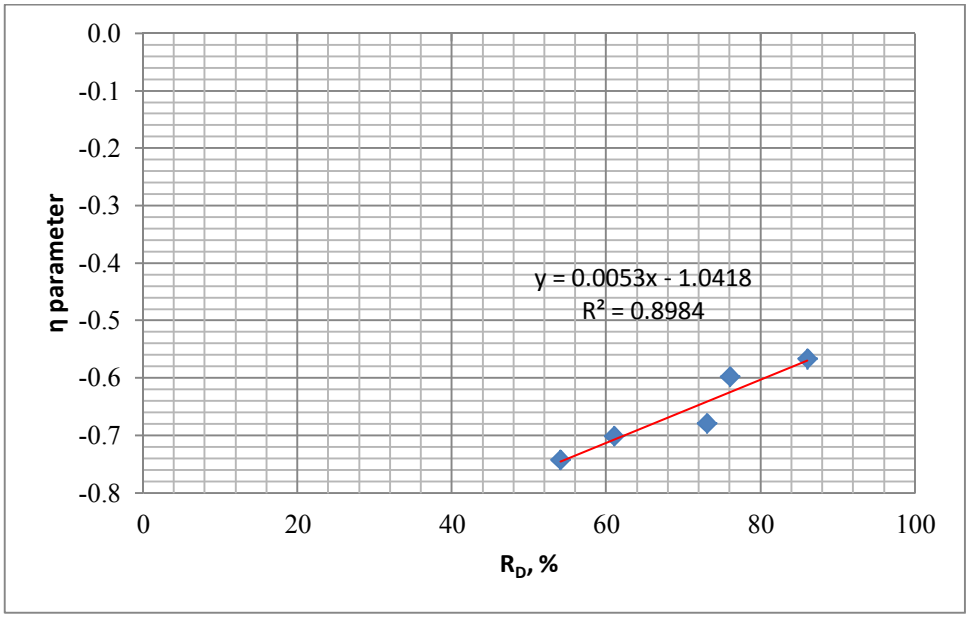


(b)

Figure 4.21. Variation of fitting parameters with R_D , for $\sigma'_v = 10\ Kpa$ a)ζparameter b) η parameter.

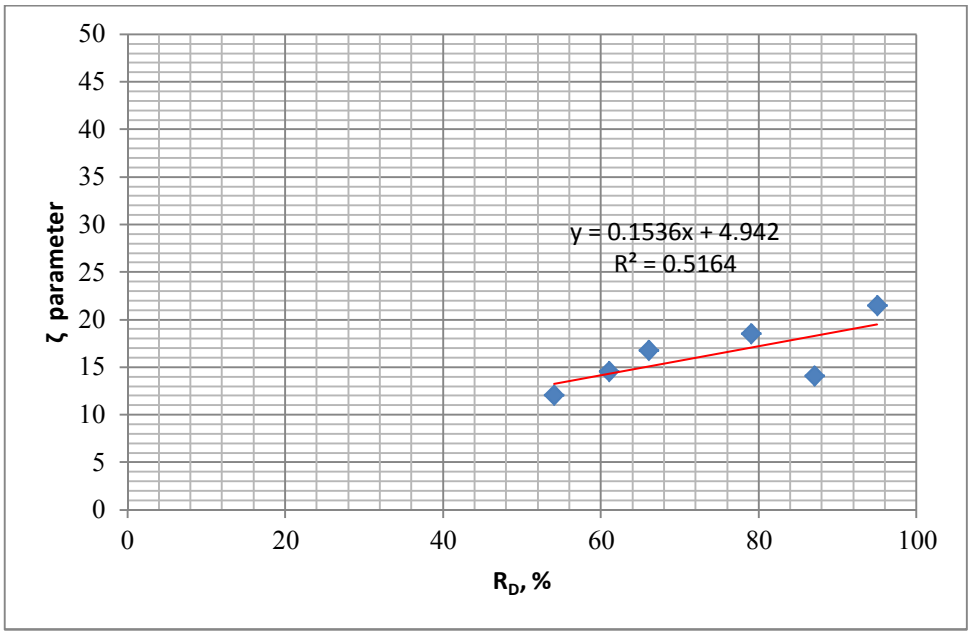


(a)

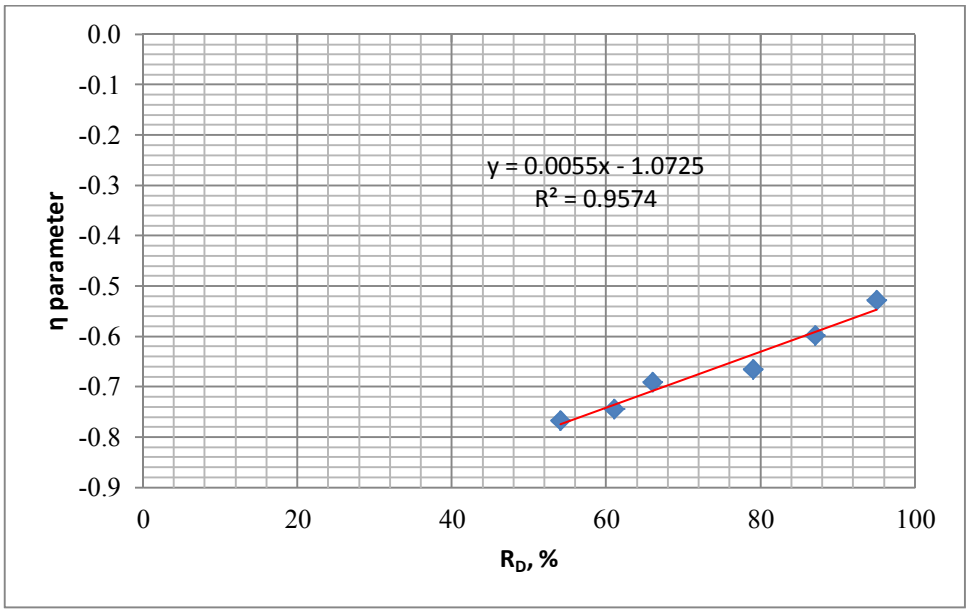


(b)

Figure 4.22. Variation of fitting parameters with R_D , for $\sigma'_v = 50\ Kpa$ a)ζparameter b) η parameter.

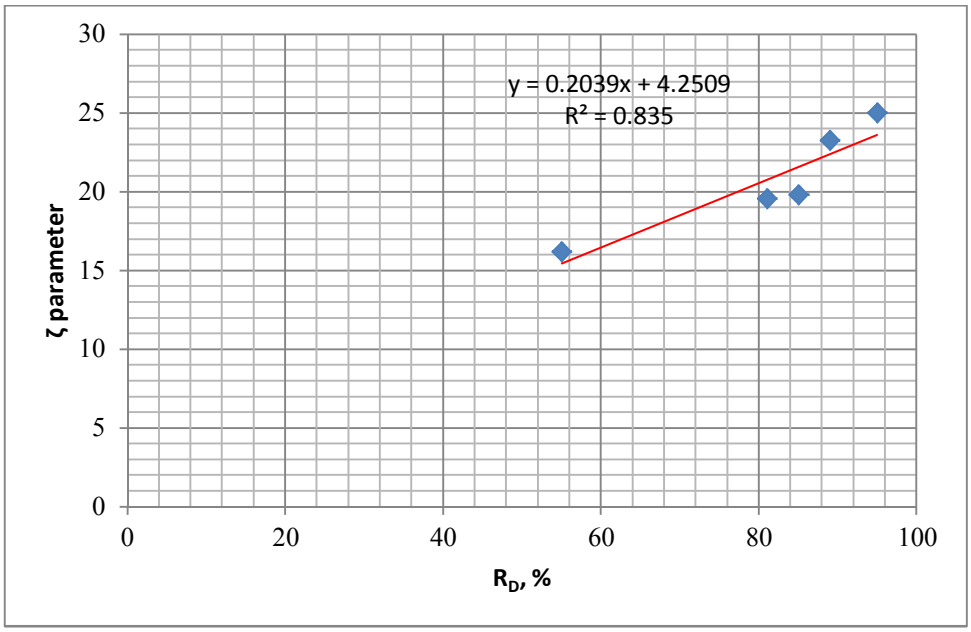


(a)

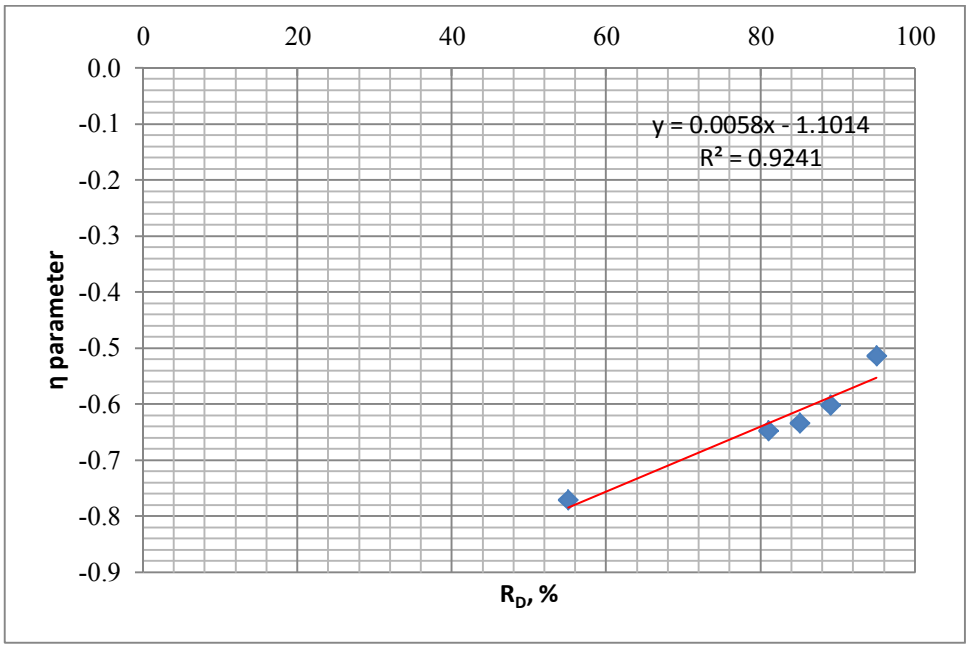


(b)

Figure 4.23. Variation of fitting parameters with R_D , for $\sigma'_v = 70\ Kpa$ a)ζparameter b) η parameter.

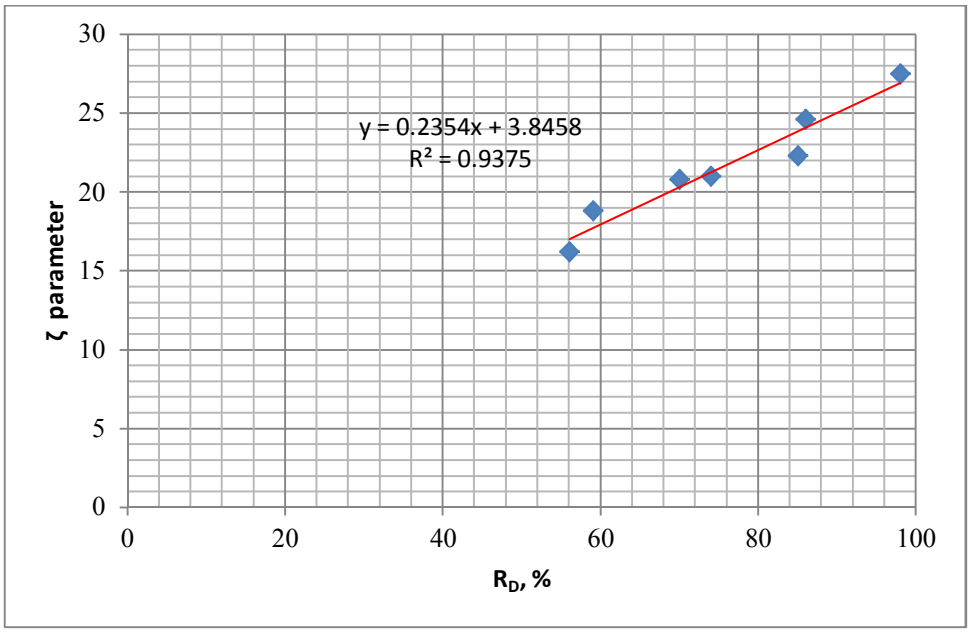


(a)

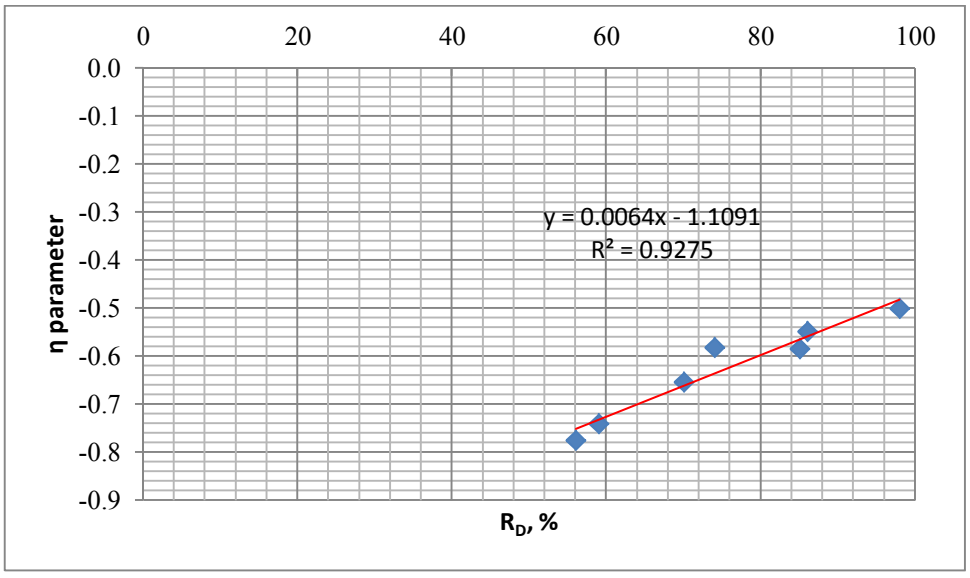


(b)

Figure 4.24. Variation of fitting parameters with R_D , for $\sigma'_v = 90\ Kpa$ a)ζparameter b) η parameter.

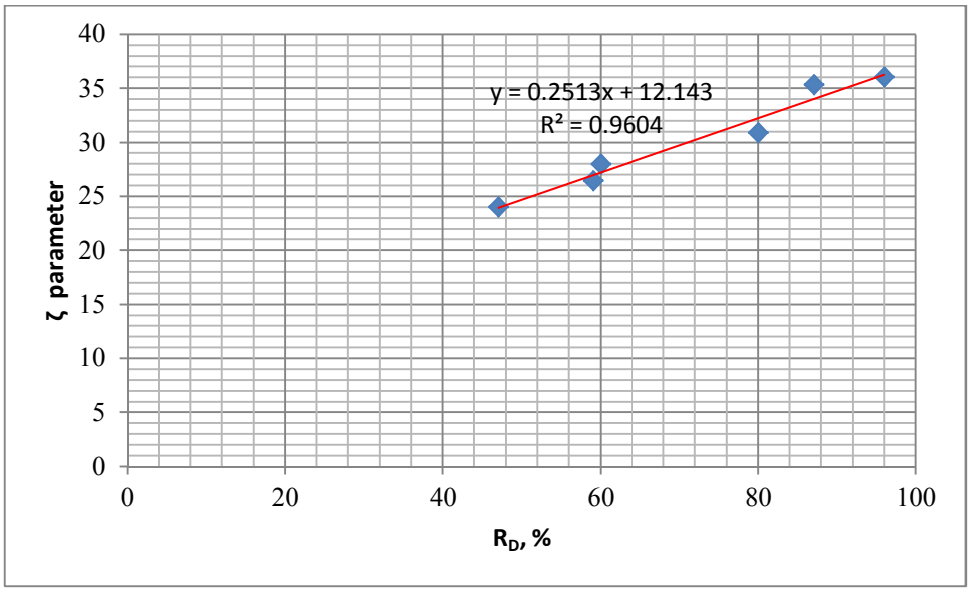


(a)

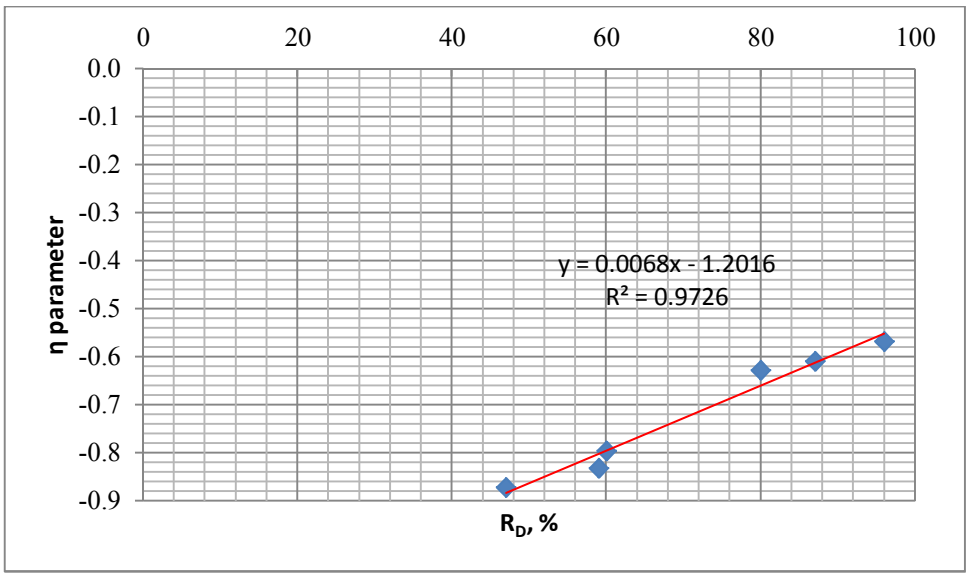


(b)

Figure 4.25. Variation of fitting parameters with R_D , for $\sigma'_v = 110\ Kpa$a)ζparameter b) η parameter.

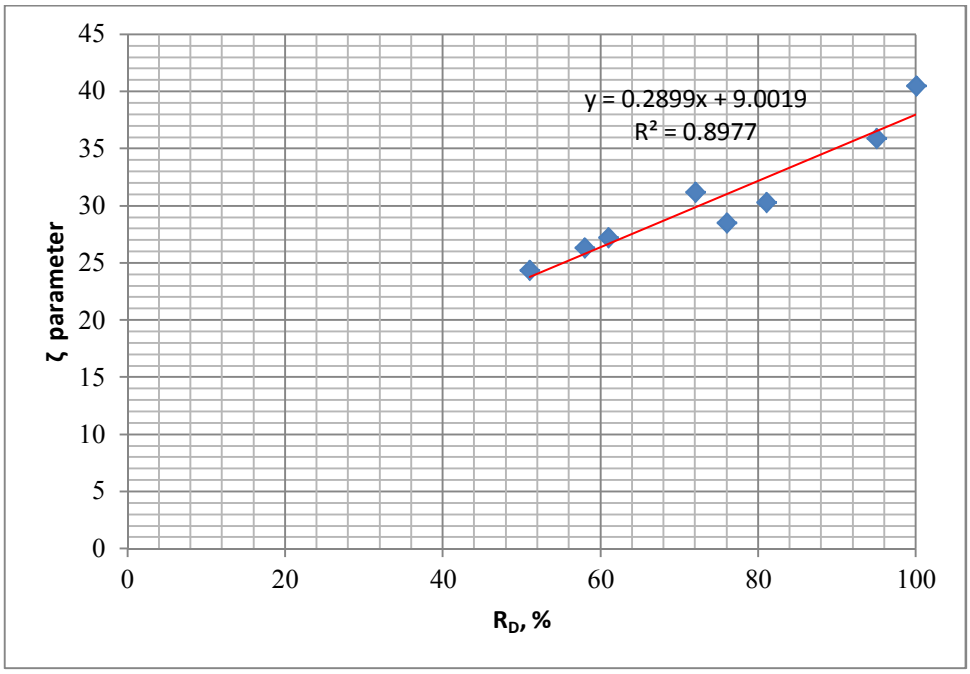


(a)

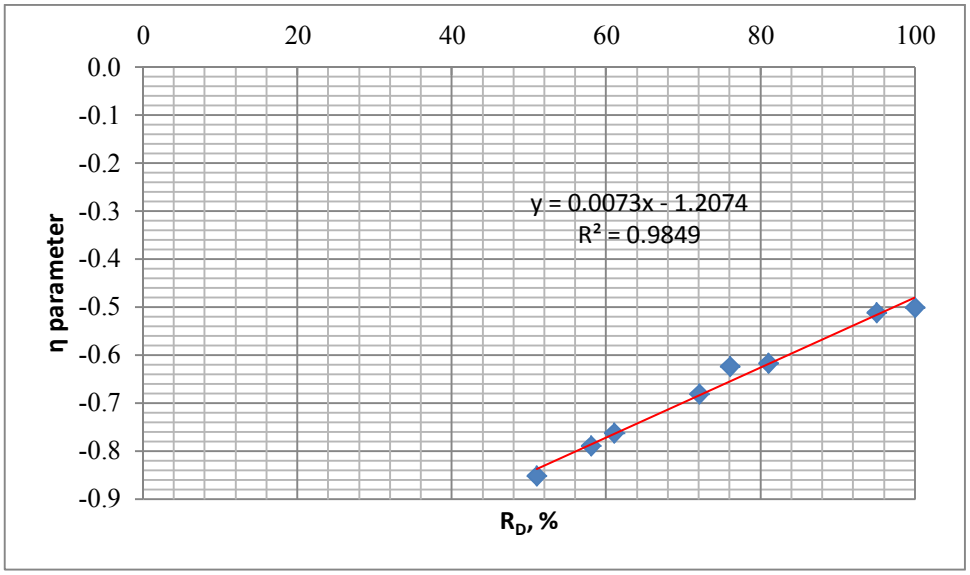


(b)

Figure 4.26. Variation of fitting parameters with R_D , for $\sigma'_v = 130\ Kpa$ a)ζparameter b) η parameter

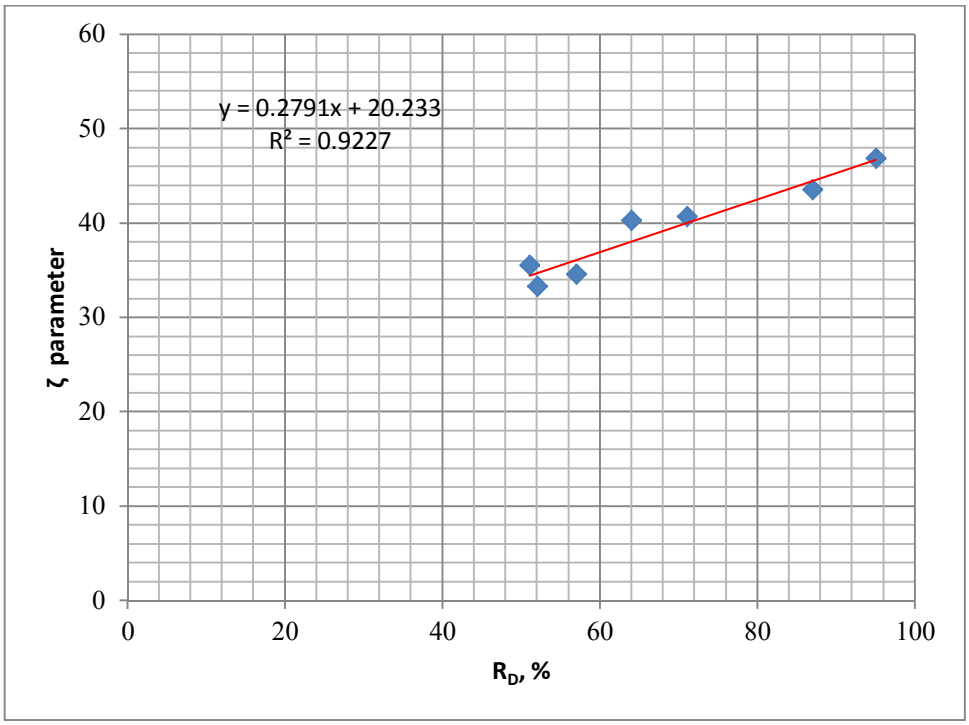


(a)

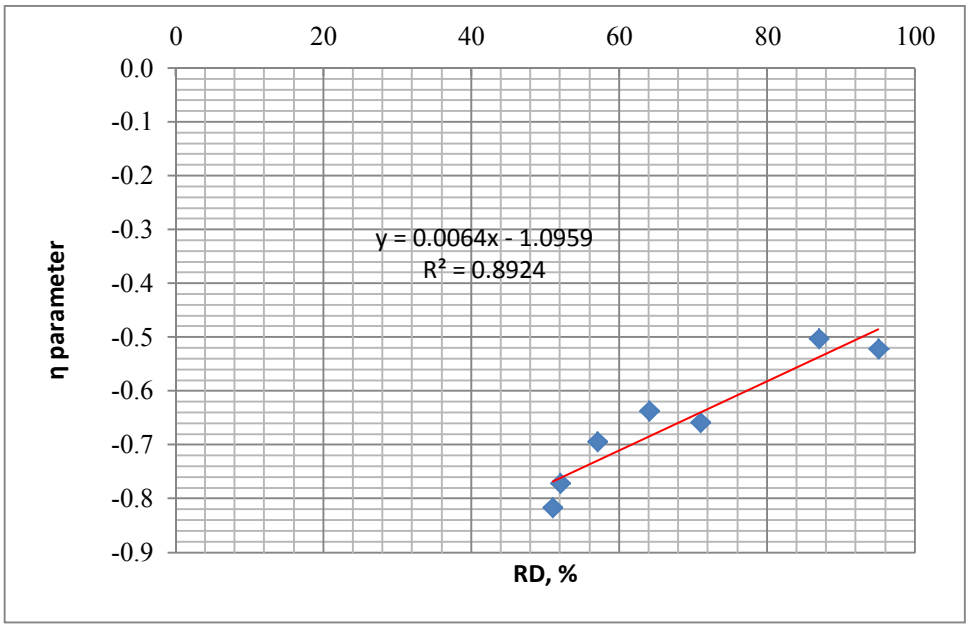


(b)

Figure 4.27. Variation of fitting parameters with R_D , for $\sigma'_v = 160\ Kpa$
a)ζparameter b) η parameter.



(a)



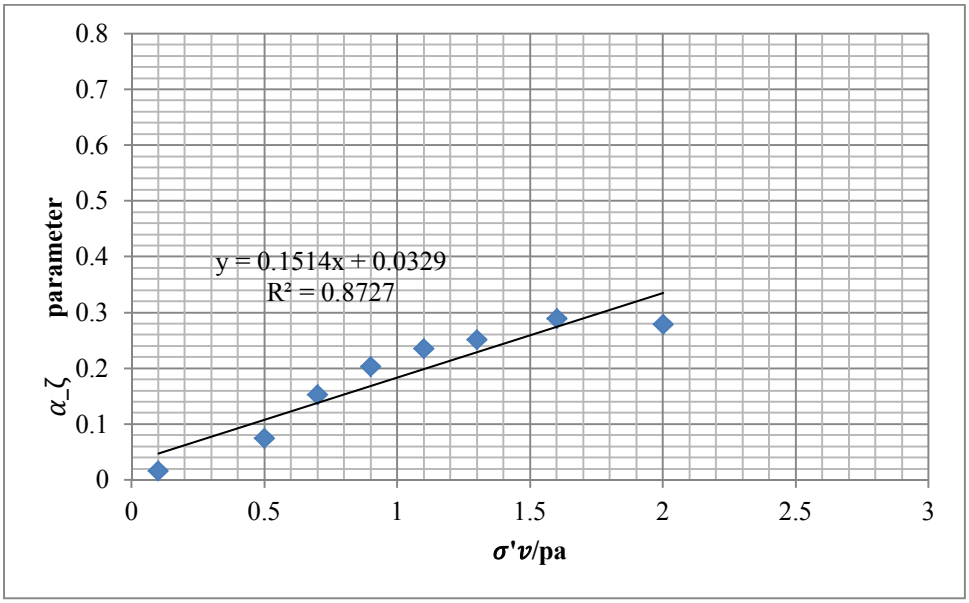
(b)

Figure 4.28. Variation of fitting parameters with R_D , for $\sigma'_v = 200\ Kpa$a)ζparameter b) η parameter.

Table 4.8gives a summary of the equations and their corresponding R^2 values for ζ and η parameters. Since Equation 4.4 is dependent both on σ'_v and R_D, so, this time, to consider the effect of σ'_v on G function, we need to monitor variations of α_ζ, β_ζ, α_η and β_η with respect to normalized vertical effective stress (σ'_v/P_a), Figure 4.29. Values of α_ζ, β_ζ, α_η and $\beta_\eta$are available in Table 4.9.

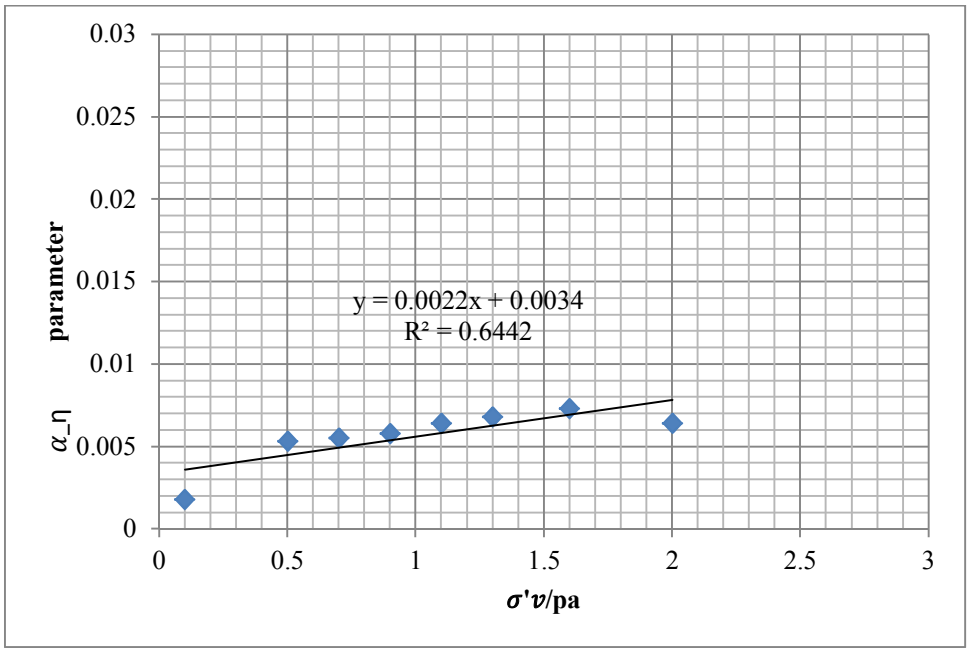
Table 4.8.Summary of the equations corresponding to trend-lines for ζ and η parameters

σ'_v, Kpa	Equation forζ parameter	R^2	Equation for η parameter	R^2
10	ζ = 0.016053x + 1.6959	0.9216	η = 0.0018x - 0.735	0.7984
50	ζ = 0.0752x + 4.6139	0.9924	η = 0.0053x - 1.0309	0.8064
70	ζ = 0.15364x + 4.942	0.7164	η = 0.0055x - 1.0725	0.9574
90	ζ = 0.20387x + 4.2509	0.835	η =0.0058x - 1.1014	0.9241
110	ζ = 0.23542x + 3.8458	0.9375	η =0.0064x - 1.1091	0.9275
130	ζ =0. 25129x + 12.143	0.9604	η = 0.0068x - 1.2016	0.9726
160	ζ = 0.28992x + 9.0019	0.8977	η = 0.0073x - 1.2074	0.9849
200	ζ = 0.2791x + 20.233	0.9849	η = 0.0064x - 1.0959	0.8924

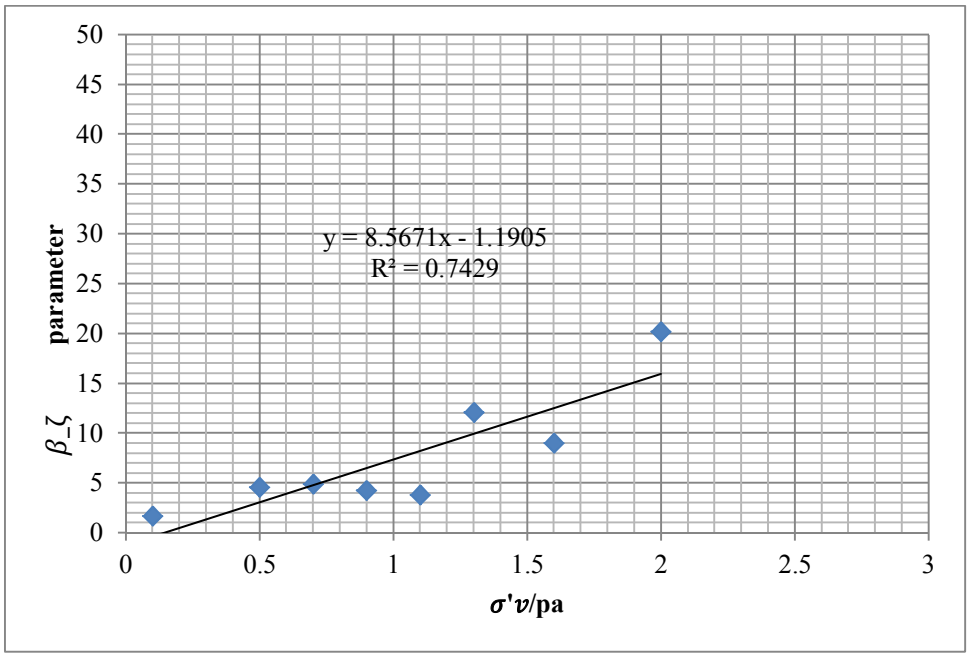


(a)

Figure 4.29. Fitting parameters variation with σ'_v/P_a, a)$\alpha_\zeta - \sigma'_v/P_a$.

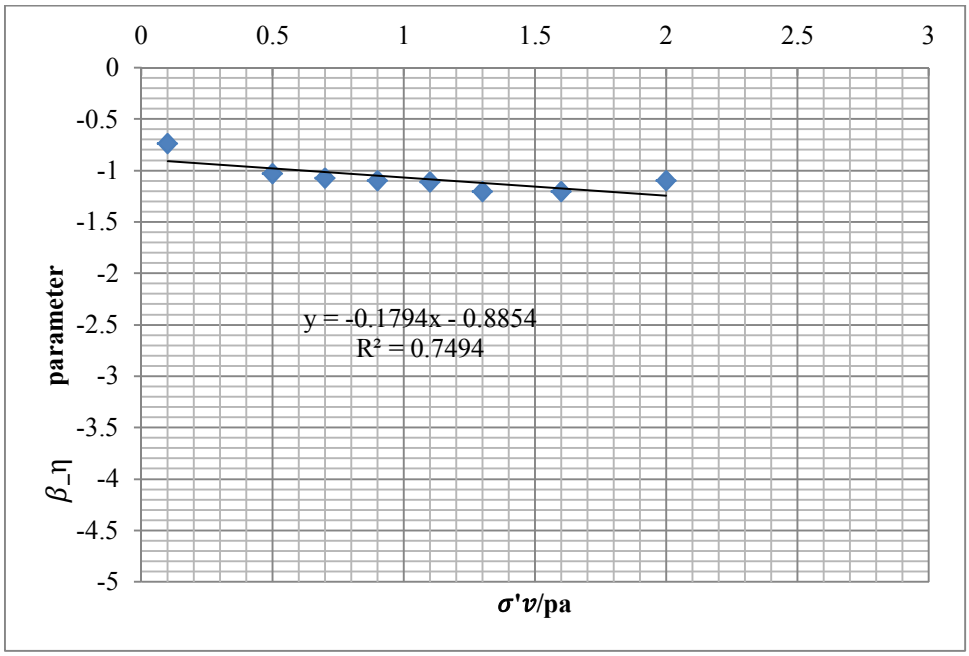


(b)



(c)

Figure 4.29. Fitting parameters variation with $\sigma'_v/\mathrm{P_a}$, b) $\alpha_\eta - \sigma'_v/P_a$ c) $\beta_\zeta - \sigma'_v/P_a$ (Cont.).



(d)

Figure 4.29. Fitting parameters variation with σ'_v/P_a, d) $\beta_\eta - \sigma'_v/P_a$ (Cont.).

A general linear equation defined for the fitting parameters of Silivri sand, similarly, the same behavior observed for SOG sand in Figure 4.29, so the $k_{1,\ldots,8}$ parameters, which are fitting parameters of α_ζ , β_ζ , α_η and β_η for SOG sand, are summarized in Table 4.10.

Table 4.9. Fitting parameters variation with σ'_v/P_a

σ'_v, Kpa	α_ζ	β_ζ	α_η	β_η
10	0.016053	1.6959	0.0018	- 0.735
50	0.092704	3.5265	0.0053	- 1.0309
70	0.15364	4.942	0.0055	- 1.0725
90	0.20387	4.2509	0.0058	- 1.1014
110	0.23542	3.8458	0.0064	- 1.1091
130	0.25129	12.143	0.0068	- 1.2016
160	0.28992	9.0019	0.0073	- 1.2074
200	0.2791	20.233	0.0064	- 1.0959

Table 4.11gives a summary of the equations and their corresponding R^2 values for α_ζ , β_ζ , α_η and β_η parameters. Having unit-independent parameters, and inserting them into Equation 4.7, mathematical equation for variation of G with respect to σ'_v , R_D and γ can be computed. Equation 4.12 is a power function that renders calculation of shear modulus for any shear strain between 0.1 to 10 %, so, if the values of $k_{1,\dots,8}$in Table 4.10 are used, the result will be the equation for the SOG sand :

$$\frac{G}{P_a} = \left[\left(k_1\left(\frac{\sigma'_v}{P_a}\right) + k_2\right)R_D + k_3\frac{\sigma'_v}{P_a}\right) \; + \; k_4\right] * \gamma^{\left[\left(k_5\left(\frac{\sigma'_v}{P_a}\right)+k_6\right)R_D + k_7\left(\frac{\sigma'_v}{P_a}\right)+ k_8\right]} \quad (4.12)$$

Table 4.10. Summary of $k_{1,\dots,8}$ values of trend-lines for α_ζ , β_ζ , α_η and β_η parameters.

k_1	k_2	k_3	k_4	k_5	k_6	k_7	k_8
0.1514	0.0329	8.5671	- 1.1905	0.0022	0.0034	-0.1794	- 0.8854

Table 4.11 Summary of the equations corresponding and R^2 values of trend-lines for α_ζ , β_ζ , α_η and β_η parameters.

Unit-independent parameter	Corresponding linear equation	R^2
α_ζ	α_ζ= 0.1514x + 0.0329	0.8798
α_η	α_η= 0.0022x + 0.0034	0.6442
β_ζ	β_ζ= 8.5671x - 1.1905	0.7429
β_η	β_η= -0.1794x - 0.8854	0.7494

5. DISCUSSION

In Chapter 4, it has been shown that the variation of shear modulus with shear strain at constant confinement, leads to a relationship with a power function form. As the variations of the parameters of the shear modulus-shear strain function are quantified for varying relative density and vertical effective stress values, a complete function for calculating the shear modulus from measurable parameters is obtained. On the other hand, to have unit independent fitting parameters, both G and σ'_v were normalized by atmospheric pressure (P_a=100 Kpa).

In this section, results obtained for both type of sands that were tested by DSS device are plotted, in addition, proposed equations are also plotted to have an idea of how the functions would fit experimental data.

5.1. Comparison of Obtained Results for Silivri Sand with Proposed Equation

The shear modulus is dependent on shear strain, and for this study which considers large strains, shear strain variation range is between 0.1 and 10%. Both results for Silivri sand and plot of Equation 4.12, using available data for relative density and vertical effective stress, are shown in Figures 5.1 to 5.5.

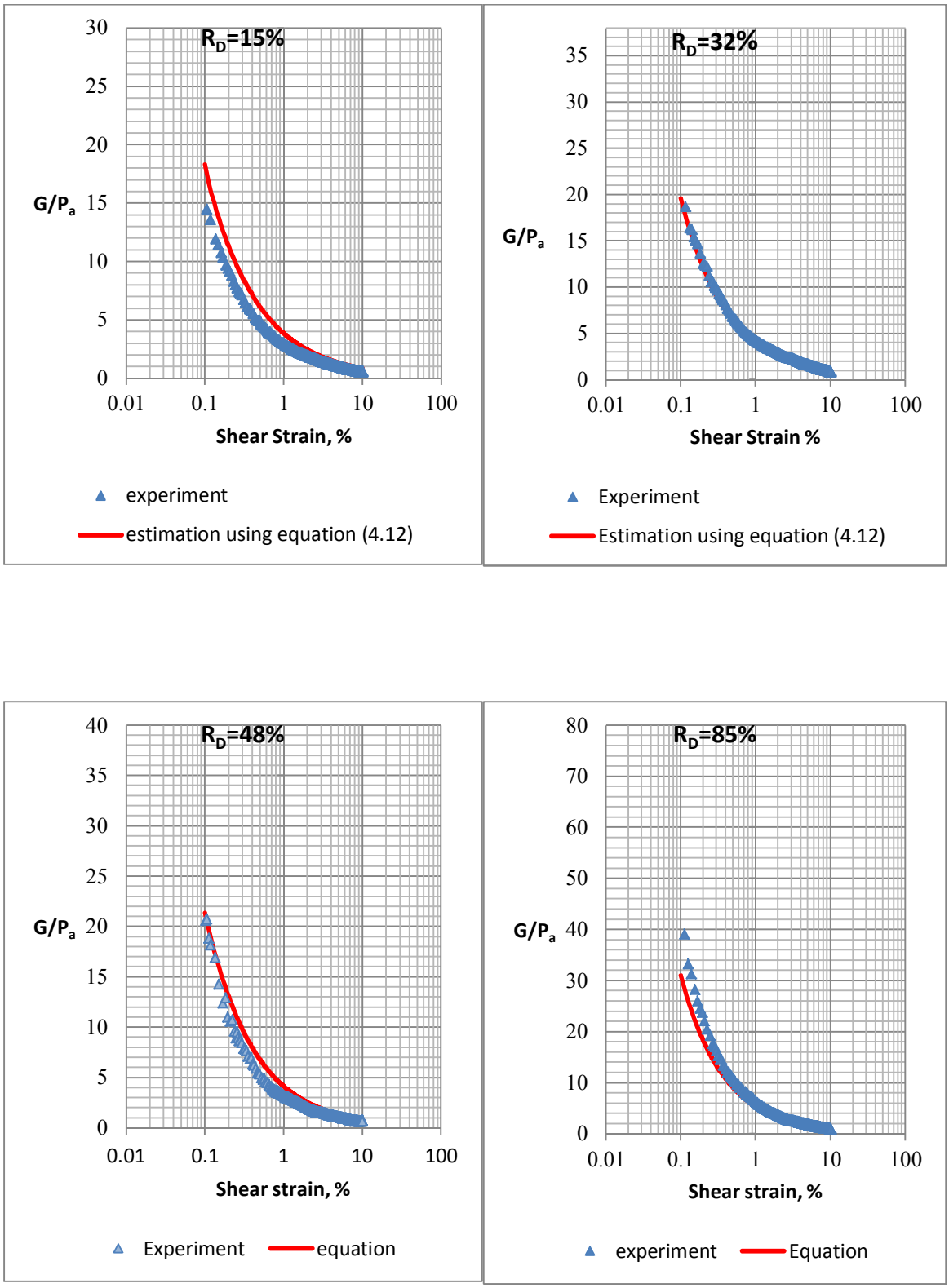


Figure 5.1. Comparison of obtained data from DSS test for Silivri sand with proposed equation at σ'_v =10 Kpa.

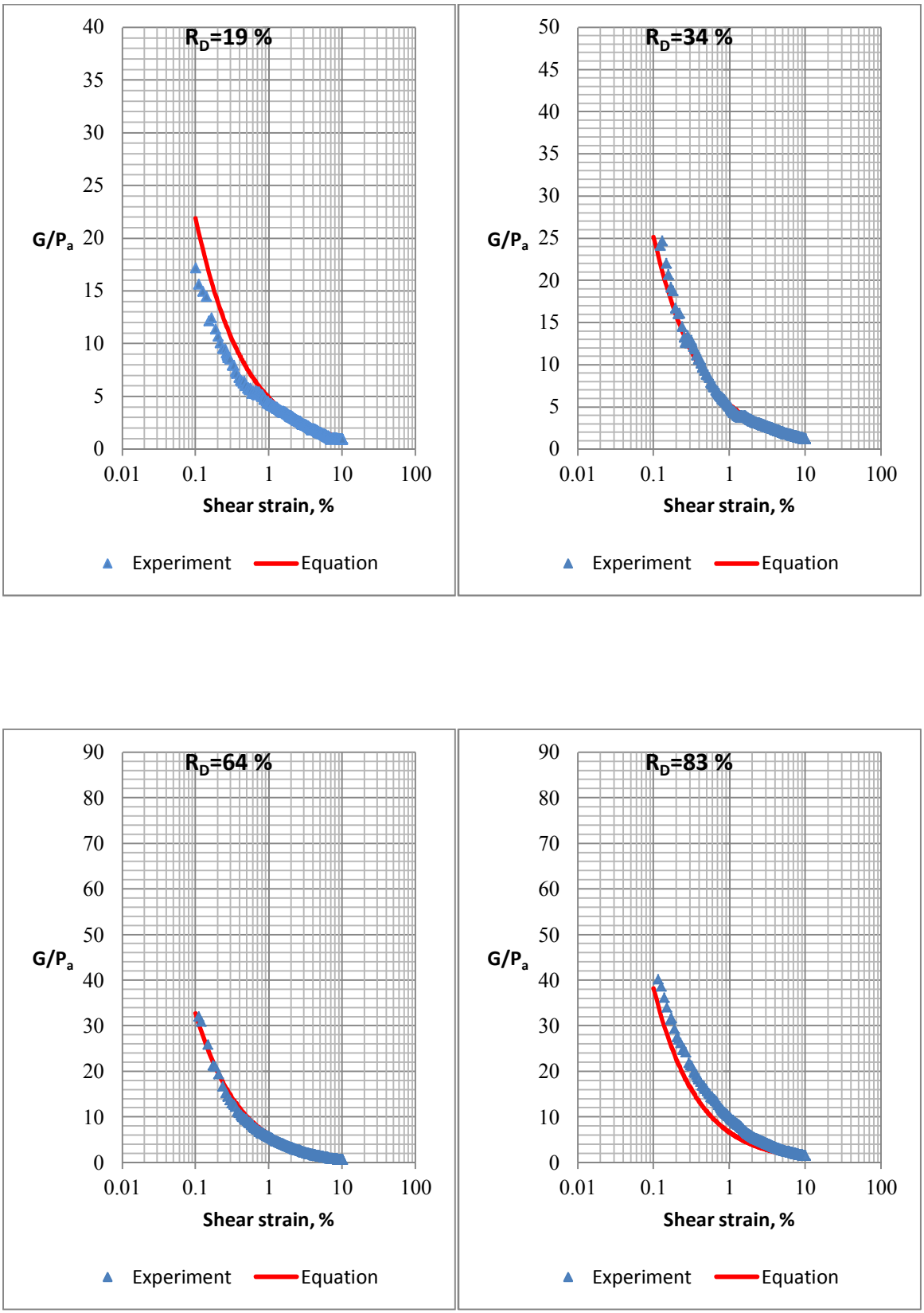


Figure 5.2. Comparison of obtained data from DSS test for Silivri sand with proposed equation at σ'_v =20 Kpa.

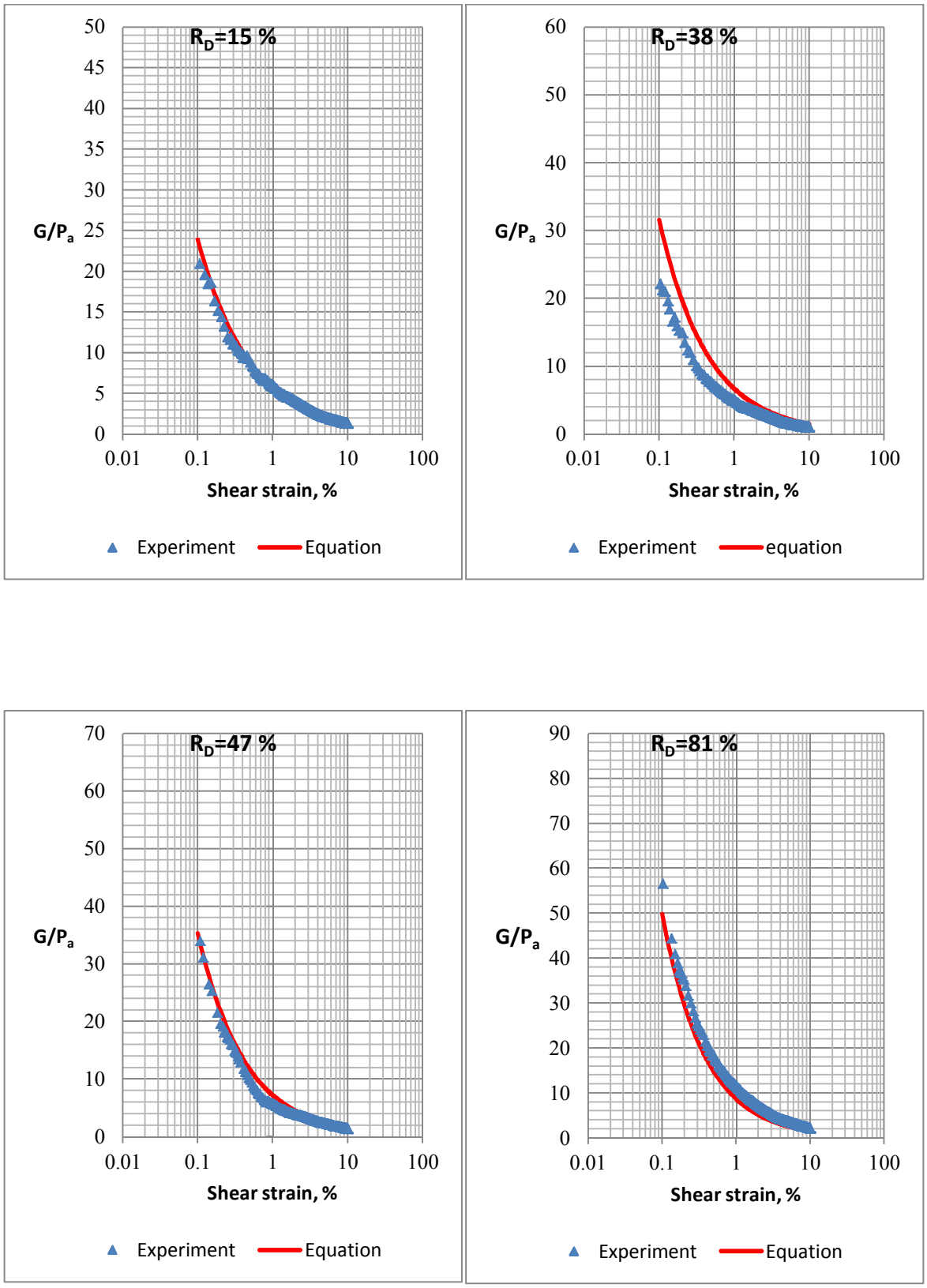


Figure 5.3. Comparison of obtained data from DSS test for Silivri sand with proposed equation at σ'_v =30 Kpa.

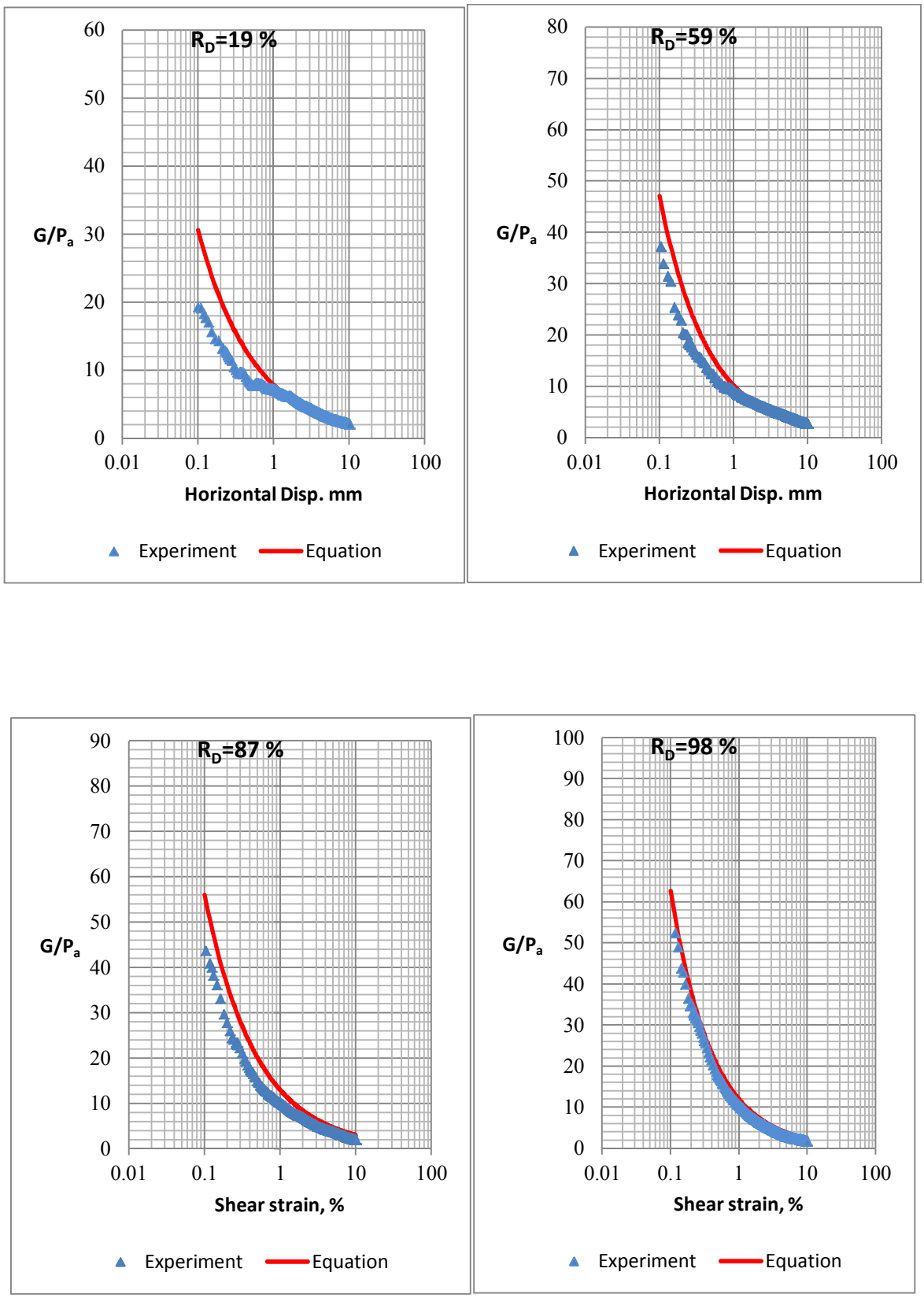


Figure 5.4. Comparison of obtained data from DSS test for Silivri sand with proposed equation at σ'_v =50 Kpa.

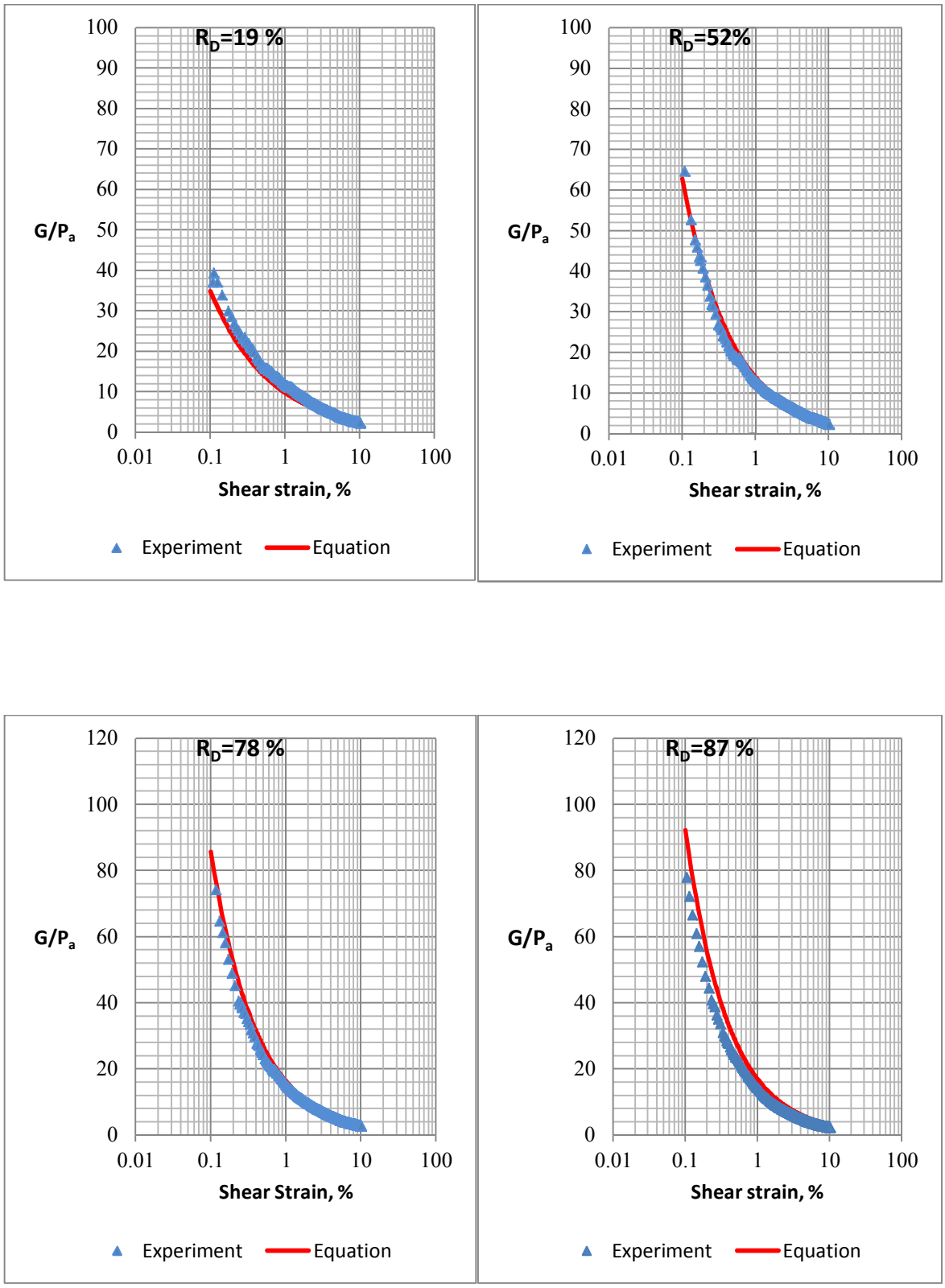


Figure 5.5. Comparison of obtained data from DSS test for Silivri sand with proposed equation at σ'_v =70 Kpa.

Analyzing plotted data points versus the results of the proposed equation of Silivri sand, for each combination of relative density and vertical effective stress at 10kpa, as shown in Figure 5.1, a high fitting level can be seen. It shows the possibility of estimation of shear modulus, as a function of R_D and σ'_v, with an empirical equation, which is the first objective of this study.

Similarly, for the σ'_v higher than 10kpa, as shown in Figures 5.2 to 5.5, proposed power function for G (Equation 4.12), have a good fitting level with data points.

5.2.Comparison of Obtained Results for Standard Ottawa Graded Sand with Proposed Equation

The second objective of this thesis was to evaluate proposed equation for another type of sand, a standard Ottawa graded sand. This way it will be possible to evaluate the universal applicability of the proposed equation (Equation 4.12). Following the same procedure, using Equation 4.12 with the parameters suitable for SOG, applicability of the proposed equation to different sands was shown in Figures 5.6 to 5.13.

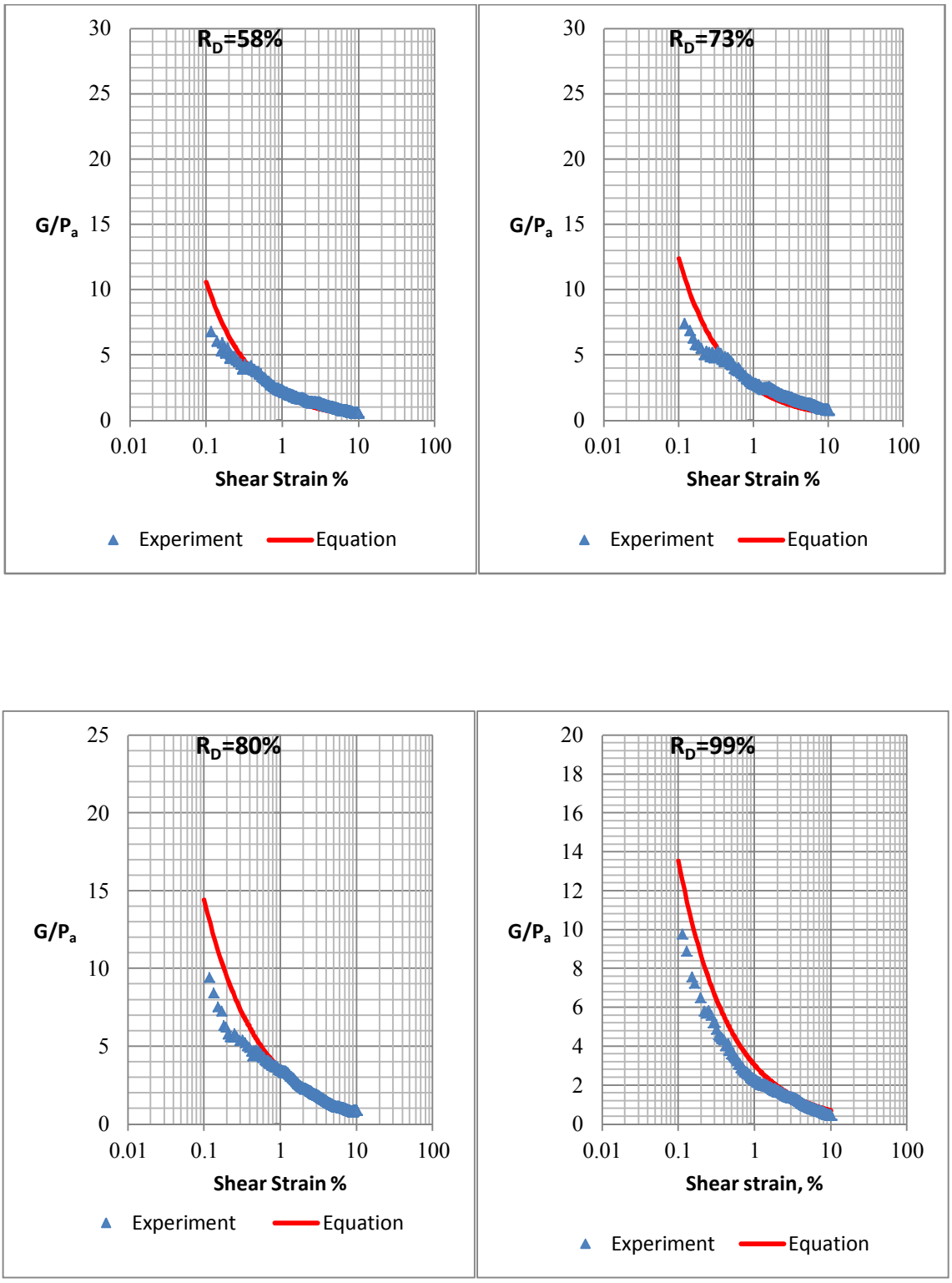
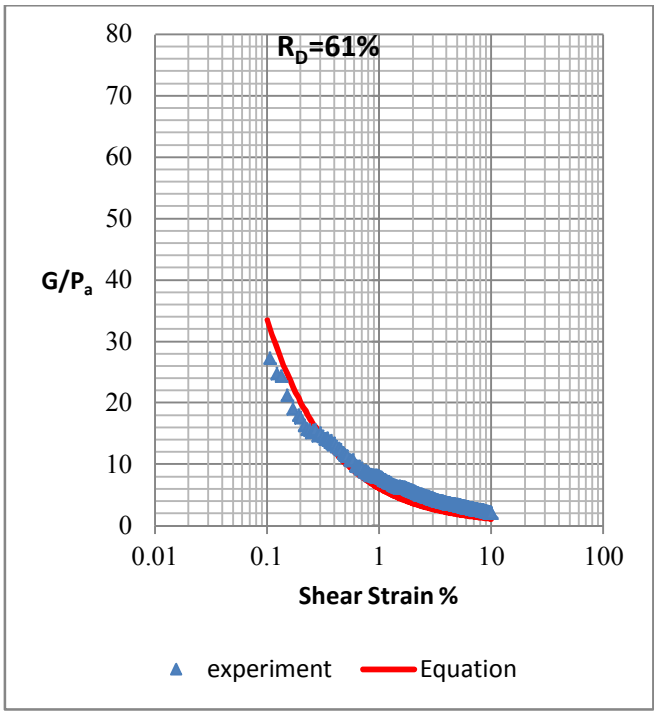


Figure 5.6. Comparison of obtained data from DSS test for SOG sand with proposed equation at σ'_v =10 Kpa.



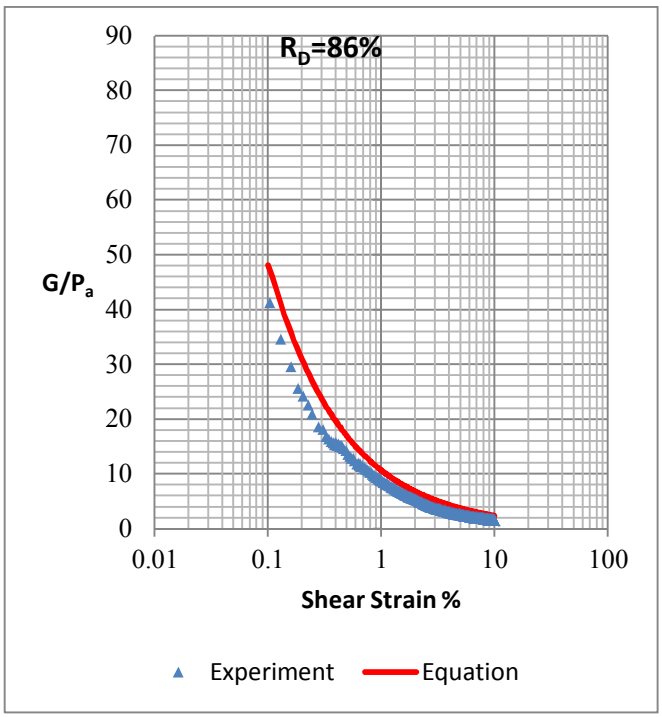


Figure 5.7. Comparison of obtained data from DSS test for SOG sand with proposed equation at σ'_v =50 Kpa.

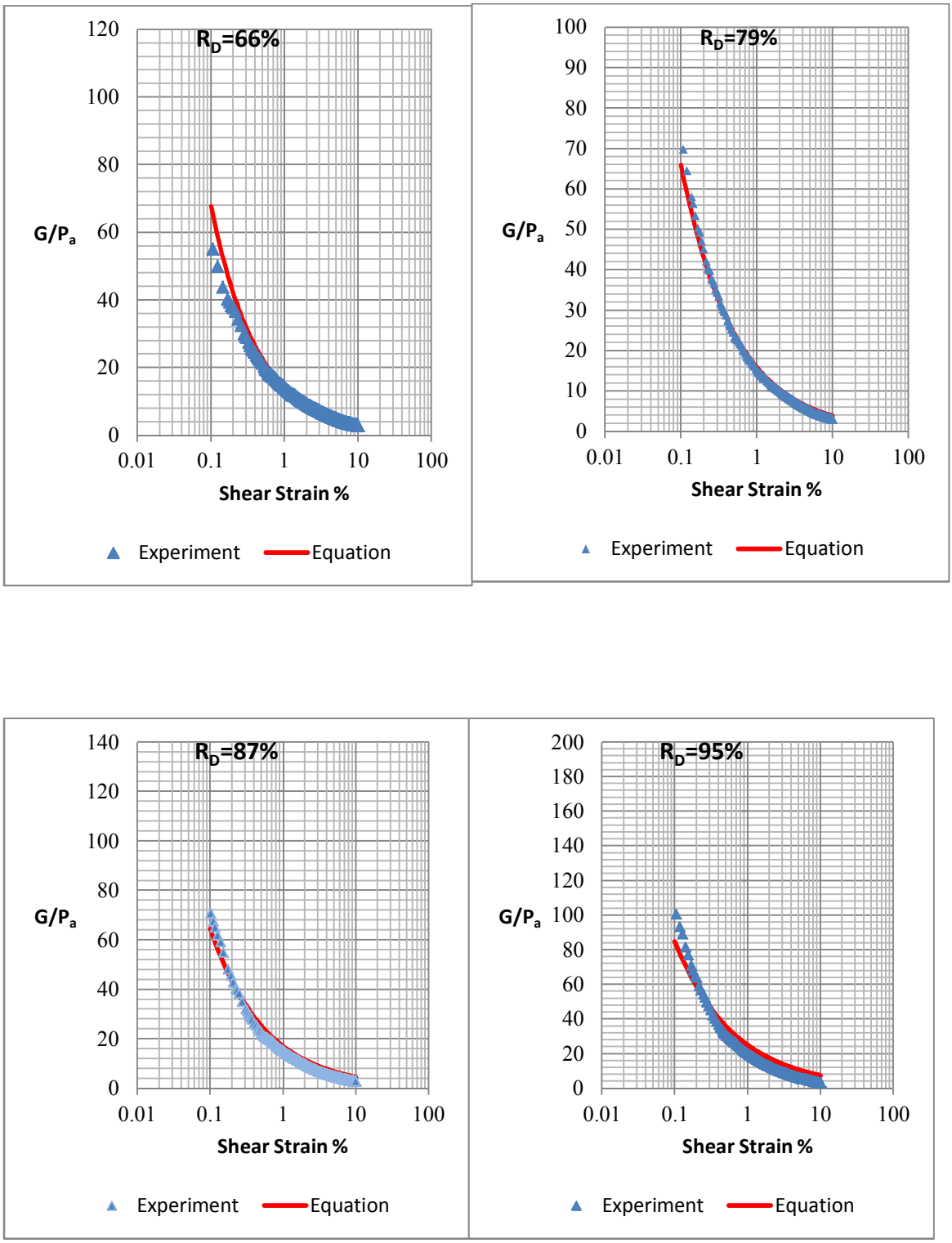


Figure 5.8. Comparison of obtained data from DSS test for SOG sand with proposed equation at σ'_v =70 Kpa.

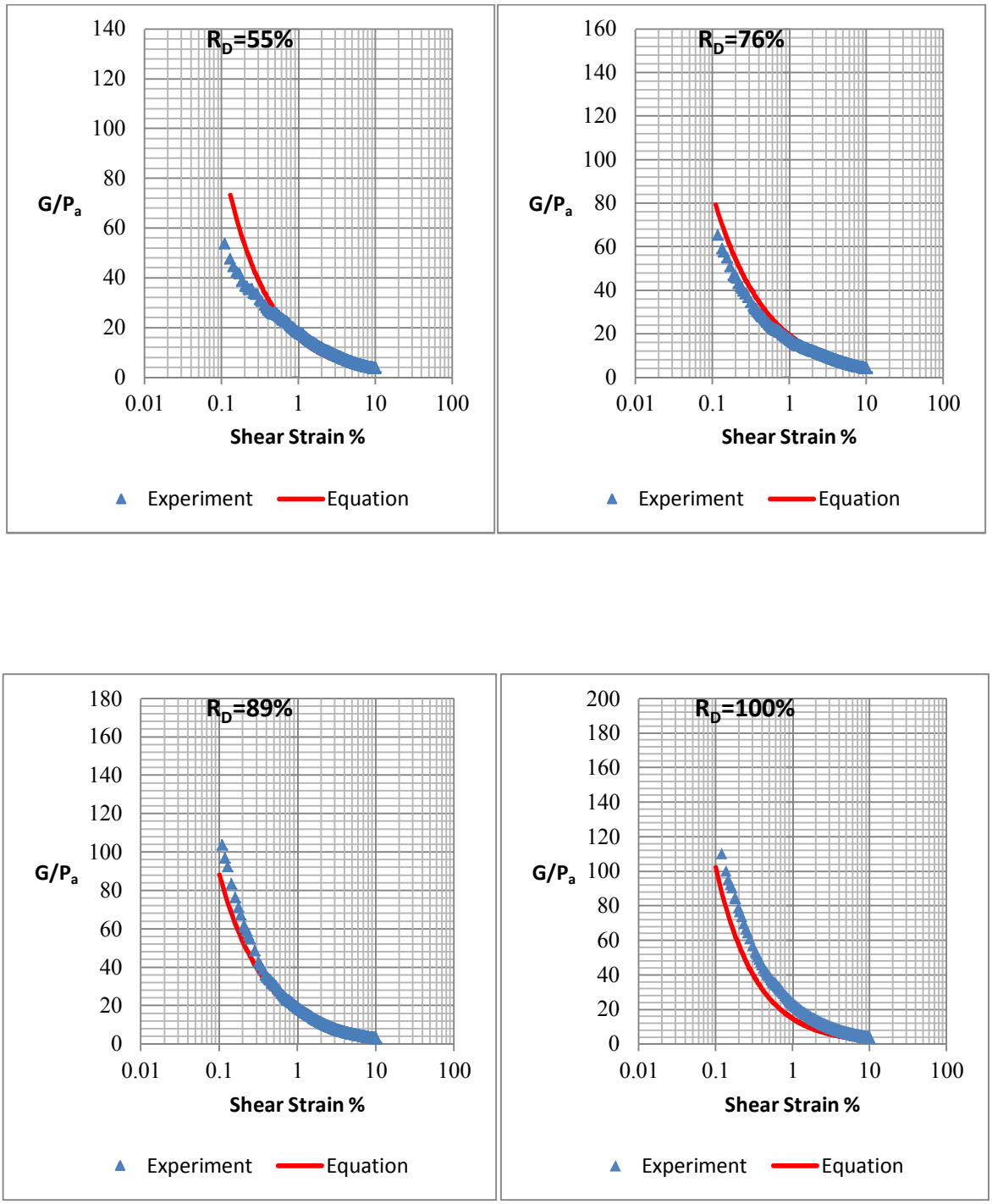


Figure 5.9. Comparison of obtained data from DSS test for SOG sand with proposed equation at σ'_v =90 Kpa.

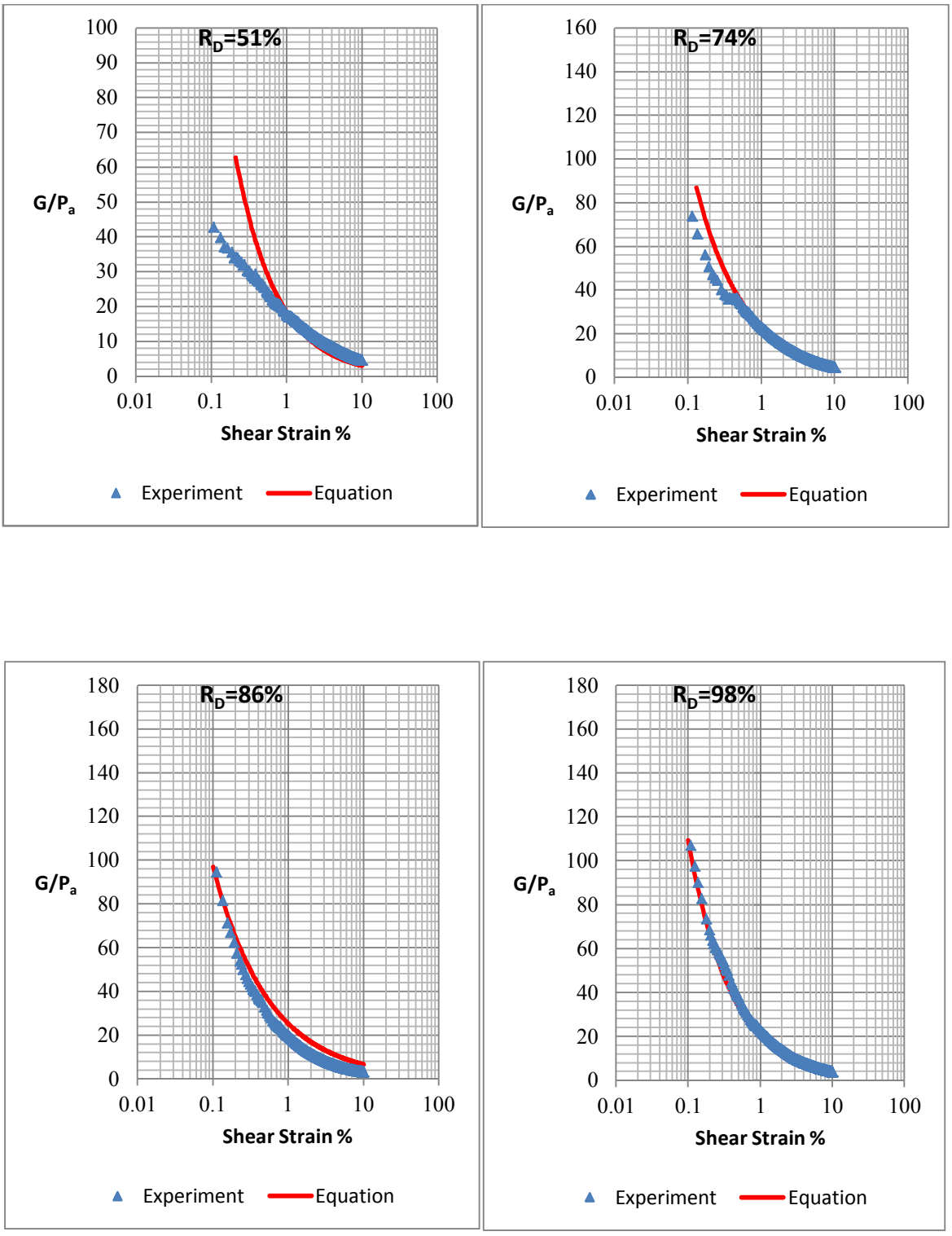


Figure 5.10. Comparison of obtained data from DSS test for SOG sand with proposed equation at σ'_v =110 Kpa.

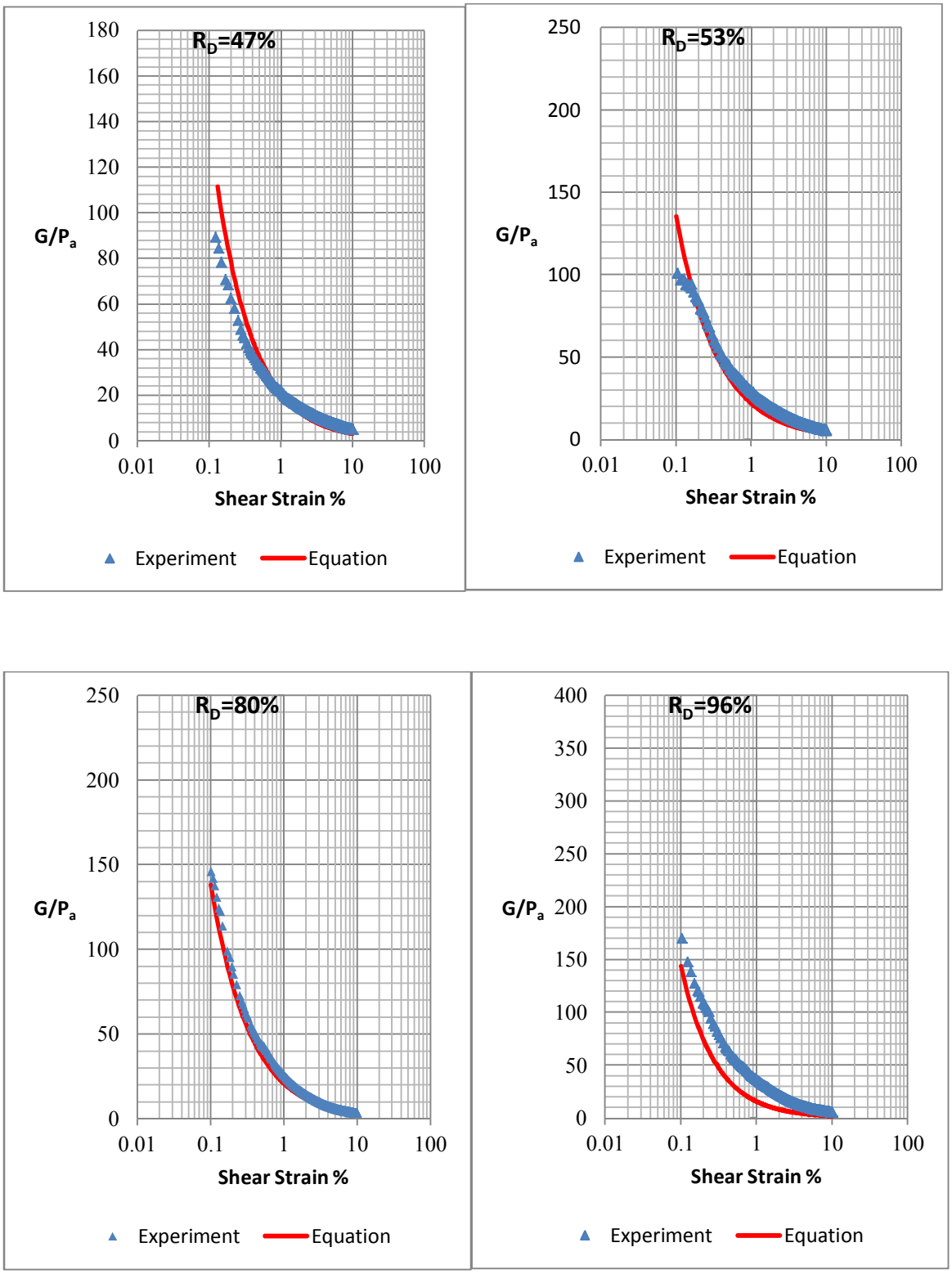


Figure 5.11. Comparison of obtained data from DSS test for SOG sand with proposed equation at σ'_v =130 Kpa.

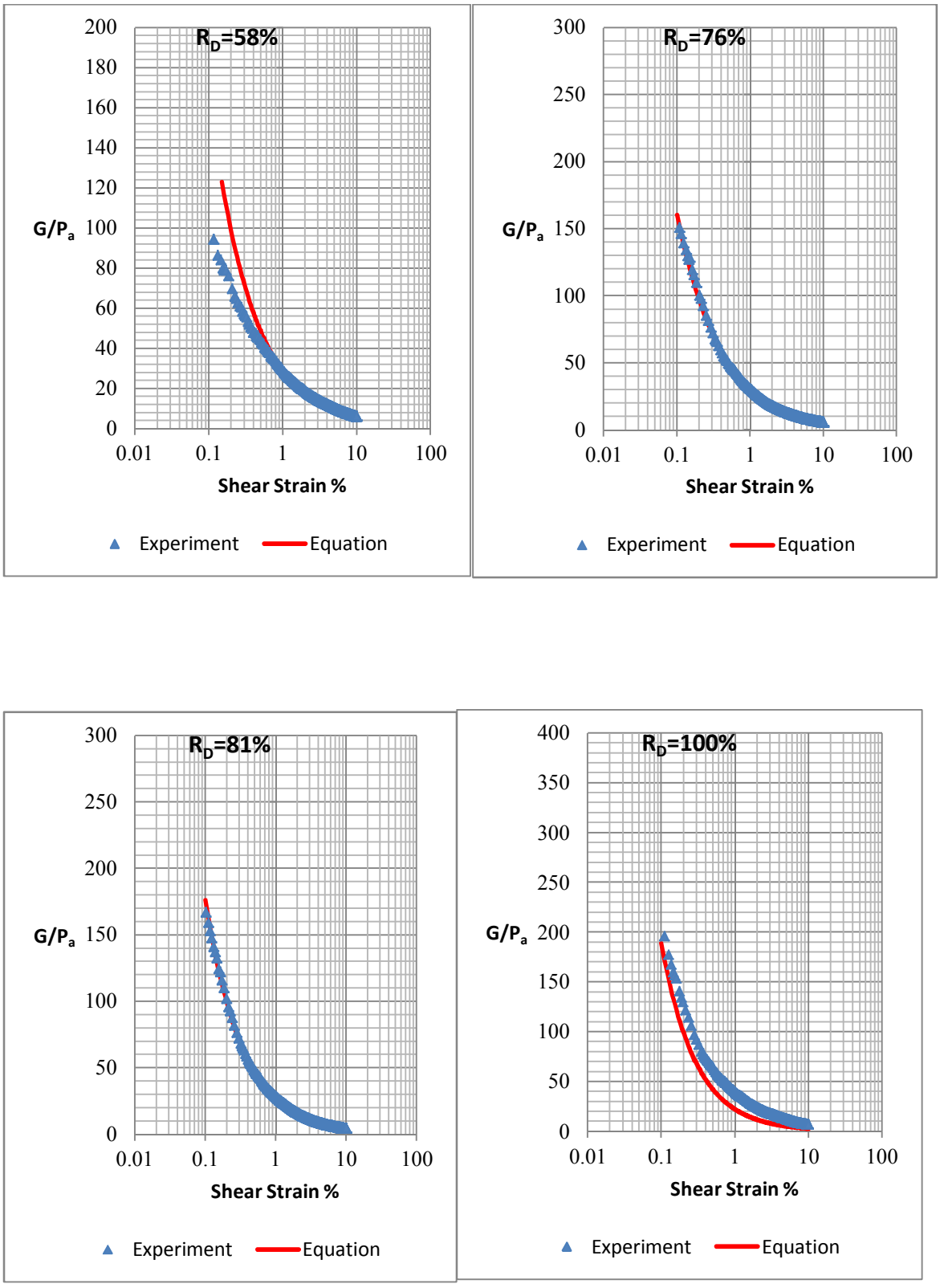


Figure 5.12. Comparison of obtained data from DSS test for SOG sand with proposed equation at σ'_v =160 Kpa.

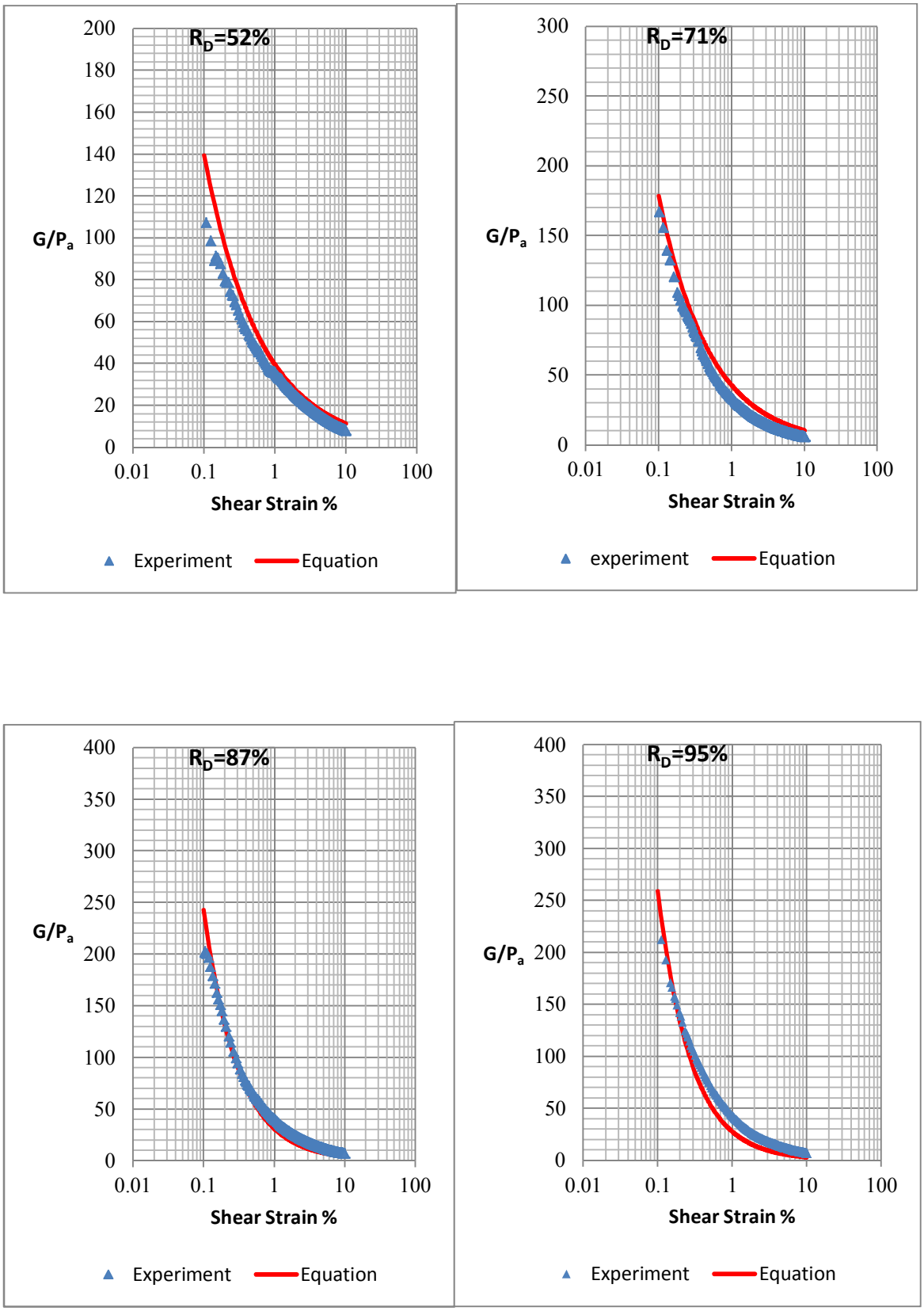


Figure 5.13 Comparison of obtained data from DSS test for SOG sand with proposed equation at σ'_v =200 Kpa.

Comparing plots for data points and Equation 4.12 (the parameters suitable for SOG sand are inserted in the equation), for each combination of R_D at σ'_v =10kpa, shown in Figure 5.6, a high fitting level can be seen. Identically, for the σ'_v higher than 10kpa, as shown in Figures 5.7 to 5.13, proposed power function for G (Equation 4.12), have a good fitting level with data points of SOG sand.

6. CONCLUSIONS

An experimental study including more than 200 DSS tests were done on two different clean cohesionless soils. The objectives of this thesis were understanding and quantifying the influences of relative density (R_D) and vertical effective stress (σ'_v) on shear modulus as a function of shear strain. According to the results obtained from DSS experimental program, following conclusions can be drawn:

(i) Shear modulus of cohesionless soils is dependent on both relative density and confinement pressure.

(ii) For a combination of R_D and σ'_v, plot of obtained data points for tangent shear modulus and shear strain between 0.1 and 10%, results in a power function.

(iii) High R^2fits were obtained between power trendlines and experimental data.

(iv) Keeping vertical effective stress constant and increasing relative density, results in higher shear modulus, on the other hand, the values of ζ and η parameters also increase.

(v) An empirical equation is obtained that yields shear modulus as a function of shear strain,R_D and σ'_v. The outstanding advantage of proposed equation is that it uses directly measurable and calculable parameters.

$$\frac{G}{P_a} = \left[\left(k_1\left(\frac{\sigma'_v}{P_a}\right) + k_2\right)R_D + k_3\left(\frac{\sigma'_v}{P_a}\right) + k_4\right] * \gamma^{\left[\left(k_5\left(\frac{\sigma'_v}{P_a}\right)+k_6\right)R_D + k_7\left(\frac{\sigma'_v}{P_a}\right)+ k_8\right]}$$

(vi) By conducting the experimental program on two different sands (Silivri and standard Ottawa graded sand), it has been shown that the proposed equation is valid for different soils.

(vii) By conducting approximately 15 tests (three various vertical effective stress and five different relative density for each), unit-less fitting parameters of proposed equation can be obtained for a soil type. Consequently, being able to predict stiffness of sands using proposed equation leads to have a better understanding of soil behavior during ground motions.

6.1. Recommendations for Future Work

The results of this thesis suggest that the shear modulus can be quantified with respect to vertical effective stress, relative density and shear strain. Conducted tests were primarily on reconstituted samples, and future study should focus on testing a group of high quality undisturbed specimens. To increase the validity of these findings more tests could be run on an even wider range of soils.

Furthermore, to get a higher fitting level between actual results and proposed equation, optimization needed to be done on empirical equation with mathematical approaches. Additionally, the effect of each of variables should be studiedin order to have a better estimation of future experimental programs.

Coefficients of relative density and normalized vertical effective stress can be also investigated for small shear strains, which, in this region minor strength degradation occurs.

REFERENCES

1. Afifi, S. S., and F. E.,Richart, "Stress-history Effects on Shear Modulus of Soils",*Soils and Foundations,*Vol.13, No. 1, pp. 77-95, 1973.

2. Afifi, S. S., and R. D. Woods, "Long-term Pressure Effects on Shear Modulus of Soils",*J. Soil Mek and Found Div.,* ASCE, Vol. 97, No. 10, pp. 1445-1460, 1971.

3. Airey, D. and R. D. Woods, "Discussion of Specimen Size Effect *in* Simple ShearTest",*Journal of Geotechnical Engineering Division*, ASCE, Vol. 110, No. 3, pp. 439-442, 1984.

4. Abadkon, A.,2012, *Strength and Dilatancy of Anisotropic Cohesionless Soils*, Ph.D.Dissertation, Boğazici University.

5. Arthur, JRF., JDC.Rodriguez, "Principal Stress Rotation: a Missing Parameter",*J Geotech Eng Div*,ASCE, Vol. 106, No 4, pp. 419–433, 1980.

6. Baxter, A.S., M. Bradshaw, "DSS Test Results Using Wire-Reinforced Membranes and Stacked Rings", In: GeoFlorida,*Advances in Analysis, Modeling & Design (GSP 199)*, Florida, USA, 2010, ASCE.

7. Bjerrum, L., and A. Landva, "Direct Simple ShearTests on a Norwegian Quick Clay",*Géotechnique*, Vol. 16, No. 1, pp. 1–20, 1966.

8. Brylawski, E., and T., Berre, "*Membrane Correction - DSS Apparatus"*, GEONOR, Inc., 1992; rev 1997.

9. DeGroot, D. J., C. C., Ladd, andJ. T., Germaine,"Direct Simple Shear Testing of Direct Shear",*Géotechnique*, Vol. 17, pp. 309-328, 1992.

10. Dyvik, R., T., Berre, and S., Lacasse, "Comparison of Truly Undrained and Constant Volume Direct Simple Shear Tests",*Géotechnique*, Vol. 37, No. 1, pp. 3–10, 1987.

11. Franke, E., M., Kiekbusch, "A New Direct Simple Shear Device",*Geotech. Test. J.*, Vol. 2, No. 4, pp. 190–199, 1979.

12. Hardin, B. O., andF. E., Richart, "Elastic Wave Velocities in Granular soils",*J. Soil Mech. and Found. Div., ASCE,*Vol.89(1), pp. 33-65, 1963.

13. Iwasaki, T., F., Tatsuoka, "Shear Moduli of Sands UnderCyclic Torsional Shear Loading",*Soils and Foundations,*Vol.18, No. 1, pp. 39-56, 1978.

14. Kaveh H. Z., 2012, *AnAssesmentof the DynamicProperties of AdapazarıSoils by Cyclic Direct Simple Shear Test*,M.S.Thesis, Middle East Technical University.

15. Kjellam, W., "Testing the Shear Strength of Clay in Sweden",*Géotechnique*, pp 225-232, 1951.

16. Kokusho, T., Y., Yoshida, "Dynamic Properties of Soft Clay for Wide Strain Range" *Soils and Foundations,* Vol. 22, No 4, pp. 1-18, 1982.

17. Ladd, C.C., "Stability Evaluation During Staged Construction: 22nd Terzaghi Lecture",*Journal of Geotechnical Engineering*, ASCE, Vol. 117, No. 4, pp. 537-615, 1991.

18. Ladd, C.C., andD.J.,DeGroot, "Recommended Practice for Soft Ground Site Characterization",*Proceedings of the 12th Panamerican Conference on Soil Mechanics and Geotechnical Engineering*, Boston,Lecture JGE117, pp. 540-615, 2003.

19. Marte Gutierrez, K. Ishihara, "Non-coaxiality and Energy DissipationGranular Materials",*Soils Foundation*, Vol. 40, No. 2, pp. 49–59, 2000.

20. Marr, W. A.,"Universal Shear Device",*GEOCOMP Corporation*, 2003.

21. Marte Gutierrez, J. Wang, M. Yoshimine, "Modeling of the Simple Shear Deformation of Sand: Effects of Principal Stress Rotation", *Acta Geotechnica*,Vol. 4, No. 3, pp 193-201, 2009.

22. Morgenstern, N.R., andJ.S. Tchalenko, "Microscopic Structure in Kaolin Subjected to Direct Shear", *Géotechnique,* Vol.17,pp. 309-328, 1967.

23. Potts, D.M., G.T., Dounias, and P.R.,Vaughan, "Finite Element Analysis of the Direct simple shear"*Géotechnique,* Vol.37, No.1, pp. 11-23, 1987.

24. Roscoe, K. H., A. N., Schofield, "On the Yielding of Soils", *Géotechnique,* Vol. 8, pp. 22–53, 1958.

25. Roscoe, KH., "The influence of strains in soil mechanics 10th Rankine Lecture", *Géotechnique*, Vol. 20, No. 2, pp. 129–170, 1970.

26. Saada A. S., and F. C.,Townsend, "State of the Art: Laboratory Strength Testing of Soil"*ASTM STP* 740,Young R.N. and Townsend F.C. (Editors), pp. 7-77, 1981.

27. Saada, A. S., G., Fries, and C. C., Ker, "An Evaluation of Laboratory Testing Techniques in Soil Mechanics", *Soils and Foundations*, Vol. 23, No. 2, pp. 98-112, 1983.

28. Seth M., "Comparison of Direct Simple Shear Confinement Methods on Clay andShear Box Test",*Géotechnique*, Vol. 37, No. 1, pp. 11-23.

29. Sowers, G. F.,"Strength Testing of Soils. Laboratory Shear Testing of Soils",*ASTM STP* 361, Am. Soc. Testing Mats, p. 4, 1963.

30. Terzaghi, K., R. B., Peck, and G., Mesri, *Soil Mechanics in Engineering Practice*, 3rd Ed., John Wiley & Sons, New York, p. 549, 1996.

31. Vucetic M. and Lacasse S., "Specimen Size Effect in Simple Shear Test", *Journal of Geotechnical Engineering Division*, ASCE, Vol.108,pp. 1567-1585, 1982.

32. Young, R. N., and F. C., Townsend,"Normalized Stress-Strain for Undrained Shear Tests",*Géotechnique*,Vol. 47,pp. 387-409, 1981.

33. Yu, P., and F. E., Richart, "Stress Ratio Effects on Shear Modulus of Dry Sands",*J. Geotech. Engrg. Div.,* ASCE, Vol. 110, No.3, pp. 331-345, 1984.